This article was published in Water Research, 88, 39-59, 2016
http://dx.doi.org/10.1016/j.watres.2015.09.044

# Chemical and Photochemical Degradation of Polybrominated Diphenyl Ethers in Liquid Systems – A Review

Mónica S. F. Santos[a*], Arminda Alves[a] and Luis M. Madeira[a*]

[a] LEPABE – Laboratory for Process, Environmental, Biotechnology and Energy Engineering, Faculty of Engineering, University of Porto, R. Dr. Roberto Frias, s/n, 4200-465 Porto, Portugal

**Abstract**

Polybrominated diphenyl ethers (PBDEs) are brominated flame retardants which have received a great deal of attention due to their persistence, potential to bioaccumulate and possible toxic effects. PBDEs have been globally detected in humans, wildlife and environment, highlighting the urgency of looking for effective removal technologies to mitigate their spread and accumulation in the environment. Among all environmental compartments, the water has raised particular attention. This paper aims to provide information about the suitability of the main degradation processes investigated to date (photolysis, zerovalent iron and $TiO_2$ photocatalysis) for the degradation of PBDEs in water matrices. The most relevant criteria behind the design of a system for such purpose are discussed in detail for each individual process. The comparative analysis suggests that the oxidative degradation by $TiO_2$ is the most appropriated technology to treat waters contaminated with PBDEs because higher debromination and mineralization degrees are achieved, preventing the formation/accumulation of lower brominated PBDE congeners and promoting the cracking of aromatic cores.

* Corresponding authors. Tel.: +351-225081519; Fax: +351-225081449; E-mail adresses: mssantos@fe.up.pt (Mónica S. F. Santos), mmdeira@fe.up.pt (Luís M. Madeira)

## Contents



## Nomenclature

ACN – acetonitrile

BFRs – brominated flame retardants

CB – conduction band

DFT – density functional theory

$e_{CB}^{-}$ – conduction band electrons

$E_{ex}$ – the lowest singlet vertical excitation energy

$E_{LUMO}$ – energy of the lowest unoccupied molecular orbital

FR – flame retardants

GC-ECD – gas chromatography with electron capture detector

GC-MS – gas chromatography with mass spectrometer detector

$H_{ads}$ – atomic hydrogen

$H_f$ – Gibbs free energy of formation

HO-PBDEs – hydroxylated polybrominated diphenyl ether

HO-PBDFs – hydroxylated polybrominated dibenzofurans

$h_{VB}^{+}$ – photogenerated holes

$M$ - noble metal

MeOH – methanol

MeO-PBDEs – methoxylated polybrominated diphenyl ethers

MeO-PBDFs – methoxylated polybrominated dibenzofurans

MZVI – microscale zerovalent iron particles

NZVI – nanoscale zerovalent iron particles

NZVI/Ag - bimetallic iron-silver nanoparticles

NZVI/Ni – bimetallic iron-nickel nanoparticles

NZVI/Pd – bimetallic iron-palladium nanoparticles

PBDEs – polybrominated diphenyl ethers

PBDFs – polybrominated dibenzofurans

PCBs – polychlorinated biphenyls

PCDFs- polychlorinated dibenzofurans

POPs – Persistent Organic Pollutants

$q_{Br}^{+}$ – average formal charge on Br

S-NZVI – nanoscale zerovalent iron particles prepared from steel pickling waste liquor

THF – tetrahydrofuran

VB – valence band

WWTPs – wastewater treatment plants

ZVI – zerovalent iron

## 1. Introduction

Accidental fires inflict a heavy toll in terms of economic loss, human suffering and, in the extreme, death. As a response to this challenge, there was a need to produce and

use flame retardants (FR), as a mean to reduce the likelihood of ignition, to hind the fire spread and to provide some extra time in the early stages of a fire when it is much easier to escape (D'Silva et al. 2004). For a long time, flame retardants were associated to safety and protection and were used in a large number of applications including: the industries of plastics, textiles, electronic equipment and building materials. Among the organohalogenated flame retardants the bromine-based ones are the most effective and applied (Olukunle et al. 2012). Their popularity on fire prevention is related in part to the weak bond between bromine and the carbon atoms, which enables the bromine atom to interfere at a more favorable point in the combustion process (D'Silva et al. 2004). Brominated flame retardants (BFRs) can be classified in reactive or additive, depending on the manner they are incorporated in the material. Reactive flame retardants are chemically bonded to the material while additive flame retardants are not covalently bonded and are often applied to the substrate surface as a spray in a coating formulation (Xiao et al. 2007). For that reason, additive BFRs are easily leached out from the surface of the material and thus released into the environment during their natural operational life and also during processing, recycling or combustion (D'Silva et al. 2004, Fulara and Czaplicka 2012). Polybrominated diphenyl ethers (PBDEs) are an example of additive flame retardants having structures similar to polychlorinated biphenyls (PCBs) with an oxygen atom between the aromatic rings (Fig. S1 of the supporting information) (Polo et al. 2004). Theoretically, there are 209 PBDEs congeners differing in the number and/or position of the bromine atoms in the aromatic ring. These compounds are commercially available as mixtures of PBDEs with different degrees of bromination. Three main commercial formulations exist (Penta-BDE, Octa-BDE and Deca-BDE), which are designated according to the degree of bromination of the major PBDE constituent.

The main properties of technical PBDE mixtures are indicated in Table S1 of the supporting information (ATSDR and EPA, 2004, ENVIRON International Corporation, 2003a, ENVIRON International Corporation, 2003b, Hardy et al. 2002). In the United States, several states have adopted legislation to ban the Penta-BDE and Octa-BDE mixtures and, owing to growing concerns, the main US chemical producer (Great Lakes Chemical Corporation) voluntarily agreed to stop its manufacturing (Bacaloni et al. 2009). The Deca-BDE mixture was phased out at the end of 2013 (Dishaw et al. 2014).

At European Union (EU), the uses of Penta-BDE and Octa-BDE commercial mixtures were completely banned since 2004, after a comprehensive risk assessment analysis under the Existing Substances Regulation 793/93/EEC (Directive 2003/11/EC, 2003). In May 2009, at the 4$^{th}$ meeting of the parties of the Stockholm Convention for Persistent Organic Pollutants (POPs), the Penta-BDE and Octa-BDE commercial mixtures were officially classified as POPs substances and were included in the Annex A (elimination of production and use of all intentionally produced POPs) (http://chm.pops.int/Convention/ThePOPs/TheNewPOPs/tabid/2511/Default.aspx, Möller et al. 2011). The use of Deca-BDE formulation in EU is restricted and its inclusion in Annexes A, B and /or C of the Stockholm Convention is still under consideration (http://chm.pops.int/Convention/POPsReviewCommittee/Chemicals/tabid/243/Default.aspx). Although the use of PBDEs has been restricted or even ceased, human and environment exposure will continue for decades due to the big "reservoir" of existing products containing PBDEs. As such, urgent needs regarding the search for effective removal methodologies to mitigate the spread and accumulation of these compounds in the environment arise. As PBDEs have high tendency to adsorb to particulate matter due to their chemical properties, a high effort in the investigation of removal/degradation methodologies for the remediation of contaminated soils, sediments and sewage sludge would be expected. However, most of the studies reported in the literature use the bacterial or microorganisms existing in the referred matrices, but for the biodegradation of PBDEs in the liquid phase. Relatively few exceptions were found to be effectively focused in the remediation of solid matrices contaminated with PBDEs (Ahn et al. 2006, Hua et al. 2003, Lu and Zhang 2014, Söderström et al. 2003, Wu et al. 2012, Wu et al. 2013, Xie et al. 2014). For that reason, this review will only consider the studies about removal/degradation of PBDEs in liquid systems. Additionally, because biodegradation has been extensively described (Xia 2012), only the recent advances in chemical and photochemical degradation processes will be discussed.

Because our main objective is to provide information about how waters contaminated with PBDEs could be treated, the most relevant criteria to take into account in the designi of a system for such purpose will be addressed. These criteria are (i) the

degradation rate of the PBDE; (ii) the overall degradation degree of the parent compound; (iii) the global debromination percentage; (iv) the kind of degradation by-products formed and (iv) the toxicity of such by-products.

The degradation rate will be discussed in the following sections in terms of its variation with some parameters such as: the type of solvent used in the reaction; the amount of $TiO_2$ photocatalyst; the presence of organic matter; the size and the amount of zerovalent iron particles; etc. Quantum yields are discussed as well. This analysis will be helpful to identify which conditions could bring the maximum degradation rate and the maximum degradation degree of the parent compound.

Since PBDEs could be degraded to generate potentially more persistent and/or less toxic brominated species, the favorable elimination methods are expected to achieve a full debromination. The degree of debromination will be evaluated by the global debromination percentage at the end of the process.

A detailed analysis of the degradation mechanisms will be also attempted in the following sections to identify the most probable degradation by-products and to draw conclusions about their toxicity.

## 2. Degradation technologies of PBDEs in liquid systems

Relatively few data concerning the occurrence of PBDEs in waters has been reported, which is not surprising as their partitioning and accumulation characteristics (Table S1) make other matrices more attractive for study. Nevertheless, the contamination of this matrix by PBDEs should not be ruled out since, even at low doses, a long term exposure to these compounds could bring some problems to humans, wildlife and the environment. Actually, although the use of PBDEs commercial mixtures has been restricted or even ceased, the introduction of such hazardous in the environment will continue for a long period due to the equipment/materials in use and in stock. Although wastewater treatment plants (WWTPs) are contributing to the drop on PBDEs contamination levels, additional treatment strategies are still being required; PBDEs concentrations from 1 to 4300 ng/L and from non-detected to 270 ng/L have been measured in influents and effluents from WWTPs, respectively (Anderson and MacRae 2006, Clara et al. 2012, Clarke et al. 2010, Kim et al. 2013, North 2004, Peng et al. 2009, Rocha-Gutierrez and Lee 2011, Vogelsang et al. 2006). Actually, the discharge

of effluents contaminated with PBDEs into water courses lead to their contamination, rising concern about the occurrence of PBDEs in source waters for drinking water supply (Wols and Hofman-Caris 2012).

Some degradation techniques have been explored for the effective removal of PBDEs from contaminated liquids. Photolysis, reductive dehalogenation by zerovalent iron and photocatalysis with $TiO_2$ constitute the main degradation methodologies reported in the literature concerning this matter (Fig. 1 a). A detailed and critical analysis is indicated in the next sections for each degradation methodology. Among them, direct photolysis is undoubtedly the most studied technique followed by reductive dehalogenation by zerovalent iron and the photocatalysis with $TiO_2$ (Fig. 1 a). Beyond those, it is worth mentioning one study about hydrothermal degradation of PBDEs under high-temperature and high-pressure conditions (Nose et al. 2007), and two other regarding the electrochemical debromination of the commercial decabromodiphenyl ether flame retardant (Konstantinov et al. 2008) and BDE-47 (Su et al. 2012). Regarding the PBDE congeners most investigated, it can be concluded from Fig. 1 b that BDE-209 is the most studied congener followed by BDE-47 and BDE-99. A total contribution of only 18% of the studies reported in the literature is reserved for the investigation of other PBDEs. It seems that a great concern exists about the BDE-209 degradation, which may be driven by the necessity of understanding how this compound could contribute to the accumulation of lower brominated PBDEs in environmental waters. Indeed, although BDE-209 is generally considered highly recalcitrant but safe (Keum and Li 2005), it may be a source of environmentally abundant BDEs (BDEs 47, 99, 100, 154 and 183) (Keum and Li 2005) and other metabolites, which have been considered more dangerous for humans and wildlife (Darnerud et al. 2001, Fang et al. 2008, Hardy 2000, Millischer et al. 1979). The results depicted in Fig. 1 b for the other congeners, seem to be in accordance with the most abundant congeners identified in wastewaters. Up to the author's knowledge, BDEs 47, 99, 209 and 100 are the most predominant PBDE congeners in influents and effluents from WWTPs (Anderson and MacRae 2006, Clara et al. 2012, North 2004, Rocha-Gutierrez and Lee 2011, Vogelsang et al. 2006), being BDE 209 more often associated to particulate matter (Kim et al. 2013, Peng et al. 2009, Ricklund et al. 2009).

Another relevant aspect that deserves attention is the initial concentration of the parent compound in PBDEs degradation studies. As can be checked from Fig. 1 c, a great percentage of the available studies were carried out using high initial PBDEs concentrations (mg/L level), which is really far from real conditions. Actually, the solubilities of PBDEs in water are extremely low (few μg/L) and, for that reason, the degradation of PBDEs in realistic environmental conditions would occur at much lower contamination levels than the ones considered in most reported cases. As demonstrated, the performances of hydrothermal and electrolytic treatments (denoted as "Others" in Fig. 1 c) were only inspected for the degradation of high PBDEs concentrations in liquid-phase (mg/L). The higher percentage of studies performed at μg/L level was observed for photolysis treatment (only 38%), which highlights the need to invest in experiments under conditions as much as possible closer to the reality. If the solvent in which the degradation process takes place is considered for the analysis, the scenario is even worst (Fig. 1 d). Since the experiments performed with pure water are conducted at μg/L level (see in Table S1 the low solubility of PBDEs in water), it is evident that the most studies that were carried out at low concentration levels (μg/L) were done in organic solvent instead of pure water. Degradation of PBDEs in pure water and at initial concentrations of μg/L is a research topic really scarcely addressed. In fact, it seems very difficult to carry out experiments in pure water due to the extremely low solubility of PBDEs in this solvent (Table S1), which significantly enhances the relative importance of any sorption process on container walls or other materials used during the experiments (Bezares-Cruz et al. 2004). The use of organic solvents not only allows to avoid the relative importance of such sorption processes, but also to use higher initial PBDEs concentrations, which are more easily quantifiable/monitored. In real waters the scenario is even worst due to the presence of organic species that adsorb the PBDEs and affect the performance of the degradation processes. From the analytical point of view, lower levels of PBDEs would require highly sensitive methodologies such as GC-ECD and even GC-MS. Additionally, transparency to UVB light and the ability to act as a hydrogen donor are favorable properties of some organic solvents that suggest a more facile reaction in these solvents (Bezares-Cruz et al. 2004). So, these may be the reasons why most researchers start by investigating the PBDEs degradation in other kind of solvents,

namely hexane (Bezares-Cruz et al. 2004, Fang et al. 2008), tetrahydrofuran (Christiansson et al. 2009, Konstantinov et al. 2008, Sun et al. 2012), mixtures of hexane/benzene/acetone (Watanabe and Tatsukawa 1987), etc. However, care must be taken because the kinetic constants, degradation mechanisms and reaction products may be drastically influenced by the conditions under which the reaction is processed, and some predictions concerning real scenarios may clearly fail.

### 2.1. Photolysis

The starting event for any photochemical reaction is the absorption of a photon by a molecule. For a photon to be absorbed, the compound absorption spectrum must overlap the light source emission spectrum at least in one wavelength of the UV-visible spectrum (Rubio-Clemente et al. 2014). Following absorption of a photon, the molecule is converted to an electronically excited state having a new electronic configuration with a greater potential energy than the ground state (Eq. (1)). As a consequence, the excited compounds ($X^*$) can return to the ground state by energy dissipation (Eq. (2)) or be transformed into intermediate products by photochemically induced reactions (Eq. (3)) (Rubio-Clemente et al. 2014). These intermediate species may ultimately be transformed and mineralized into carbon dioxide, water and inorganic ions – Eq. (4) (Rubio-Clemente et al. 2014).

$$X + h\nu \rightarrow X^* \quad (1)$$

$$X^* \rightarrow X \quad (2)$$

$$X^* \rightarrow Intermediates \quad (3)$$

$$Intermediates \rightarrow\rightarrow CO_2 + H_2O + inorganic\ \ ions \quad (4)$$

#### 2.1.1. Photolysis: kinetics and photoreactivities

All studies found about PBDEs photodegradation in liquid-phase are compiled in Table S2 of the supporting information. As can be seen, the photodegradation of PBDEs typically follows a pseudo-first order kinetic model; however, different photodegradation rate constants (0.003 to 31.94 $h^{-1}$) and quantum yields (0.0102 to 0.60) have been reported, as a consequence of the PBDE congener under investigation

and the different conditions employed in the experiments. First of all, the photoreactivity of PBDEs depends on their molecular structures. Many molecular structural descriptors have been used in quantitative structure-property relationship (QSPR) models to characterize all PBDE congeners, and they can be subdivided into two groups: the quantum chemical descriptors and the geometrical molecular descriptors. The most relevant quantum chemical descriptors for PBDEs are the molecular weight ($M_W$), the atomic charges on bromine ($q_{Br}$) and hydrogen atoms ($q_H$), the frontier molecular orbital energies ($E_{LUMO}$ and $E_{HOMO}$), the standard heat of formation ($\Delta H_f$), the total energy ($TE$) and the electronic energy ($EE$) (Chen et al. 2007, Fang et al. 2009, Niu et al. 2006). On the other hand, the molecular surface area and the molecular volume of PBDEs can be highlighted among other geometrical descriptors in the development of QSPR models (Fang et al. 2009). According to the published QSPR models, it seems that the substitution pattern of bromine atoms on the PBDE molecules has greater relevance to the photolysis quantum yields (fraction of the excited molecules that underwent photolysis) than the number of bromines (Chen et al. 2007, Fang et al. 2009, Niu et al. 2006). Actually, the main descriptors influencing the quantum yields ($q_{Br}$, $q_H$, $E_{LUMO}$ and $E_{HOMO}$) lack of a linear/straight relationship with the degree of bromination and the results seem to be a consequence of the specific PBDE substitution pattern (Fig. S2 of the supporting information). Contrarily, the bromination degree of PBDEs seems to be the governing factor for the photodegradation rates, attending on the descriptors with high importance in the projection (such as $M_W$, $\Delta H_f$, $TE$ and $EE$) – Fig. S2 (Chen et al. 2007, Fang et al. 2009, Niu et al. 2006). Generally, higher brominated diphenyl ethers degrade faster than the lowers (Fig. 2).

Beyond the natural PBDEs photoreactivity, the reaction rate and quantum yields can be influenced by other parameters such as the type of the solvent/reaction medium (Li et al. 2010b, Rayne et al. 2006, Sanchez-Prado et al. 2012) and the intensity/kind of radiation used (Christiansson et al. 2009, Kuivikko et al. 2007). Low quantum yields and reaction rates have been obtained for the photolytic degradation of PBDEs in poor hydrogen donating solvents (e.g. water) – Table S2 (Li et al. 2008, Li et al. 2010b, Xie et al. 2009). Eriksson et al. (2004) studied the photochemical decomposition of 15 PBDEs

304 in different solvents and observed that the reaction rate in methanol/water solution
305 was consistently around 1.7 times lower than in pure methanol and 2-3 times lower
306 than in THF (the best hydrogen donor solvent among these three) (Eriksson et al.
307 2004). Similarly, Xie and co-workers (2009) obtained lower rate constants (2 times
308 lower) and quantum yields (1.3 times lower) for BDE-209 in methanol than in THF (Xie
309 et al. 2009). Leal et al. (2013) demonstrated that water suppresses significantly the
310 photolytic degradation of BDE-209 (rate constant of 0.6 $h^{-1}$ and quantum yield of 0.23)
311 – Table S2 (Leal et al. 2013). Low photolysis rates and quantum yields for experiments
312 conducted in water were also reported by Xue Li and his team (Li et al. 2008, Li et al.
313 2010b), when they compared the BDE-47 and 99 degradation performances in
314 aqueous micellar solutions of nonionic surfactants with the ones achieved in water
315 alone (1.4 to 2.4 times lower). The authors attributed the better results in surfactant
316 solutions to their hydrogen donating capacities through the polyethylene oxide chains
317 and/or hydrocarbon moieties (Li et al. 2008). Moreover, they showed that depending
318 on the surfactant structure, different enhancement performances are attained; Tween
319 80 proved to be more effective than Brij 35 and Brij 58 (1.5 times better either in terms
320 of rate constant or quantum yield) (Li et al. 2008).
321 However, hydrogen donating capacity does not fully explain the photodegradation
322 kinetics/quantum yields of PBDEs in different solvents. For example, Davis and
323 Stapleton (2009) observed a faster photodegradation of nona-PBDEs in toluene
324 relative to methanol or THF, which is not in line with the proposed order of hydrogen
325 donation capacity (Davis and Stapleton 2009). Methanol is clearly the worst hydrogen
326 donor solvent among the three (Eriksson et al. 2004), but it would be expected that
327 THF may be a better hydrogen donor than toluene; THF has an electron-withdrawing
328 oxygen atom in the ring which may potentially increase the acidity of its protons (Davis
329 and Stapleton 2009). The higher degradation performance in toluene may be explained
330 by the fact that toluene's aromatic ring, a good chromophore, may facilitate the
331 indirect photodegradation of PBDEs (Davis and Stapleton 2009). Actually, nonbonding
332 electrons on the oxygen atoms in methanol and in THF may also act as chromophores,
333 but the transition of electrons from nonbonding to antibonding orbitals (toluene)
334 occurs at a lower energy than the transition of electrons from bonding to antibonding
335 orbitals (methanol and THF) (Schwarzenbach et al. 2005). Still looking at the influence

of the reaction solvent on the photodegradation rates and quantum yields, the light attenuation effect is another point that should not be ruled out. For example, although acetone can hardly act as hydrogen donor or a photosensitizer for the photodegradation of PBDEs, Xie et al. (2009) demonstrated that the light attenuation effect caused by acetone is the main reason for the quite slow photodegradation of BDE-209 in this solvent (Fig. 3 and Table S2) (Xie et al. 2009). Xue Li and co-workers also observed that acetone in the Brij 35/acetone system may virtually perform as a light barrier and retard BDE-47 photodegradation (Li et al. 2008). Further, the degradation of BDE-47 in the nonionic surfactant Tween 80 was significantly affected when the concentration of Tween 80 increases from $4.20\times10^{-4}$ M to $1.68\times10^{-3}$ M (quantum yield and rate constant decrease approximately 5 times), which is related to strong light absorption at 253.7 nm (8.5 times absorption increase) (Li et al. 2008).

The interaction between PBDE molecules and the reaction medium also play an important role in the overall photodegradation perfomance (Wang et al. 2012, Xie et al. 2009). Such interactions may modify the properties of the target analytes and lead to different photoreactivities as detailed above; this may explain some results obtained by Xie and co-workers concerning BDE-209 degradation in different solvents (Fig. 4) (Xie et al. 2009).

Recently, Sun and co-workers (2013) demonstrated that it is possible to degrade BDE-209 under visible light irradiation due to the formation of a halogen-binding-based complex through the interaction between PBDE-209 and carboxylate present in the solvent, which exhibits visible-light absorption (Sun et al. 2013).

The presence/absence of organic matter should also be discussed. Leal et al. (2013) studied the effect of different humic substances on the photodecomposition of BDE-209 and they verified that humic and fulvic acids inhibit the degradation process in a similar way, while XAD-4 does not have any effect (Table S2) (Leal et al. 2013). Two reasons were pointed out to justify such findings: light screening by the humic substances and the association of the target compound with the hydrophobic sites of the humic material (Leal et al. 2013). The natural absorbing components in waters from the Atlantic Ocean and the Baltic Sea (natural particles and dissolved organic matter) were also responsible for the different degradation rates obtained by Kuivikko and co-workers (Kuivikko et al. 2007). As the photolytic solar radiation is much more

steeply attenuated by absorbing components of the coastal than of the open ocean, shorter photolytic half-lives were attained in the Atlantic ocean (9.6, 648, 2760 h in Atlantic Ocean against 43.2, 2904 and 12624 h in the Baltic Sea, respectively for BDE-209, 99 and 47).

**2.1.2. Photolysis: mechanism and degradation by-products**

Photodegradation of PBDEs generally leads to the formation of lower brominated PBDE congeners by consecutive reductive debromination (see e.g. Fig. 2). The debromination of an excited PBDE organic molecule may proceed by either homolytic (Scheme 1a) or heterolytic (Scheme 1b) pathways. The two species formed in the photochemically induced aryl bromine bond homolysis (aryl and bromine radicals) can be recombined to yield no net photochemical reaction or the resulting aryl radical can be transformed in a lower brominated PBDE by hydrogen abstraction (Scheme 1a). The hydrogen abstraction step is highly dependent on the kind of solvent in which the degradation reaction proceeds; the more labile is the solvent, with regard to hydrogen atom donation, the higher the photodebromination rate by homolytic pathway.

In heterolytic bond cleavage, the electrons are unequal distributed by the fragments, forming an aryl cation and a bromide ion ($Br^-$) (Scheme 1b). If the photochemical aryl-bromine heterolytic cleavage represents the dominant mechanism, the conversion of the starting material will be strongly dependent on the nucleophilicity of the solvent. Indeed, strong nucleophilic solvents (such as water and methanol) will allow the "trapping" of the aryl cation to yield organic molecules with lower bromine content (Scheme 1b). In contrast, the use of weak nucleophilic solvents will conduct to lower or insignificant conversions of the starting material by this pathway due to the recombination of aryl cation-bromide ion pairs as no nucleophile is present to trap the aryl cation (Scheme 1b). These reactions are potentially responsible for the formation of a wide range of PBDE derivatives: hydroxylated polybrominate diphenyl ethers (HO-PBDEs) when the "trapping" is made by water molecules, methoxylated polybrominated diphenyl ethers (MeO-PBDEs) when MeOH is being used, etc. As can be checked from Table S2, no study reported the formation of MeO-PBDEs, HO-PBDEs or related species in the photochemical degradation of a variety of PBDEs and solvents. The high photoreactivity of such PBDE derivatives (Bastos et al. 2009, Xie et al. 2013)

might be a reason for these findings. However, it is important to emphasize that some PBDEs degradation by-products were assigned to methoxylated polybrominated dibenzofurans (MeO-PBDFs) (Christiansson et al. 2009, Eriksson et al. 2004) and hydroxylated polybrominated dibenzofurans (HO-PBDFs) (Christiansson et al. 2009) when the reaction took place in MeOH and water, respectively. In fact, polybrominated dibenzofurans (PBDFs), which are per se PBDE degradation products, may also react with the surrounding medium to lead the above mentioned species as occur with PBDEs. Summarizing, all studies stated the formation of lower brominated PBDEs congeners and no or few evidences of the presence of PBDE/PBDFs derivatives (eg. HO-PBDEs and HO-PBDFs) in the reaction medium were noticed (Table S2). Sequential dehalogenation is frequently reported as the main mechanism involved in the photodegradation of PBDEs under solar light (Bezares-Cruz et al. 2004, Davis and Stapleton 2009) or UV radiation (Bendig and Vetter 2010, Christiansson et al. 2009, Eriksson et al. 2004, Fang et al. 2008, Watanabe and Tatsukawa 1987). This may suggest that the photolytic cleavage of the aryl-bromine bond is more likely to occur via homolytic pathway. Moreover, it was verified and discussed previously (section 2.1.1.) that the reaction in poor hydrogen donating solvents (e.g. water, methanol) is quite limited compared to other solvents with higher hydrogen donating capabilities.

Concerning the bromines photoreactivity, the available studies report a relatively strong stability of the bond between the aromatic carbons and the *para* bromines, compared to those with *ortho* and *meta* bromines (Davis and Stapleton 2009, Wang et al. 2013a, Wei et al. 2013, Xie et al. 2009, Zeng et al. 2008). Li et al. (2007) investigated the relative reactivity among PBDEs isomers based on net charges of individual atoms calculated by a semiempirical method (Li et al. 2007). They showed that the net positive charges of both *ortho* and *meta* bromine atoms in PBDEs are generally higher than that of *para* bromines in all homologs (Fig. 5) (Li et al. 2007). Years later, Hu and co-workers (2012) also proved that the density functional theory (DFT) can also be satisfactorily used to predict the positional preference of the debromination product formation. They found, for example, that the theoretical debromination preference of BDE-209 by nanoscale zerovalent iron particles was *meta*-Br > *ortho*-Br > *para*-Br (Hu et al. 2012). These predictions are consistent with the experimental results obtained by Wei and co-workers about photolytic debromination of thirteen PBDEs in hexane by

sunlight (Wei et al. 2013); the vulnerability rank order was *meta*≥*ortho*>*para* for the lighter PBDEs (≤8 Br). However, they did not find evident differences in debromination preference among *ortho*, *meta* and *para* bromines for heavier congeners (Wei et al. 2013), which may be explained by the high complexity of the highly brominated molecular structures and the high relevance of the bromine substitution pattern for the overall degradation process in such cases (Fang et al. 2008).

Typically, the unsymmetrical substituted diphenyl ethers were usually photodegraded by debromination on the more substituted ring as observed in many studies for PCBs (Chang et al. 2003, Fang et al. 2008, Li et al. 2010b, Sánchez-Prado et al. 2006). The photodegradation of BDE-100 is not again in line with this generalized rule since BDE-75, which is frequently detected as a BDE-100 degradation product, results from the loss of a bromine atom from the *ortho* position of the less substituted ring. Such finding may be justified by both the steric effect of three adjacent *ortho* bromine atoms (2,2´,6) and the stable structure of the specific brominated phenyl ring with 2,4,6 substitution pattern (Fang et al. 2008). Nevertheless, according to PCBs photodegradation studies, it is not expected that lower brominated PBDEs congeners would be formed as a consequence of the debromination of the less substituted ring at *meta* or *para* positions (Miao et al. 1999).

Beyond the debromination of PBDEs, other relevant degradation pathways may occur and are responsible for the formation of other classes of compounds. One of the most important is the dibenzofuran-type ring closure process via an intramolecular elimination of HBr, which is responsible for the formation of polybrominated dibenzofurans – PBDFs (Scheme 1c) (Christiansson et al. 2009, Eriksson et al. 2004, Fang et al. 2008, Li et al. 2008, Li et al. 2010b, Rayne et al. 2006, Sanchez-Prado et al. 2012, Sánchez-Prado et al. 2006, Söderström et al. 2003, Watanabe and Tatsukawa 1987, Wei et al. 2013). It has been widely reported that PBDFs are more toxic compounds than the original ones (PBDEs) (Li et al. 2010b, Rayne et al. 2006, Sanchez-Prado et al. 2012), and so this pathway is not desired. Typically, lower brominated PBDFs (di- to penta-BDFs) are identified in the reaction medium instead of highly brominated congeners (Christiansson et al. 2009, Eriksson et al. 2004, Rayne et al. 2006, Sanchez-Prado et al. 2012, Watanabe and Tatsukawa 1987). Rayne et al. (2006) and Watanabe and Tatsukawa (1987) argue that PBDEs with >6 bromine substituents

prefer to undergo photodebromination to the hexa-BDE level and be rearranged afterwards into PBDFs (Rayne et al. 2006, Watanabe and Tatsukawa 1987). However, Eriksson and co-workers (Eriksson et al. 2004) suggested that the formation of the furan ring is possible for PBDEs of any level of bromination as long as one *ortho* position is nonbrominated. Despite of this, the lower brominated PBDFs are more often detected because highly halogenated PBDFs are very photosensitive with high quantum yields and high absorption coefficients (Christiansson et al. 2009, Eriksson et al. 2004, Lenoir et al. 1991, Watanabe et al. 1994).

Another possible degradation pathway of PBDEs is the aryl-ether bond cleavage. The photochemically induced aryl-ether bond cleavage may also proceed by homolytic (Scheme 1d and Scheme 1e) or heterolytic (Scheme 1f) pathways. One type of homolytic cleavage reaction that preserves a diaryl system is the photo-Fries rearrangement to produce hydroxybiphenyls (Scheme 1d) (Rayne et al. 2006). According to the studies found in the literature about photodegradation of PBDEs (Table S2), only one paper reported the formation of brominated hydroxybiphenyl compounds (Rayne et al. 2006). Although photo-Fries rearrangements are favored in hydroxylic solvents (or their presence as co-solvents) (Ogata et al. 1970), the presence of these compounds in such solvents was sometimes not observed may be due to the extremely low initial PBDEs concentrations used (Rayne et al. 2006, Sanchez-Prado et al. 2012). Indeed, such low concentrations (~$10^{-9}$ M) may favor preferential hydrogen abstraction as well as the reaction of dissolved oxygen with aryl radicals to yield bromophenols (Scheme 1e) (Rayne et al. 2006).

An alternative photodegradation pathway for PBDEs is the heterolytic aryl-ether bond cleavage yielding bromophenolate ion and aryl cation (Scheme 1f). The bromophenolate ion may be protonated to produce hydroxylated bromobenzenes and/or phenol and the aryl cation may suffer a nucleophilic attack to yield –OR substituted bromobenzenes. Hydroxylated bromobenzenes (Bendig and Vetter 2013, Christiansson et al. 2009) and tetra- and penta-bromobenzenes (Watanabe and Tatsukawa 1987) were identified as photodegradation by-products of decabrominated diphenyl ether in high hydrogen donor solvents (e.g. hexane and THF) (Table S2).

Regarding the global debromination efficiency, the experiments carried out in poor hydrogen donor solvents seem to lead to lower debromination percentages (e.g. 0% in

496 water and 7-12% in methanol) – Table S2 (Davis and Stapleton 2009, Sanchez-Prado et
497 al. 2012). Chromophore solvents (e.g. toluene) or good hydrogen donor solvents (e.g.
498 THF) contribute positively to this criterion, but percentages not higher than 50% were
499 generally achieved (Table S2). Few exceptions are associated to the use of surfactant
500 solutions (~70% of global debromination) (Li et al. 2008, Li et al. 2010b).
501
502 **2.2. $TiO_2$ photocatalysis**
503 The first step of every semiconductor sensitised photoreactions is the photo-activation
504 of the material by the photogeneration of electron-hole ($e^-$–$h^+$) pairs. Semiconductors
505 are characterized for having an electronic band structure in which the highest fully
506 occupied energy band is called valence band (VB) and the lowest empty band is called
507 conduction band (CB) (Hoffmann et al. 1995). The absorption of a photon, whose
508 energy is equal or higher than the band gap energy of the semiconductor, allows the
509 promotion of an electron ( $e^-_{CB}$ ) from the VB to the CB leaving a hole ( $h^+_{VB}$ ) behind – Eq.
510 (5).
511

$$TiO_2 + h\nu \rightarrow TiO_2(e^-_{CB} + h^+_{VB}) \quad (5)$$

512
513 Upon excitation, the fate of the separated electron and hole can follow different
514 pathways (Fig. S3 of the supporting information). In the absence of suitable electron
515 and hole scavengers, the excited-state conduction-band electrons and valence-band
516 holes can recombine on the surface or in the bulk of the photocatalyst and dissipate
517 the input energy as heat (Hoffmann et al. 1995) – Eq. (6).
518

$$TiO_2(e^-_{CB} + h^+_{VB}) \rightarrow TiO_2 + energy \quad (6)$$

519
520 However, if a suitable scavenger or surface defect state is available to trap the charge
521 carriers, the undesired recombination pathway is prevented and subsequent redox
522 reactions may occur (Chong et al. 2010) – Eq. 7.
523

$$(\mathrm{Ox})_{ads} + (\mathrm{Red})_{ads} \xrightarrow{\mathrm{TiO_2\ h\nu \geq Eg}} \mathrm{Ox}^- + \mathrm{Red}^+ \quad (7)$$

Under photocatalytic conditions, the reduction of organic compounds can be achieved either by the attack of CB electrons or reductant species, which are generated from the one-electron oxidation of electron donors or the solvent (Sun et al. 2008).

According to a great number of experimental evidences, compounds prefer to undergo oxidation reactions (mainly driven by highly oxidative species) over photo-activated $TiO_2$ surfaces instead of react directly with free electrons (Folli 2010). Such highly oxidative species (e.g. hydroxyl radicals ( $HO^{\bullet}$ ), superoxides ( $O_2^{\bullet -}$ ), peroxides ( $HO_2^-$ )) are generated by initial interaction of oxygen with conduction band electrons (Eqs. 8 to 12) (Folli 2010) and water and/or surface OH groups with valence band positive holes (Eqs. 13 and 14).

$$TiO_2(e_{CB}^-) + (O_2)_{ads} \rightarrow TiO_2 + (O_2^{\bullet -})_{ads} \quad (8)$$

$$(O_2^{\bullet -})_{ads} + (H^+)_{ads} \rightarrow (HO_2^{\bullet})_{ads} \quad (9)$$

$$TiO_2(e_{CB}^-) + (HO_2^{\bullet})_{ads} \rightarrow (HO_2^-)_{ads} \quad (10)$$

$$(HO_2^-)_{ads} + (H^+)_{ads} \rightarrow (H_2O_2)_{ads} \quad (11)$$

$$(O_2^{\bullet -})_{ads} + (H_2O_2)_{ads} \rightarrow (OH^-)_{ads} + (HO^{\bullet})_{ads} + (O_2)_{ads} \quad (12)$$

$$TiO_2(h_{VB}^+) + (H_2O)_{ads} \rightarrow TiO_2 + (HO^{\bullet})_{ads} + (H^+)_{ads} \quad (13)$$

$$TiO_2(h_{VB}^+) + (HO^-)_{ads} \rightarrow TiO_2 + (HO^{\bullet})_{ads} \quad (14)$$

Beyond the hydroxyl radical reactions, the direct oxidation by photogenerated holes ( $h_{VB}^+$ ) cannot be ruled out in a photocatalytic process (Hoffmann et al. 1995).

### 2.2.1. $TiO_2$ photocatalysis: kinetics and photoreactivities

All studies found about photocatalytic degradation of PBDEs in liquid systems using $TiO_2$ are summarized in Table S3 of the supporting information. Similarly to that was indicated for photolysis, the overall apparent rate constant for the degradation of

PBDEs over photo activated $TiO_2$ surface depends on a number of parameters. The influence of some of them will be explained during this section. The amount and the crystalline form of the photocatalyst used are two of the main important factors. Anatase and rutile are the two basic catalytic crystalline forms of $TiO_2$, being anatase characterized for having a higher adsorptive ability towards organic compounds (Stafford et al. 1993) and a larger band gap (Mo and Ching 1995) than rutile. For that reason, the use of mixtures of anatase and rutile, where anatase acts as an oxidation centre and rutile as a reduction one, proved to bring the highest photocatalytic efficiencies (Fig. 6 c) (Bickley et al. 1991, Bojinova et al. 2007, Chow et al. 2012).

As the reaction occurs at the surface of $TiO_2$, the higher the amount of the catalyst the higher the number of active sites and consequently the higher the degradation performance (Huang et al. 2012). However, for too high $TiO_2$ loads the turbidity of the dispersion increases and inherently the penetration depth of UV irradiation decreases, reducing light utilization efficiency and limiting the photo excitation of $TiO_2$ (Huang et al. 2012). For example, Huang and co-workers (2013) observed an increase on the BDE-209 debromination efficiency when the amount of $TiO_2$ was increased from 0 to 0.1 g/L (21.2 to 96 % BDE-209 removal, respectively), but a further decrease was noticed for increasing amounts of the photocatalyst (Fig. 7) (Huang et al. 2012). Even concerning the influence of the photocatalyst nature on the kinetic constant, Wei et al. (2013) demonstrate very recently that it is possible to enhance PBDEs degradation by using a surface-metalized $TiO_2$ photocatalyst – complete degradation of BDE-209 was observed after only 4 min of irradiation on Pd-$TiO_2$ surface versus only about 40% on unamended $TiO_2$ system at the same irradiation time (Fig. 8) (Li et al. 2014). The supported Pd particles can catalytically activate donors of hydrogen/electron to reduce many halogenated compounds (this will be discussed in detail in section 2.3).

The presence of humic acids is another relevant point for the reaction performance. Humic acids are photosensitizers which can transfer absorbed energy to a chemical or generate oxygen reactive species to enhance the breakdown of organic pollutants (Aguer et al. 1999, Chow et al. 2012, Sandvik et al. 2000). Nevertheless, an increase on the humic acids concentration does not always mean an increase on the degradation rates because the photosensitization effect of humic acids depends on their adsorption on the surface of $TiO_2$. Chow et al. (2012) demonstrated that the degradation of BDE-

209 over $TiO_2$ depends on the humic acid concentration – the reaction rate increase until a humic concentration of 20 mg/L and then decrease (Fig. 6 b) (Chow et al. 2012). Concerning the kind of solvent used, its positive or negative effect on the apparent overall rate constant depends on the main degradation process involved. Huang et al. (2013) showed that the debromination of BDE-209 over $TiO_2$ within 12 h of UV-illumination was negligible in air-saturated acetonitrile after deducting the direct photolysis (Huang et al. 2012). Moreover, they also verified that an increase of the water content led to an increase on the BDE-209 degradation efficiency (Fig. 9), which can be explained by the following reasons: (i) BDE-209 is less soluble in water than in acetonitrile and, for that reason, the amount of BDE-209 molecules adsorbed on the $TiO_2$ surface increases with increasing amount of water – 3.3% and 95% of BDE-209 is adsorbed on the surface of $TiO_2$ in acetonitrile and water, respectively (Huang et al. 2012); (ii) the presence of acetonitrile decreases the adsorption of water molecules on the $TiO_2$ surface, and then minimizes the conversion of holes to $HO^{\bullet}$ (Eqs. 13 and 14) (El-Morsi et al. 2000); (iii) the reaction of $HO^{\bullet}$ with aromatic hydrocarbons is much slower in acetonitrile than in water (DeMatteo et al. 2005, Poole et al. 2005). The same behavior was observed by Zhang and co-workers when the photocatalytic degradation of BDE-209 was investigated in pure water and water/THF systems under air-saturated conditions (Zhang et al. 2014). However, Sun and co-workers (2009) reported that only 1% of water in anoxic acetonitrile is enough to stop the degradation of BDE-209 over $TiO_2$ under UV irradiation in the presence of isopropyl alcohol (Sun et al. 2008). Since the isopropyl alcohol is an electron donor, it will react with the photogenerated holes as well as with any highly oxidative species, preventing the degradation of BDE-209 via oxidation. Because the only way to degrade BDE-209 under such conditions is via reductive process, the results suggest that the amount of photogenerated electrons in aqueous $TiO_2$ dispersions is very limited (water layer on the surface of $TiO_2$ would hinder the interaction between PBDEs and the surface) and hence the photocatalytic reduction of BDE-209 is negligible (Sun et al. 2008). Years later, the same authors proved that it is possible to degrade BDE-209 via reductive process in an aqueous system if the pollutant is pre-adsorbed on the surface of $TiO_2$ (Fig. 10) (Sun et al. 2012). Moreover, it was shown that the degradation of PBDEs can be enhanced/suppressed by the addition of bases/acids, respectively (Fig. 6 a) (Sun et al. 2008). Generally, the

609 adsorption of bases on the surface of $TiO_2$ shifts the Fermi level (flat band potential)
610 toward a negative potential; on the contrary the adsorption of acids tends to positively
611 shift the conduction band edge (Kusama et al. 2008, Sun et al. 2008, Ward et al. 1983).
612 The results obtained by Sun et al. (2009) are in line with this: great depression of BDE-
613 209 degradation by addition of acids (formic acid, acetic acid and trifluoroacetic acid)
614 and opposite behavior when bases were added (pyridine, triethylamine and
615 dimethylformamide) (Sun et al. 2008). Chow and co-workers (2012) also verified that
616 the photocatalytic degradation of BDE-209 and production of lower congeners were
617 the most vigorous at pH 12. They also attribute such behavior to the readily generation
618 of hydroxyl radicals at higher pH (Chow et al. 2012, Shourong et al. 1997) and to the
619 repulsion of mono-charged $TiO_2$ particles which increases the effective surface area
620 and thus enhances the degradation (Chow et al. 2012).
621
622 **2.2.2. $TiO_2$ photocatalysis: mechanism and degradation by-products**
623 The degradation of PBDEs over photo activated $TiO_2$ can be achieved via reductive (An
624 et al. 2008, Chow et al. 2012, Li et al. 2014, Sun et al. 2008, Sun et al. 2012) or
625 oxidative processes (An et al. 2008, Huang et al. 2012, Zhang et al. 2014). When the
626 main mechanism is via reductive process, the degradation of PBDEs is a consequence
627 of their reaction with the conduction electrons or other reductant species. This is the
628 case of the following works: (i) degradation of BDE-209 in anoxic acetonitrile over
629 photo activated $TiO_2$ in the presence of isopropyl alcohol (Sun et al. 2008), (ii)
630 photocatalytic debromination of preloaded BDE-209 on the $TiO_2$ surface in aqueous
631 system in the presence of methanol (Sun et al. 2012) and (iii) photocatalytic
632 debromination of BDE-209 on $TiO_2$ with surface-loaded palladium (Pd-$TiO_2$) in
633 methanol (Li et al. 2014). In such cases, the oxidative process was prevented adding
634 isopropyl alcohol (Sun et al. 2008) or methanol (Li et al. 2014, Sun et al. 2012) to
635 scavenge the VB holes and preloading of BDE-209 molecules to avoid the formation of
636 the depressive water barrier, which would block the electron transformation channel
637 between PBDEs and the surface (Sun et al. 2012). As expected in reduction reactions,
638 the degradation of BDE-209 over unamended $TiO_2$ conducted to the formation of
639 lower brominated PBDEs and at best to diphenyl ether (Li et al. 2014, Sun et al. 2008,
640 Sun et al. 2012). For the reaction carried out over surface-palladized $TiO_2$, phenolic

intermediates originating from the cleavage of the C-O-C ether bond were also detected, probably due to the Pd-catalyzed hydrogenation of the oxygen (Li et al. 2014).

Concerning the bromines reactivity, it was evident from the available studies that bromines at *ortho* position seemed to be more reactive than those at *meta* and *para* positions in reactions accomplished in organic solvents and over unamended $TiO_2$ (Li et al. 2014, Sun et al. 2008). This is consistent with the bond dissociation energies of aryl-bromine bonds for BDE-209 anion: *ortho* (190.4 kJ/mol), *meta* (196.3 kJ/mol) and *para* (196.4 kJ/mol) (Sun et al. 2008). However, Sun and co-workers demonstrated in 2012 that *meta* substituted PBDEs are more reactive than *ortho* substituted ones, when they studied the photocatalytic reductive debromination of preloaded BDE-209 over $TiO_2$ surface in aqueous system (Sun et al. 2012). Two possible interpretations for the findings in water experiments were pointed out (Sun et al. 2012): (1) stronger interaction with $TiO_2$, due to BDE-209 unsolvability in water, may decrease the aryl-bromine bond energy at *meta* position making it of lower energy than the correspondent one at *ortho* position due to steric effects; (2) the interaction might change the breaking of aryl-bromine bond from the stepwise mechanism (Eq. 15) to the concerted one (Eq. 16).

$$\mathrm{R-X} + e^- \rightarrow \mathrm{R-X^{\bullet -}} \rightarrow \mathrm{R^{\bullet}} + \mathrm{X^-} \quad (15)$$

$$\mathrm{R-X} + e^- \rightarrow \left[\mathrm{R\ldots X\ldots}e^-\right] \rightarrow \mathrm{R^{\bullet}} + \mathrm{X^-} \quad (16)$$

This is likely because the trapped electron (Ti III<) can polarize C–Br bond, and the surface Ti site of $TiO_2$ is strong Lewis acid to accept the leaving bromine. The same bromine position preference (i.e. *meta* position) was also observed in experiment done over surface-palladized $TiO_2$, which is in agreement with the findings for PBDE reduction by ZVI (view section 2.3.2.).

Taicheng An and co-workers (2008) studied the photocatalytic degradation of BDE-209 over $TiO_2$ immobilized on hydrophobic montmorillonite and also concluded that the major degradation step appeared to be the reductive debromination (An et al. 2008). However, they noticed that hydroxyl radical reactions were also relevant pathways for the overall BDE-209 degradation, being the bromination degree and the localization of

670 the substrate in the montmorillonite layers the major parameters affecting their
671 preponderance (An et al. 2008). For example, substrates localized in the hydrophobic
672 or interspacial regions (isolated within clay layers) are less susceptible to undergo
673 hydroxyl radical reactions than substrates located at the external surfaces near
674 particles of $TiO_2$, where hydroxyl radicals are generated (An et al. 2008). Moreover,
675 compounds become more reactive towards hydroxyl radical reactions and more
676 resistant to reductive debromination as the level of bromination decreases (An et al.
677 2008, Huang et al. 2012, Li et al. 2014). The degradation intermediates were lower
678 brominated PBDEs which appear to be the result of reduction reactions and
679 hydroxylated PBDEs, brominated phenoxy phenols, phenoxy phenols and small
680 carboxylic acids, which seem to be a consequence of hydroxyl radical reactions
681 (oxidation process) (An et al. 2008, Xie et al. 2015).
682 Up to the author's best knowledge, only one paper was published to date about
683 oxidative degradation (as main mechanism) of PBDEs over $TiO_2$-mediated
684 photocatalysis in liquid-phase. The referred work deals with the degradation of BDE-
685 209 in aqueous solution on the $TiO_2$ surface and was published by Huang and partners
686 in 2013 (Huang et al. 2012). The oxidative mechanism for the photocatalytic
687 degradation of PBDEs over $TiO_2$ in aqueous systems is presented in Scheme 2 using
688 BDE-209 as model congener. Similar OH addition and HBr/Br elimination pathways
689 have been observed for the reaction of $HO^{\bullet}$ with fluoroquinolone pharmaceuticals
690 (Santoke et al. 2009) and hexafluorobenzene (Kobrina 2012).
691 As shown in Scheme 2a, the addition of highly oxidative species (herein represented by
692 $HO^{\bullet}$) to a PBDE molecule leads directly to an aromatic-OH adduct radical, whereas the
693 oxidation by $h_{VB}^{+}$ results in the formation of a radical cation, which will react quickly
694 with water, leading to the same OH-adduct radical after a subsequent deprotonation.
695 The addition of $HO^{\bullet}$ or $h_{VB}^{+}$ may occur in any substituted position of the aromatic ring,
696 but different intermediates are expected accordingly. Since the ether oxygen is an
697 electron donor through resonance, it increases the electron density of the carbons
698 which are directly linked to it (*ipso* carbons) making them favorable to the electrophilic
699 attack by $h_{VB}^{+}$/$HO^{\bullet}$ species. The *ipso* addition leads to the ether linkage cleavage and
700 the formation of bromophenols (intermediate I) and bromophenoxyl radicals

(intermediate II) (route a of Scheme 2). *Para* carbons exhibit the least steric hindrance, among the four possible substitution positions and, for that reason, the electrophilic attack lead to the formation of an aromatic-OH adduct radical, which undergo a rapid HBr elimination to form BDE-phenoxy radical with three mesomeric structures (intermediate III) (route b of Scheme 2). BDE-phenoxy radical can in turn be transformed into bicyclic benzoquinone derivatives by HBr elimination (intermediate IV) and/or can be oxidized to bromophenols and brominated benzoquinones and their radicals by two consecutive $h_{VB}^{+}$/HO$^{\bullet}$ additions (intermediates I, II, V, VI, VII and VIII). These intermediate species are then transformed into ring cleavage derivatives leading to brominated dienoic acids and other ring-opening intermediates, which could be converted into short chain acids (route c and d of Scheme 2). Huang and co-workers did not find any aromatic intermediates during the photocatalytic oxidation of BDE-209, but they observed the accumulation of aliphatic carboxylic derivatives dissolved in solution (Huang et al. 2012). They proposed that the initial attack of $h_{VB}^{+}$/HO$^{\bullet}$ on BDE-209 should be slower enough than the following oxidation reactions of the generated less-brominated hydroxylated PBDEs to ensure the rapid consumption of aromatic intermediates as soon as they are formed on $TiO_2$ surface (Huang et al. 2012). Additionally, they advance that the accumulation of aliphatic carboxylic derivatives should be the result of the diffusion of substrates away from the $TiO_2$ surface (where the reactions with $h_{VB}^{+}$/HO$^{\bullet}$ species take place) due to their strong hydrophilic characteristics (Huang et al. 2012). It is important to emphasize that the generation of aromatic ring-opening intermediates such as brominated dienoic acids is a clear evidence of a photocatalytic oxidative degradation mechanism because the cracking of aromatic cores is impossible in reductive reaction pathways (Huang et al. 2012).

Compared to the reduction process, the oxidation one seems to be a good alternative since it generally leads to higher debromination and mineralization degrees (Table S3). Global debromination percentages higher than 80% were typically found in studies where the oxidation process was identified as the main degradation mechanism (Huang et al. 2012, Zhang et al. 2014). Moreover, it seems that the higher the amount of water in the reaction medium, the higher the global debromination percentage (e.g. >80% in $H_2O$ against <50% in $H_2O$:THF (1:1, v/v)) (Zhang et al. 2014); 96% in $H_2O$

against 15.4% in acetonitrile (Huang et al. 2012)). Regarding the reduction processes, the global debromination efficiency was generally no higher than 50% (Chow et al. 2012, Li et al. 2014, Sun et al. 2008), unless a surface-metalized $TiO_2$ photocatalyst has been used (Li et al. 2014).

**2.3. Zerovalent iron (ZVI)**

Zerovalent iron (ZVI) has been intensively studied for the remediation of a wide range of contaminants such as chlorinated organic carbons (Matheson and Tratnyek 1994), toxic metals (Lien and Wilkin 2005) and inorganic compounds (Liou et al. 2005). Recently, this process has shown to be also effective to reduce PBDEs through reductive debromination. According to Matheson and Tratnyek, the dehalogenation of halogenated compounds by ZVI can be described by three different pathways (Fig. S4 of the supporting information) (Ciblak 2011, Matheson and Tratnyek 1994). The first one involves a ZVI surface that undergoes oxidation by water, causing a direct electron transfer from the surface to the halogenated compound (Fig. S4 a). The second pathway corresponds to the reduction of the contaminant by intermediate product of corrosion ($Fe^{2+}$) in aqueous solution (Fig. S4 b). The electron transfer from ligand ferrous ions through the ZVI oxide shell is thought to be relatively slow and is probably not so effective (Li 2007). The reductive dehalogenation by produced hydrogen as a product of corrosion with water is the last pathway (Fig. S4 c). However, dissolved hydrogen gas has been shown of little reactivity in the absence of a suitable catalytic surface (Li 2007).

Noble metals ($M$), with lower reactivities than $Fe^0$ (e.g. Cu, Pd, Ag, Ni), are excellent hydrogenation catalysts when applied on ZVI surface and could generate atomic hydrogen ($H_{ads}$) through the dissociative chemisorption of $H_2$ (Eq. (19)), itself generated via water reduction (Eq. (17) and (18)). In a bimetallic system, depending on the strength of interaction, active atomic hydrogen ($H_{ads}$) could be surface-adsorbed or be absorbed within the metal additive lattice behaving like hydride ($H^-$) (Cwiertny et al. 2006, Cwiertny et al. 2007). This will determine the reaction mechanism involved in the debromination of PBDEs by bimetallic systems. If the atomic hydrogen is surface-adsorbed, the dehalogenation will proceed by homolytic pathway (Scheme 1a

763 and Eq. (22)). Otherwise, $H_{ads}$ would react via nucleophilic attack at a halogen
764 substituent rather than via addition at a carbon center (Scheme 1b and Eq. (23)). The
765 abundance of $H^+$ is controlled by its formation from the solution reactions (Eqs. (20)
766 and (21)) and its removal by the bimetallic system to form the atomic hydrogen (Eqs.
767 (18) and (19)) (Graham and Jovanovic 1999).
768
769 Surface reactions

$$Fe^0 \rightarrow Fe^{2+} + 2e^- \quad (17)$$

$$2H_2O + 2e^- \rightarrow H_2(g) + 2OH^- \quad (18)$$

$$2M + H_2(g) \rightarrow 2M\cdots H_{ads} \quad (19)$$

770
771 Solution reactions

$$2H_2O \rightarrow 2H^+ + 2OH^- \quad (20)$$

$$2HBr \rightarrow 2H^+ + 2Br^- \quad (21)$$

772
773 Debromination Reaction

$$2M\cdots H_{ads} + RBr_n \rightarrow RBr_{n-1} + HBr \quad (22)$$

$$M\cdots H_{ads} + RBr_n \rightarrow RBr_{n-1} + Br^- \quad (23)$$

774
775 **2.3.1. Zerovalent iron: kinetics and reactivity**
776 As can be observed in Table S4 of the supporting information, the debromination of
777 PBDEs by ZVI is always well described by a pseudo-first order reaction. However, very
778 frequently a two-step kinetic behavior is observed: a fast removal step at the
779 beginning of the reaction and a follow-up slow removal step (Cai et al. 2014, Fang et al.
780 2011a, b, Keum and Li 2005, Luo et al. 2012, Peng et al. 2013). This phenomenon is
781 probably due to the iron oxidation and concomitant formation of an oxide or
782 hydroxide layer (passivated layer) during the ZVI mediated reduction reaction, which
783 covers some reaction sites and hinders the transfer of electrons (Fang et al. 2011a, b,
784 Keum and Li 2005, Kluyev et al. 2002, Peng et al. 2013). One way to reduce this

785 negative effect is to perform the reaction at lower pHs because iron oxides are soluble
786 in acidic conditions (Shih and Tai 2010, Yang and Lee 2005).
787 Concerning the apparent kinetic constants, it is difficult to make any comparative
788 judgment since it depends on many factors that are not well controlled from one study
789 to another. Some of the main aspects which determine the reaction rate are the
790 nature and properties of the reducing agent used. For example, the use of bimetallic
791 systems instead of the unamended ZVI (uncatalyzed $Fe^0$ particles) usually improves the
792 dehalogenation reaction rate – Fig. 11. In bimetallic systems, the noble metal (of lower
793 reactivity) could alter the electronic properties of iron and enhance the rate of iron
794 corrosion by forming a galvanic couple with it (Kluyev et al. 2002, Ni and Yang 2014, Xu
795 and Zhang 2000). Additionally, it also favors water reduction and formation of
796 activated H-species, as explained above, which in turn can contribute to increased
797 rates of contaminant reduction (Ni and Yang 2014, Schrick et al. 2002). Fang et al.
798 (2011) studied the degradation of BDE-209 by nanoscale zerovalent iron particles
799 (NZVI) and bimetallic iron-nickel nanoparticles (NZVI/Ni) and obtained apparent
800 pseudo-first order rate constants of 0.031 $h^{-1}$ and 1.662 $h^{-1}$, respectively. Zhuang and
801 co-workers also showed that the iron normalized rate constants obtained with
802 bimetallic iron-palladium nanoparticles (NZVI/Pd) were 2, 3, and 4 orders of magnitude
803 greater for tri-, di- and mono-BDEs, respectively, than with NZVI (Zhuang et al. 2010,
804 Zhuang et al. 2011). Additionally, Fang et al. (2011) verified a slow removal of BDE-209
805 by NZVI within a test period of 3 h and about 93.4% BDE-209 removal within 90 min by
806 NZVI/Ni (Fang et al. 2011a). Recently, Ni et al. (2014) also confirmed that the use of a
807 second metal (nickel) on the $Fe^0$ nanoparticles surface allow the increase of the BDE-
808 209 apparent degradation rate constant from 0.164 to 0.287 $h^{-1}$ (Ni and Yang 2014).
809 However, the excessive deposition of the second metal on the ZVI surface (bimetallic
810 system) may cause the complete covering of $Fe^0$ particles, being unfavorable for the
811 dehalogenation (Ni and Yang 2014, Xu et al. 2012, Zhuang et al. 2012). For example,
812 Zhuang et al. (2012) obtained a drop in reactivity above 0.3 Pd/Fe wt.% (Zhuang et al.
813 2012).
814 Another point that influences the remediation by bimetallic systems is the kind of
815 metal ion applied on the ZVI surface. Tan and co-workers investigated the effect of
816 three transition metal ions ($Cu^{2+}$, $Co^{2+}$ and $Ni^{2+}$) on the debromination of BDE-209 by

817 NZVI and verified that such ions contribute positively to the process (Tan et al. 2014).
818 They concluded that the BDE-209 removal efficiency is higher for bimetallic systems
819 (i.e. in the presence of the above mentioned cations), being the highest value attained
820 in the experiment performed with 0.05 mM of $Ni^{2+}$ (rate constant of 42.32 $h^{-1}$ against
821 21.79 $h^{-1}$ and 13.82 $h^{-1}$ for 0.05 mM of $Cu^{2+}$ and $Co^{2+}$, respectively) (Tan et al. 2014).
822 These results may be explained by the different abilities of the ions to promote the
823 dehydrogenation of BDE-209. The promotion mechanism of these ions was also
824 verified in the reductive degradation of BDE-209 by a nanoscale zerovalent metal
825 prepared from steel pickling waste liquor (NZVM) (rate constant of 1.10 $h^{-1}$ for NZVM,
826 46.59 $h^{-1}$ for NZVM with 0.05 mM $Ni^{2+}$, 23.03 $h^{-1}$ for NZVM with 0.05 mM $Cu^{2+}$ and
827 16.16 $h^{-1}$ for NZVM with 0.05 mM $Co^{2+}$) (Cai et al. 2014).
828 The use of particles with different dimensions also constitutes another relevant point
829 for the overall reaction rate. As the degradation of PBDEs by ZVI occurs on the surface
830 of the metal, NZVI exhibits higher reactivity than microscale zerovalent iron particles
831 (MZVI) thanks to the great specific surface area and, consequently, the higher number
832 of reactive sites. For example, Shih and co-workers (2010) verified that the reactivity of
833 NZVI was about 7-fold higher than that of MZVI (Shih and Tai 2010). Zhuang et al.
834 (2010) compared the rate constants normalized by the mass of ZVI obtained for the
835 debromination of BDE-7 by NZVI and MZVI and concluded that NZVI gives the highest
836 rate constant ($2.29\times10^{-4}$ against $3.56\times10^{-6}$ L/d.g) (Zhuang et al. 2010). Removal
837 efficiencies of 24% and 4.5% were also obtained for the degradation of BDE-209 by
838 NZVI and Fe powder, respectively (Fig. 11) (Fang et al. 2011b). However, NZVI has
839 adverse effects on organisms in the environment (Barnes et al. 2010, Lee et al. 2008, Li
840 et al. 2010c, Peng et al. 2013) and its reactivity is sometimes affected by the tendency
841 to aggregate and to form particles with larger dimensions (Ni and Yang 2014, Tso and
842 Shih 2015, Wang et al. 2013b). For that reason, some studies evaluate the efficacy of
843 NZVI immobilized on different supports (Ni and Yang 2014, Zhuang et al. 2011). For
844 example, the reaction rate of resin-bound NZVI is about 55% higher than that of
845 dispersed NZVI (Fig. 12) (Ni and Yang 2014).
846 In the same line, it is obvious that an increase of ZVI dosage has a positive effect on the
847 conversion; increase of the number of active sites and reactive surface areas (Fang et
848 al. 2011a, Peng et al. 2013). In contrast, an increase of the PBDEs concentration might

849 lead to a decrease of the reaction rate, for a fixed surface reaction area, due to
850 competitive adsorption among molecules (Bokare et al. 2008, Fang et al. 2011a, b).
851 The presence of organic matter also influences the degradation process by ZVI. It is
852 reported in the literature that organic matter (e.g. humic substances) affects
853 negatively the process by decreasing the ZVI reactivity. The benzene carboxylic and
854 phenolic hydroxyl groups of the humic acids (HA) can chemisorb on the active sites of
855 ZVI surface, inhibiting the pollutants removal. Tan et al. (2014) studied the
856 debromination of BDE-209 by NZVI and verified that as the concentration of HA
857 increased, its inhibitory effect intensified and the rate constant decrease (1.02 $h^{-1}$ for 0
858 mM HA, 0.71 $h^{-1}$ for 10 mM HA, 0.49 $h^{-1}$ for 20 mM HA and 0.30 $h^{-1}$ for 40 mM HA) (Tan
859 et al. 2014). The same was concluded by Cai et al. (2014) when they investigated the
860 degradation of BDE-209 by a NZVM produced from steel pickling waste liquor (1.10 $h^{-1}$
861 for 0 mM HA, 0.76 $h^{-1}$ for 10 mM HA, 0.48 $h^{-1}$ for 20 mM HA and 0.37 $h^{-1}$ for 40 mM HA
862 (Cai et al. 2014).
863 Besides the above mentioned issues, environmental conditions such as the type of
864 solvent, the pH and the temperature would further contribute to such differences
865 observed in kinetic constants and even in reaction mechanisms (Table S4).
866
867 **2.3.2. Zerovalent iron: mechanism and degradation by-products**
868 A stepwise mechanism (Eq. 15) was observed in the debromination of: (i) BDE-209 by
869 NZVI immobilized on a resin (Li et al. 2007); (ii) six PBDEs (substituted with one to ten
870 bromines) by ZVI (Keum and Li 2005); (iii) BDE-209 and BDE-3 by MZVI (Peng et al.
871 2013); (iv) BDE-209 and BDE-47 by bimetallic iron-silver nanoparticles (NZVI/Ag) (Luo
872 et al. 2012); (v) BDE-21 by NZVI (Zhuang et al. 2010); BDE-209 by NZVI/Ni immobilized
873 on a resin (Ni and Yang 2014); (vi) BDE-209 by NZVI/Ni (Fang et al. 2011a); (vii) BDE-
874 209 by nanoscale zerovalent iron particles prepared from steel pickling waste liquor (S-
875 NZVI) (Fang et al. 2011b); (viii) BDE-47 by NZVI/Ag with ultrasound (Luo et al. 2011);
876 (ix) several environmental-abundant PBDEs by NZVI and bimetallic iron-palladium
877 nanoparticles (NZVI/Pd) (Zhuang et al. 2012). However, sometimes the following
878 sequential dehalogenation reactions could not fully explain the instant formation of
879 some degradation by-products, indicating that a concerted mechanism (i.e.,
880 simultaneous) pathway was sometimes involved (Eq. 16). For example, Shih et al.

(2010) studied the degradation of BDE-209 by ZVI and concluded that it seemed to be a multiple debromination reaction (Shih and Tai 2010). Zhuang and co-workers (2010) also demonstrated that the debromination of BDE 5 and 12 by NZVI seemed to suggest that near simultaneous (concerted mechanism) loss of *ortho*- and *meta*- or *meta*- and *para*-bromines might be possible. One year later, the same research group verified that NZVI/Pd promotes concerted debromination, especially in case of the existence of adjacent bromines (Zhuang et al. 2011).

According to the studies compiled in Table S4, direct electron transfer (Fig. S4 a) appears to be the major reaction mechanism between PBDEs and unamended ZVI (Liang et al. 2014, Peng et al. 2013, Shih and Tai 2010, Zhuang et al. 2010, Zhuang et al. 2012).

Concerning the bromines reactivity, the *meta*-position is the most susceptible to the debromination by unamended ZVI, followed by the *ortho* and *para*-positions (Keum and Li 2005, Li et al. 2007, Ni and Yang 2014, Shih and Tai 2010, Zhuang et al. 2010, Zhuang et al. 2011, Zhuang et al. 2012). These results are in line with the theoretical studies based on net charge (Li et al. 2007) and DFT concepts (Hu et al. 2012) referred previously (section 2.1.2.). Although this trend favors *per se* the accumulation of para-bromines, Zhuang et al. (2010) discovered that another factor may contribute to their persistence – a sigmatropic shift of bromine (Hu et al. 2012, Zhuang et al. 2010). This intramolecular migration of the substituent with simultaneous rearrangement of the π system explains, for example, the formation of BDEs 2 (3-monoBDE) and 3 (4-monoBDE), instead of BDEs 1 (2-monoBDE) and 2 (3-monoBDE), from the BDE-5 (2,3-diBDE) reaction with NZVI (Zhuang et al. 2010).

Regarding the reductive debromination of PBDEs by bimetallic systems, it is of general concern that the sorbed atomic hydrogen, rather than galvanic corrosion, is the main responsible for the enhanced reactivity of iron-based bimetal (Bransfield et al. 2006, Xu et al. 2012). For that reason, the mechanism that controls the PBDE debromination by catalyzed ZVI is the catalytic hydrogenation (Fang et al. 2011a, b, Li et al. 2007, Luo et al. 2012, Ni and Yang 2014, Zhuang et al. 2011, Zhuang et al. 2012) and the solvent in which the reaction take place is of extremely importance. Since the main reducing agent in these reactions is the hydrogen atom, protic solvents are required for the reduction. Fang and co-workers (2011) demonstrated that non or negligible

913 degradation of BDE-209 by NZVI particles prepared from steel pickling waste liquor
914 was attained when pure THF or a mixture of THF and ethanol were used as solvents,
915 respectively (Fig. 13) (Fang et al. 2011b). They also observed a notable enhancement of
916 BDE-209 degradation when they increased the amount of water in the solvent (Fang et
917 al. 2011a) - Fig. 13. Indeed, the ionization constants of these solvents followed this
918 trend: water ($1\times10^{-14}$) > ethanol ($1\times10^{-30}$) > THF (aprotic solvent) (Fang et al. 2011a). In
919 all studies found in the literature (Table S4), the susceptibility of bromine for
920 debromination by bimetallic systems follows the order of *para*- > *meta*- > *ortho*-
921 position (Zhuang et al. 2011, Zhuang et al. 2012). This can be explained by steric
922 considerations, where steric hindrance could inhibit the formation of any precursor
923 complex between H atom and PBDEs (Zhuang et al. 2011, Zhuang et al. 2012). The
924 *ortho*-bromines are most hindered by neighboring oxygen, while *para*-bromines bear
925 the least hindrance from the oxygen atom and the other phenyl ring (Zhuang et al.
926 2011).
927 Although the toxicity of PBDEs is not yet fully studied, there are evidences that at least
928 one *para*-bromine atom beside two *ortho* (2,6)-bromine atoms should be presented on
929 one phenyl ring to form a common structural feature for estrogenic PBDEs (Meerts et
930 al. 2001). Therefore, fast and preferred elimination of *para*-bromines by catalyzed ZVI
931 (bimetallic systems) would likely reduce their estrogenic potencies, while the
932 preferential removal of *meta*-bromine by unamended ZVI would not (Zhuang et al.
933 2011, Zhuang et al. 2012).
934 None of the products that could be derived from oxidation, hydroxylation or
935 heterolytic fission of the ether bond were reported in the available studies of PBDEs
936 degradation by ZVI (unamended or catalyzed); only lower brominated PBDEs and
937 diphenyl ether, which typically are more toxic than the higher brominated PBDEs, were
938 reported as the degradation products. Regarding the global debromination efficiency,
939 it can be concluded that the higher the ZVI particle size, the lower the debromination
940 percentage, being 86% for the system NZVI/$H_2O$ against 59% for ZVI/$H_2O$ – Table S4
941 (Keum and Li 2005, Shih and Tai 2010). On the other hand, the available studies
942 suggest that an increase on the amount of water in the reaction medium leads to an
943 increase on the debromination efficiency – 86% global debromination in $H_2O$ using
944 NZVI versus 46% in $H_2O$:acetone (1:1, v/v) using NZVI (Li et al. 2007, Shih and Tai 2010).

## 2.4. Comparison of the degradation processes

Independently of the removal process used, the degradation reaction is often well described by pseudo-first order kinetics. Regarding their performances for the degradation of PBDEs in liquid systems, it is quite difficult to make any comparative judgment due to the wide range of conditions employed. Maximum kinetic constants of 6.7, 20 and 46.59 $h^{-1}$ were obtained for BDE-209 degradation by photolysis, photocatalysis with $TiO_2$ and zerovalent iron processes, respectively. Care should however be taken when analyzing these results, which merely refer to BDE removal, independently of the reaction mechanism.

A great gap still exists concerning the degradation of PBDEs in waters. Actually, many studies which supposedly report the degradation of PBDEs in waters, use co-solvents (even at extremely low percentages) to promote the solubility and stability of PBDEs in the reaction medium. As shown, the effect of such co-solvents should not be completely neglected. Since the contamination of environmental waters by PBDEs is an increasing issue of concern, efforts directed towards the investigation of their degradation under real conditions are urgent. Despite of this, the available results suggest that the photolysis and the reductive degradation through $TiO_2$ photocatalysis seem not to be effective approaches for the treatment of waters contaminated with PBDEs. Either low degradation performances or low global debromination percentages were achieved in both cases (see sections 2.1. and 2.2.) (Sanchez-Prado et al. 2012, Sun et al. 2008, Sun et al. 2012). Photolysis showed only to be efficient for the degradation of PBDEs in high hydrogen donor solvents (e.g. hexane, THF) or in those which could act as photosensitizers (e.g. toluene); even so, global debromination percentages not higher than 50% were generally obtained. Moreover, hydroxylated PBDEs/PBDFs derivatives are likely to be formed, which are known to exhibit significantly higher thyroid hormone activities than PBDEs (Li et al. 2010a) and can photogenerate polybromodibenzo-p-dioxins (Arnoldsson et al. 2012). On the other hand, the extent of the reaction between PBDEs with the conduction electrons generated by the photoexcitation of $TiO_2$ (reduction process) is limited in water due to the formation of the depressive water barrier, which blocks the electron transformation channel between PBDEs and the surface (Sun et al. 2008). Thus, the

977 application of $TiO_2$ photocatalyst for the treatment of waters contaminated with
978 PBDEs seems to be only practicable when no electron donors are present (otherwise
979 they react with photogenerated holes or highly oxidative species avoiding the
980 oxidation of the target compounds) and ideally in the presence of oxygen so that the
981 oxidation mechanism prevails. In such conditions, global debromination levels of 96%
982 can be achieved. The reductive degradation of PBDEs in water by unamended or
983 catalyzed ZVI conducts to satisfactory global debromination degrees (e.g. 59-86% of
984 debromination), but the resulting by-products are assigned to lower brominated PBDE
985 congeners, which are potentially more persistent and toxic than the original ones.
986 Summarizing, $TiO_2$ via an oxidative process (which depends on the operating
987 conditions) seems to constitute a promising approach for developing green and
988 effective methods to remove PBDEs and their family members from contaminated
989 waters. Contrarily to the reduction processes, the oxidation one leads to higher
990 debromination and mineralization degrees and prevents de formation/accumulation of
991 highly toxic PBDEs congeners and aromatic intermediates. In the author's opinion, and
992 because the compounds become more reactive towards hydroxyl radical reactions and
993 more resistant to reductive debromination as the level of bromination decreases, the
994 reductive processes should be followed by an oxidative one to allow the cracking of
995 aromatic cores and put fully detoxification/mineralization of PBDEs in priority. For
996 example, Luo et al. (2011) observed that the effluent resultant from the degradation of
997 BDE-47 by NZVI revealed high acute toxicity, but toxicity was not detected after the
998 addition of hydrogen peroxide to this effluent (Luo et al. 2011). Alternatively, after
999 reductive debromination reactions lower brominated PBDEs can be biodegraded by
1000 microorganisms (Keum and Li 2005, Kim et al. 2012). Among the processes which only
1001 allow the debromination of PBDEs at best to diphenyl ether (reductive processes), the
1002 degradation by catalyzed ZVI should be the preferred one. Actually, the fast and
1003 preferred elimination of *para*-bromines by catalyzed ZVI would likely reduce estrogenic
1004 potencies of PBDEs, while the preferential removal of *meta*-bromine by the others
1005 would not.
1006
1007
1008

## Conclusions

PBDEs can be removed from waters through distinct mechanisms. Among the chemical and photochemical processes discussed in this paper (photolysis, zerovalent iron and $TiO_2$ photocatalysis), the oxidative degradation route by $TiO_2$ photocatalysis seems to be the most suitable for the treatment of waters containing PBDEs. It allows achieving higher debromination and mineralization degrees, avoiding the formation/accumulation of lower brominated PBDE congeners and promoting the cracking of aromatic cores. Photolysis appears to be the less effective degradation methodology.


## Acknowledgements

Mónica S. F. Santos is grateful to the Portuguese Foundation for Science and Technology (FCT) for her postdoctoral grant (ref. SFRH/BPD/104039/2014). This work was funded by FEDER funds through the Operational Programme for Competitiveness Factors – COMPETE, ON.2 - O Novo Norte - North Portugal Regional Operational Programme and National Funds through FCT - Foundation for Science and Technology, in the scope of the P2020 Partnership Agreement under the projects: UID/EQU/00511/2013-LEPABE and NORTE-07-0124-FEDER-000025 - RL2_ Environment&Health.


## References


ATSDR and EPA, 2004. Toxicological profile for polybrominated biphenyls and polybrominated diphenyl ethers. U.S. Department of Health and human Services, Agency for Toxic Substances and Disease Registry, Georgia.

Directive 2003/11/EC, 2003. Directive 2003/11/EC of the European Parliament and of the Council of 6 February 2003 amending for the 24th time Council Directive 76/769/EEC relating to restrictions on the marketing and use of certain dangerous substances and preparations (pentabromodiphenyl ether, octabromodiphenyl ether). Official Journal of the European Union.

ENVIRON International Corporation, 2003a. Voluntary Children's Chemical Evaluation Program Pilot (VCCEPP): Tier 1 Assessment of the Potential Health Risks to Children Associated with Exposure to the Commercial octabromodiphenyl ether Product. Great Lakes Chemical Corporation, West Lafayette, Indiana, USA.

ENVIRON International Corporation, 2003b. Voluntary Children's Chemical Evaluation Program Pilot (VCCEPP): Tier 1 Assessment of the Potential Health Risks to Children Associated with Exposure to the Commercial pentabromodiphenyl ether Product. Great Lakes Chemical Corporation, West Lafayette, Indiana, USA.

http://chm.pops.int/Convention/POPsReviewCommittee/Chemicals/tabid/243/Default.aspx. Stockholm Convention, Persistent Organic Pollutants Review Committee - Recommendations for Listing Chemicals. Retrieved on 19-03-2015.

http://chm.pops.int/Convention/ThePOPs/TheNewPOPs/tabid/2511/Default.aspx. Stockholm Convention, The new POPs under the Stockholm Convention. Retrieved on 19-03-2015.

Aguer, J.P., Richard, C., Andreux, F., 1999. Effect of light on humic substances : production of reactive species. Analusis 27(5), 387-389.

Ahn, M.-Y., Filley, T.R., Jafvert, C.T., Nies, L., Hua, I., Bezares-Cruz, J., 2006. Photodegradation of Decabromodiphenyl Ether Adsorbed onto Clay Minerals, Metal Oxides, and Sediment. Environ. Sci. Technol. 40(1), 215-220.

An, T., Chen, J., Li, G., Ding, X., Sheng, G., Fu, J., Mai, B., O'Shea, K.E., 2008. Characterization and the photocatalytic activity of TiO2 immobilized hydrophobic montmorillonite photocatalysts: Degradation of decabromodiphenyl ether (BDE 209). Catal. Today 139(1–2), 69-76.

Anderson, T.D., MacRae, J.D., 2006. Polybrominated diphenyl ethers in fish and wastewater samples from an area of the Penobscot River in Central Maine. Chemosphere 62(7), 1153-1160.

Arnoldsson, K., Andersson, P.L., Haglund, P., 2012. Photochemical Formation of Polybrominated Dibenzo-p-dioxins from Environmentally Abundant Hydroxylated Polybrominated Diphenyl Ethers. Environ. Sci. Technol. 46(14), 7567-7574.

Bacaloni, A., Callipo, L., Corradini, E., Giansanti, P., Gubbiotti, R., Samperi, R., Laganà, A., 2009. Liquid chromatography–negative ion atmospheric pressure photoionization tandem mass spectrometry for the determination of brominated flame retardants in environmental water and industrial effluents. J. Chromatogr. A 1216(36), 6400-6409.

Barnes, R.J., Van der Gast, C.J., Riba, O., Lehtovirta, L.E., Prosser, J.I., Dobson, P.J., Thompson, I.P., 2010. The impact of zero-valent iron nanoparticles on a river water bacterial community. J. Hazard. Mater. 184(1–3), 73-80.

Bastos, P.M., Eriksson, J., Bergman, Å., 2009. Photochemical decomposition of dissolved hydroxylated polybrominated diphenyl ethers under various aqueous conditions. Chemosphere 77(6), 791-797.

Bendig, P., Vetter, W., 2010. Photolytical Transformation Rates of Individual Polybrominated Diphenyl Ethers in Technical Octabromo Diphenyl Ether (DE-79). Environ. Sci. Technol. 44(5), 1650-1655.

Bendig, P., Vetter, W., 2013. UV-Induced Formation of Bromophenols from Polybrominated Diphenyl Ethers. Environ. Sci. Technol. 47(8), 3665-3670.

Bezares-Cruz, J., Jafvert, C.T., Hua, I., 2004. Solar Photodecomposition of Decabromodiphenyl Ether: Products and Quantum Yield. Environ. Sci. Technol. 38(15), 4149-4156.

Bickley, R.I., Gonzalez-Carreno, T., Lees, J.S., Palmisano, L., Tilley, R.J.D., 1991. A structural investigation of titanium dioxide photocatalysts. J. Solid State Chem. 92(1), 178-190.

Bojinova, A., Kralchevska, R., Poulios, I., Dushkin, C., 2007. Anatase/rutile TiO2 composites: Influence of the mixing ratio on the photocatalytic degradation of Malachite Green and Orange II in slurry. Mater. Chem. Phys. 106(2–3), 187-192.

Bokare, A.D., Chikate, R.C., Rode, C.V., Paknikar, K.M., 2008. Iron-nickel bimetallic nanoparticles for reductive degradation of azo dye Orange G in aqueous solution. Appl. Catal., B 79(3), 270-278.

Bransfield, S.J., Cwiertny, D.M., Roberts, A.L., Fairbrother, D.H., 2006. Influence of Copper Loading and Surface Coverage on the Reactivity of Granular Iron toward 1,1,1-Trichloroethane. Environ. Sci. Technol. 40(5), 1485-1490.

Cai, Y., Liang, B., Fang, Z., Xie, Y., Tsang, E., 2014. Effect of humic acid and metal ions on the debromination of BDE209 by nZVM prepared from steel pickling waste liquor. Front. Environ. Sci. Eng., DOI 10.1007/s11783-014-0764-8.

Chang, F.-C., Chiu, T.-C., Yen, J.-H., Wang, Y.-S., 2003. Dechlorination pathways of ortho-substituted PCBs by UV irradiation in n-hexane and their correlation to the charge distribution on carbon atom. Chemosphere 51(8), 775-784.

Chen, J., Wang, D., Wang, S., Qiao, X., Huang, L., 2007. Quantitative structure–property relationships for direct photolysis of polybrominated diphenyl ethers. Ecotoxicol. Environ. Saf. 66(3), 348-352.

Chong, M.N., Jin, B., Chow, C.W.K., Saint, C., 2010. Recent developments in photocatalytic water treatment technology: A review. Water Res. 44(10), 2997-3027.

Chow, K.L., Man, Y.B., Zheng, J.S., Liang, Y., Tam, N.F.Y., Wong, M.H., 2012. Characterizing the optimal operation of photocatalytic degradation of BDE-209 by nano-sized TiO2. J. Environ. Sci. (China) 24(9), 1670-1678.

Christiansson, A., Eriksson, J., Teclechiel, D., Bergman, Å., 2009. Identification and quantification of products formed via photolysis of decabromodiphenyl ether. Environ. Sci. Pollut. Res. 16(3), 312-321.

Ciblak, A., 2011. Chemical changes and performance of iron-electrolysis for groundwater remediation. MSc thesis, Northeastern University, Boston - Massachusetts, USA.

1117 Clara, M., Windhofer, G., Weilgony, P., Gans, O., Denner, M., Chovanec, A., Zessner,
1118 M., 2012. Identification of relevant micropollutants in Austrian municipal wastewater
1119 and their behaviour during wastewater treatment. Chemosphere 87(11), 1265-1272.

1120 Clarke, B.O., Porter, N.A., Symons, R.K., Marriott, P.J., Stevenson, G.J., Blackbeard, J.R.,
1121 2010. Investigating the distribution of polybrominated diphenyl ethers through an
1122 Australian wastewater treatment plant. Sci. Total Environ. 408(7), 1604-1611.

1123 Cwiertny, D.M., Bransfield, S.J., Livi, K.J.T., Fairbrother, D.H., Roberts, A.L., 2006.
1124 Exploring the Influence of Granular Iron Additives on 1,1,1-Trichloroethane Reduction.
1125 Environ. Sci. Technol. 40(21), 6837-6843.

1126 Cwiertny, D.M., Bransfield, S.J., Roberts, A.L., 2007. Influence of the Oxidizing Species
1127 on the Reactivity of Iron-Based Bimetallic Reductants. Environ. Sci. Technol. 41(10),
1128 3734-3740.

1129 D'Silva, K., Fernandes, A., Rose, M., 2004. Brominated Organic Micropollutants—
1130 Igniting the Flame Retardant Issue. Crit. Rev. Environ. Sci. Technol. 34(2), 141-207.

1131 Darnerud, P.O., Eriksen, G.S., Jóhannesson, T., Larsen, P.B., Viluksela, M., 2001.
1132 Polybrominated diphenyl ethers: Occurence, dietary exposure, and toxicology. Environ.
1133 Health Perspect. 109(Suppl. 1), 49-68.

1134 Davis, E.F., Stapleton, H.M., 2009. Photodegradation Pathways of Nonabrominated
1135 Diphenyl Ethers, 2-Ethylhexyltetrabromobenzoate and Di(2-
1136 ethylhexyl)tetrabromophthalate: Identifying Potential Markers of Photodegradation.
1137 Environ. Sci. Technol. 43(15), 5739-5746.

1138 DeMatteo, M.P., Poole, J.S., Shi, X., Sachdeva, R., Hatcher, P.G., Hadad, C.M., Platz,
1139 M.S., 2005. On the Electrophilicity of Hydroxyl Radical: A Laser Flash Photolysis and
1140 Computational Study. J. Am. Chem. Soc. 127(19), 7094-7109.

1141 Dishaw, L.V., J Macaulay, L., Roberts, S.C., Stapleton, H.M., 2014. Exposures,
1142 mechanisms, and impacts of endocrine-active flame retardants. Curr. Opin. Pharmacol.
1143 19(0), 125-133.

1144 El-Morsi, T.M., Budakowski, W.R., Abd-El-Aziz, A.S., Friesen, K.J., 2000. Photocatalytic
1145 Degradation of 1,10-Dichlorodecane in Aqueous Suspensions of TiO2: A Reaction of
1146 Adsorbed Chlorinated Alkane with Surface Hydroxyl Radicals. Environ. Sci. Technol.
1147 34(6), 1018-1022.

1148 Eriksson, J., Green, N., Marsh, G., Bergman, Å., 2004. Photochemical Decomposition of
1149 15 Polybrominated Diphenyl Ether Congeners in Methanol/Water. Environ. Sci.
1150 Technol. 38(11), 3119-3125.

1151 Fang, L., Huang, J., Yu, G., Li, X., 2009. Quantitative structure–property relationship
1152 studies for direct photolysis rate constants and quantum yields of polybrominated
1153 diphenyl ethers in hexane and methanol. Ecotox. Environ. Safe. 72(5), 1587-1593.

1154 Fang, L., Huang, J., Yu, G., Wang, L., 2008. Photochemical degradation of six
1155 polybrominated diphenyl ether congeners under ultraviolet irradiation in hexane.
1156 Chemosphere 71(2), 258-267.

1157 Fang, Z., Qiu, X., Chen, J., 2011a. Debromination of polybrominated diphenyl ethers by
1158 Ni/Fe bimetallic nanoparticles: Influencing factors, kinetics, and mechanism. J. Hazard.
1159 Mater. 185(2-3), 958-969.

1160 Fang, Z., Qiu, X., Chen, J., 2011b. Degradation of the polybrominated diphenyl ethers
1161 by nanoscale zero-valent metallic particles prepared from steel pickling waste liquor.
1162 Desalination 267(1), 34-41.

1163 Folli, A., 2010. TiO2 photocatalysis in Portland cement systems: fundamentals of self
1164 cleaning effect and air pollution mitigation. Ph.D. thesis, University of Aberdeen, Milan,
1165 Italy.

1166 Fulara, I., Czaplicka, M., 2012. Methods for determination of polybrominated diphenyl
1167 ethers in environmental samples - Review. J. Sep. Sci. 35(16), 2075-2087.

1168 Graham, L.J., Jovanovic, G., 1999. Dechlorination of p-chlorophenol on a Pd/Fe catalyst
1169 in a magnetically stabilized fluidized bed; Implications for sludge and liquid
1170 remediation. Chem. Eng. Sci. 54(15–16), 3085-3093.

1171 Hardy, M.L., 2000. The toxicology of commercial PBDE flame retardants: DecaBDE,
1172 octaBDE, pentaBDE. Organohalogen. Comp. 47, 41-44.

1173 Hardy, M.L., Schroeder, R., Biesemeier, J., Manor, O., 2002. Prenatal Oral (Gavage)
1174 Developmental Toxicity Study of Decabromodiphenyl Oxide in Rats. Int. J. Toxicol.
1175 21(2), 83-91.

1176 Hoffmann, M.R., Martin, S.T., Choi, W., Bahnemann, D.W., 1995. Environmental
1177 Applications of Semiconductor Photocatalysis. Chem. Rev. 95(1), 69-96.

1178 Hu, J.-W., Zhuang, Y., Luo, J., Wei, X.-H., Huang, X.-F., 2012. A Theoretical Study on
1179 Reductive Debromination of Polybrominated Diphenyl Ethers. Int. J. Mol. Sci. 13(7),
1180 9332-9342.

1181 Hua, I., Kang, N., Jafvert, C.T., Fábrega-Duque, J.R., 2003. Heterogeneous
1182 photochemical reactions of decabromodiphenyl ether. Environ. Toxicol. Chem. 22(4),
1183 798-804.

1184 Huang, A., Wang, N., Lei, M., Zhu, L., Zhang, Y., Lin, Z., Yin, D., Tang, H., 2012. Efficient
1185 Oxidative Debromination of Decabromodiphenyl Ether by TiO2-Mediated
1186 Photocatalysis in Aqueous Environment. Environ. Sci. Technol. 47(1), 518-525.

1187 Keum, Y.-S., Li, Q.X., 2005. Reductive Debromination of Polybrominated Diphenyl
1188 Ethers by Zerovalent Iron. Environ. Sci. Technol. 39(7), 2280-2286.

1189 Kim, M., Guerra, P., Theocharides, M., Barclay, K., Smyth, S.A., Alaee, M., 2013.
1190 Parameters affecting the occurrence and removal of polybrominated diphenyl ethers
1191 in twenty Canadian wastewater treatment plants. Water Res. 47(7), 2213-2221.

1192 Kim, Y.-M., Murugesan, K., Chang, Y.-Y., Kim, E.-J., Chang, Y.-S., 2012. Degradation of
1193 polybrominated diphenyl ethers by a sequential treatment with nanoscale zero valent
1194 iron and aerobic biodegradation. J. Chem. Technol. Biotechnol. 87(2), 216-224.

1195 Kluyev, N., Cheleptchikov, A., Brodsky, E., Soyfer, V., Zhilnikov, V., 2002. Reductive
1196 dechlorination of polychlorinated dibenzo-p-dioxins by zerovalent iron in subcritical
1197 water. Chemosphere 46(9–10), 1293-1296.

1198 Kobrina, L.S., 2012. Radical reactions of polyfluoroarenes. Fluorine Notes 2(81).

1199 Konstantinov, A., Bejan, D., Bunce, N.J., Chittim, B., McCrindle, R., Potter, D., Tashiro,
1200 C., 2008. Electrolytic debromination of PBDEs in DE-83TM technical
1201 decabromodiphenyl ether. Chemosphere 72, 1159-1162.

1202 Kuivikko, M., Kotiaho, T., Hartonen, K., Tanskanen, A., Vähätalo, A.V., 2007. Modeled
1203 Direct Photolytic Decomposition of Polybrominated Diphenyl Ethers in the Baltic Sea
1204 and the Atlantic Ocean. Environ. Sci. Technol. 41(20), 7016-7021.

1205 Kusama, H., Orita, H., Sugihara, H., 2008. TiO2 Band Shift by Nitrogen-Containing
1206 Heterocycles in Dye-Sensitized Solar Cells: a Periodic Density Functional Theory Study.
1207 Langmuir 24(8), 4411-4419.

1208 Leal, J.F., Esteves, V.I., Santos, E.B.H., 2013. BDE-209: Kinetic Studies and Effect of
1209 Humic Substances on Photodegradation in Water. Environ. Sci. Technol. 47(24), 14010-
1210 14017.

1211 Lee, C., Kim, J.Y., Lee, W.I., Nelson, K.L., Yoon, J., Sedlak, D.L., 2008. Bactericidal Effect
1212 of Zero-Valent Iron Nanoparticles on Escherichia coli. Environ. Sci. Technol. 42(13),
1213 4927-4933.

1214 Lenoir, D., Schramm, K.W., Hutzinger, O., Schedel, G., 1991. Photochemical
1215 degradation of brominated dibenzo-p-dioxins and -furans in organic solvents.
1216 Chemosphere 22(9–10), 821-834.

1217 Li, A., Tai, C., Zhao, Z., Wang, Y., Zhang, Q., Jiang, G., Hu, J., 2007. Debromination of
1218 decabrominated diphenyl ether by resin-bound iron nanoparticles. Environ. Sci.
1219 Technol. 41, 6841-6846.

1220 Li, F., Xie, Q., Li, X., Li, N., Chi, P., Chen, J., Wang, Z., Hao, C., 2010a. Hormone Activity
1221 of Hydroxylated Polybrominated Diphenyl Ethers on Human Thyroid Receptor-β: In
1222 Vitro and In Silico Investigations. Environ. Health Perspect. 118(5), 602-606.

1223 Li, L., Chang, W., Wang, Y., Ji, H., Chen, C., Ma, W., Zhao, J., 2014. Rapid,
1224 Photocatalytic, and Deep Debromination of Polybrominated Diphenyl Ethers on Pd–
1225 TiO2: Intermediates and Pathways. Chem. Eur. J. 20(35), 11163-11170.

1226 Li, X., 2007. Zero-valent Iron (ZVI) Nanoparticles: The Core-shell Structure and Surface
1227 Chemistry. Ph.D. thesis, Lehigh University, Bethlehem - PA, USA.

1228 Li, X., Huang, J., Fang, L., Yu, G., Lin, H., Wang, L., 2008. Photodegradation of 2,2',4,4'-
1229 tetrabromodiphenyl ether in nonionic surfactant solutions. Chemosphere 73(10),
1230 1594-1601.

1231 Li, X., Huang, J., Yu, G., Deng, S., 2010b. Photodestruction of BDE-99 in micellar
1232 solutions of nonionic surfactants of Brij 35 and Brij 58. Chemosphere 78(6), 752-759.

1233 Li, Z., Greden, K., Alvarez, P.J.J., Gregory, K.B., Lowry, G.V., 2010c. Adsorbed Polymer
1234 and NOM Limits Adhesion and Toxicity of Nano Scale Zerovalent Iron to E. coli.
1235 Environ. Sci. Technol. 44(9), 3462-3467.

1236 Liang, D.-W., Yang, Y.-H., Xu, W.-W., Peng, S.-K., Lu, S.-F., Xiang, Y., 2014. Nonionic
1237 surfactant greatly enhances the reductive debromination of polybrominated diphenyl
1238 ethers by nanoscale zero-valent iron: Mechanism and kinetics. J. Hazard. Mater.
1239 278(0), 592-596.

1240 Lien, H.-L., Wilkin, R.T., 2005. High-level arsenite removal from groundwater by zero-
1241 valent iron. Chemosphere 59(3), 377-386.

1242 Liou, Y.H., Lo, S.L., Lin, C.J., Hu, C.Y., Kuan, W.H., Weng, S.C., 2005. Methods for
1243 Accelerating Nitrate Reduction Using Zerovalent Iron at Near-Neutral pH: Effects of
1244 H2-Reducing Pretreatment and Copper Deposition. Environ. Sci. Technol. 39(24), 9643-
1245 9648.

1246 Lu, M., Zhang, Z.-Z., 2014. Phytoremediation of soil co-contaminated with heavy
1247 metals and deca-BDE by co-planting of Sedum alfredii with tall fescue associated with
1248 Bacillus cereus JP12. Plant Soil 382(1-2), 89-102.

1249 Luo, S., Yang, S., Sun, C., Gu, J.-D., 2012. Improved debromination of polybrominated
1250 diphenyl ethers by bimetallic iron–silver nanoparticles coupled with microwave
1251 energy. Sci. Total Environ. 429(0), 300-308.

1252 Luo, S., Yang, S., Xue, Y., Liang, F., Sun, C., 2011. Two-stage reduction/subsequent
1253 oxidation treatment of 2,2',4,4'-tetrabromodiphenyl ether in aqueous solutions:
1254 Kinetic, pathway and toxicity. J. Hazard. Mater. 192(3), 1795-1803.

1255 Matheson, L.J., Tratnyek, P.G., 1994. Reductive Dehalogenation of Chlorinated
1256 Methanes by Iron Metal. Environ. Sci. Technol. 28(12), 2045-2053.

1257 Meerts, I.A., Letcher, R.J., Hoving, S., Marsh, G., Bergman, A., Lemmen, J.G., Van der
1258 Burg, B., Brouwer, A., 2001. In vitro estrogenicity of polybrominated diphenyl ethers,
1259 hydroxylated PDBEs, and polybrominated bisphenol A compounds. Environ. Health
1260 Persp. 109(4), 399-407.

1261 Miao, X.-S., Chu, S.-G., Xu, X.-B., 1999. Degradation pathways of PCBs upon UV
1262 irradiation in hexane. Chemosphere 39(10), 1639-1650.

Millischer, R., Girault, F., Heywood, R., Clarke, G., Hossack, D., Clair, M., 1979. Decabromobiphenyl: toxicological study. Toxicol. Eur. Res. 2, 155-161.

Mo, S.-D., Ching, W.Y., 1995. Electronic and optical properties of three phases of titanium dioxide: Rutile, anatase, and brookite. Phys. Rev. B 51(19), 13023-13032.

Möller, A., Xie, Z., Sturm, R., Ebinghaus, R., 2011. Polybrominated diphenyl ethers (PBDEs) and alternative brominated flame retardants in air and seawater of the European Arctic. Environ. Pollut. 159(6), 1577-1583.

Ni, S.-Q., Yang, N., 2014. Cation exchange resin immobilized bimetallic nickel–iron nanoparticles to facilitate their application in pollutants degradation. J. Colloid Interface Sci. 420(0), 158-165.

Niu, J., Shen, Z., Yang, Z., Long, X., Yu, G., 2006. Quantitative structure–property relationships on photodegradation of polybrominated diphenyl ethers. Chemosphere 64(4), 658-665.

North, K.D., 2004. Tracking polybrominated diphenyl ether releases in a wastewater treatment plant effluent, Palo Alto, California. Environ. Sci. Technol. 38(17), 4484-4488.

Nose, K., Hashimoto, S., Takahashi, S., Noma, Y., Sakai, S.-i., 2007. Degradation pathways of decabromodiphenyl ether during hydrothermal treatment. Chemosphere 68(1), 120-125.

Ogata, Y., Takagi, K., Ishino, I., 1970. Photochemical rearrangement of diaryl ethers. Tetrahedron 26(11), 2703-2709.

Olukunle, O.I., Okonkwo, O.J., Kefeni, K.K., Lupankwa, M., 2012. Determination of brominated flame retardants in Jukskei River catchment area in Gauteng, South Africa. Water Sci. Technol. 65(4), 743-749.

Peng, X., Tang, C., Yu, Y., Tan, J., Huang, Q., Wu, J., Chen, S., Mai, B., 2009. Concentrations, transport, fate, and releases of polybrominated diphenyl ethers in sewage treatment plants in the Pearl River Delta, South China. Environ. Int. 35(2), 303-309.

Peng, Y.-H., Chen, M.-k., Shih, Y.-h., 2013. Adsorption and sequential degradation of polybrominated diphenyl ethers with zerovalent iron. J. Hazard. Mater. 260(0), 844-850.

Polo, M., Gómez-Noya, G., Quintana, J.B., Llompart, M., García-Jares, C., Cela, R., 2004. Development of a Solid-Phase Microextraction Gas Chromatography/Tandem Mass Spectrometry Method for Polybrominated Diphenyl Ethers and Polybrominated Biphenyls in Water Samples. Anal. Chem. 76(4), 1054-1062.

Poole, J.S., Shi, X., Hadad, C.M., Platz, M.S., 2005. Reaction of Hydroxyl Radical with Aromatic Hydrocarbons in Nonaqueous Solutions: A Laser Flash Photolysis Study in Acetonitrile. J. Phys. Chem. A 109(11), 2547-2551.

Rayne, S., Wan, P., Ikonomou, M., 2006. Photochemistry of a major commercial polybrominated diphenyl ether flame retardant congener: 2,2′,4,4′,5,5′-Hexabromodiphenyl ether (BDE153). Environ. Int. 32(5), 575-585.

Ricklund, N., Kierkegaard, A., McLachlan, M.S., Wahlberg, C., 2009. Mass balance of decabromodiphenyl ethane and decabromodiphenyl ether in a WWTP. Chemosphere 74(3), 389-394.

Rocha-Gutierrez, B., Lee, W.-Y., 2011. Determination and comparison of polybrominated diphenyl ethers in primary, secondary, and tertiary wastewater treatment plants. Int. J. Environ. Anal. Chem. 92(13), 1518-1531.

Rubio-Clemente, A., Torres-Palma, R.A., Peñuela, G.A., 2014. Removal of polycyclic aromatic hydrocarbons in aqueous environment by chemical treatments: A review. Sci. Total Environ. 478(0), 201-225.

Sanchez-Prado, L., Kalafata, K., Risticevic, S., Pawliszyn, J., Lores, M., Llompart, M., Kalogerakis, N., Psillakis, E., 2012. Ice photolysis of 2,2′,4,4′,6-pentabromodiphenyl ether (BDE-100): Laboratory investigations using solid phase microextraction. Anal. Chim. Acta 742, 90-96.

Sánchez-Prado, L., Lores, M., Llompart, M., García-Jares, C., Bayona, J.M., Cela, R., 2006. Natural sunlight and sun simulator photolysis studies of tetra- to hexa-brominated diphenyl ethers in water using solid-phase microextraction. J. Chromatogr. A 1124(1–2), 157-166.

Sandvik, S.L.H., Bilski, P., Pakulski, J.D., Chignell, C.F., Coffin, R.B., 2000. Photogeneration of singlet oxygen and free radicals in dissolved organic matter isolated from the Mississippi and Atchafalaya River plumes. Mar. Chem. 69(1–2), 139-152.

Santoke, H., Song, W., Cooper, W.J., Greaves, J., Miller, G.E., 2009. Free-Radical-Induced Oxidative and Reductive Degradation of Fluoroquinolone Pharmaceuticals: Kinetic Studies and Degradation Mechanism. J. Phys. Chem. A 113(27), 7846-7851.

Schrick, B., Blough, J.L., Jones, A.D., Mallouk, T.E., 2002. Hydrodechlorination of Trichloroethylene to Hydrocarbons Using Bimetallic Nickel−Iron Nanoparticles. Chem. Mater. 14(12), 5140-5147.

Schwarzenbach, R.P., Gschwend, P.M., Imboden, D.M., 2005. Environmental Organic Chemistry. John Wiley & Sons, New Jersey, USA.

Shih, Y.-H., Tai, Y.-T., 2010. Reaction of decabrominated diphenyl ether by zerovalent iron nanoparticles. Chemosphere 78(10), 1200-1206.

1335 Shourong, Z., Qingguo, H., Jun, Z., Bingkun, W., 1997. A study on dye photoremoval in
1336 TiO2 suspension solution. J. Photochem. Photobiol. A 108(2–3), 235-238.

1337 Söderström, G., Sellström, U., de Wit, C.A., Tysklind, M., 2003. Photolytic
1338 Debromination of Decabromodiphenyl Ether (BDE 209). Environ. Sci. Technol. 38(1),
1339 127-132.

1340 Stafford, U., Gray, K.A., Kamat, P.V., Varma, A., 1993. An in situ diffuse reflectance FTIR
1341 investigation of photocatalytic degradation of 4-chlorophenol on a TiO2 powder
1342 surface. Chem. Phys. Lett. 205(1), 55-61.

1343 Su, J., Lu, N., Zhao, J., Yu, H., Huang, H., Dong, X., Quan, X., 2012. Nano-cubic
1344 structured titanium nitride particle films as cathodes for the effective electrocatalytic
1345 debromination of BDE-47. J. Hazard. Mater. 231–232(0), 105-113.

1346 Sun, C., Chang, W., Ma, W., Chen, C., Zhao, J., 2013. Photoreductive Debromination of
1347 Decabromodiphenyl Ethers in the Presence of Carboxylates under Visible Light
1348 Irradiation. Environ. Sci. Technol. 47(5), 2370-2377.

1349 Sun, C., Zhao, D., Chen, C., Ma, W., Zhao, J., 2008. TiO2-Mediated Photocatalytic
1350 Debromination of Decabromodiphenyl Ether: Kinetics and Intermediates. Environ. Sci.
1351 Technol. 43(1), 157-162.

1352 Sun, C., Zhao, J., Ji, H., Ma, W., Chen, C., 2012. Photocatalytic debromination of
1353 preloaded decabromodiphenyl ether on the TiO2 surface in aqueous system.
1354 Chemosphere 89(4), 420-425.

1355 Tan, L., Liang, B., Fang, Z., Xie, Y., Tsang, E., 2014. Effect of humic acid and transition
1356 metal ions on the debromination of decabromodiphenyl by nano zero-valent iron:
1357 kinetics and mechanisms. J. Nanopart. Res. 16(12), 1-13.

1358 Tso, C.-P., Shih, Y.-H., 2015. The reactivity of well-dispersed zerovalent iron
1359 nanoparticles toward pentachlorophenol in water. Water Res. DOI
1360 10.1016/j.watres.2014.12.038.

1361 Vogelsang, C., Grung, M., Jantsch, T.G., Tollefsen, K.E., Liltved, H., 2006. Occurrence
1362 and removal of selected organic micropollutants at mechanical, chemical and
1363 advanced wastewater treatment plants in Norway. Water Res. 40(19), 3559-3570.

1364 Wang, J.-Z., Hou, Y., Zhang, J., Zhu, J., Feng, Y.-L., 2013a. Transformation of 2,2',4,4'-
1365 tetrabromodiphenyl ether under UV irradiation: Potential sources of the secondary
1366 pollutants. J. Hazard. Mater. 263, Part 2(0), 778-783.

1367 Wang, L., Ni, S.-Q., Guo, C., Qian, Y., 2013b. One pot synthesis of ultrathin boron
1368 nitride nanosheet-supported nanoscale zerovalent iron for rapid debromination of
1369 polybrominated diphenyl ethers. J. Mater. Chem. A 1(21), 6379-6387.

1370 Wang, S., Hao, C., Gao, Z., Chen, J., Qiu, J., 2012. Effects of excited-state structures and
1371 properties on photochemical degradation of polybrominated diphenyl ethers: A TDDFT
1372 study. Chemosphere 88(1), 33-38.

1373 Ward, M.D., White, J.R., Bard, A.J., 1983. Electrochemical investigation of the
1374 energetics of particulate titanium dioxide photocatalysts. The methyl viologen-acetate
1375 system. J. Am. Chem. Soc. 105(1), 27-31.

1376 Watanabe, I., Kawano, M., Tatsukawa, R., 1994. The photolysis of halogenated
1377 dibenzofurans in hexane solution and on airborne dust by sunlight. Presented at the
1378 Dioxin '94, 14th International symposium on chlorinated dioxins, PCB and related
1379 compounds, Kyoto, Japan.

1380 Watanabe, I., Tatsukawa, R., 1987. Formation of brominated dibenzofurans from the
1381 photolysis of flame retardant decabromobiphenyl ether in hexane solution by UV and
1382 sun light. Bull. Environ. Contam. Toxicol. 39, 953-959.

1383 Wei, H., Zou, Y., Li, A., Christensen, E.R., Rockne, K.J., 2013. Photolytic debromination
1384 pathway of polybrominated diphenyl ethers in hexane by sunlight. Environ. Pollut. 174,
1385 194-200.

1386 Wols, B.A., Hofman-Caris, C.H.M., 2012. Review of photochemical reaction constants
1387 of organic micropollutants required for UV advanced oxidation processes in water.
1388 Water Res. 46(9), 2815-2827.

1389 Wu, C., Fan, C., Xie, Q., 2012. Study on electrokinetic remediation of PBDEs
1390 contaminated soil. Adv. Mat. Res. 518-523, 2829-2833.

1391 Wu, C.D., Yao, Y.F., Xie, Q.J., 2013. Synergy remediation of PBDEs contaminated soil by
1392 electric-magnetic method. Adv. Mat. Res. 726-731, 2338-2341.

1393 Xia, X., 2012. Microbial Degradation of Polybrominated Diphenyl Ethers: Current and
1394 Future. J. Bioremed. Biodeg. 4(1), 1-2.

1395 Xiao, Q., Hu, B., Duan, J., He, M., Zu, W., 2007. Analysis of PBDEs in Soil, Dust, Spiked
1396 Lake Water, and Human Serum Samples by Hollow Fiber-Liquid Phase Microextraction
1397 Combined with GC-ICP-MS. J. Am. Soc. Mass Spectr. 18(10), 1740-1748.

1398 Xie, Q., Chen, J., Shao, J., Chen, C.e., Zhao, H., Hao, C., 2009. Important role of reaction
1399 field in photodegradation of deca-bromodiphenyl ether: Theoretical and experimental
1400 investigations of solvent effects. Chemosphere 76(11), 1486-1490.

1401 Xie, Q., Chen, J., Zhao, H., Qiao, X., Cai, X., Li, X., 2013. Different photolysis kinetics and
1402 photooxidation reactivities of neutral and anionic hydroxylated polybrominated
1403 diphenyl ethers. Chemosphere 90(2), 188-194.

1404 Xie, Q., Chen, J., Zhao, H., Wang, X., Xie, H.-B., 2015. Distinct photoproducts of
1405 hydroxylated polybromodiphenyl ethers from different photodegradation pathways: a

1406 case study of 2[prime or minute]-HO-BDE-68. Environ. Sci. Process Impacts 17(2), 351-
1407 357.

1408 Xie, Y., Fang, Z., Cheng, W., Tsang, P.E., Zhao, D., 2014. Remediation of polybrominated
1409 diphenyl ethers in soil using Ni/Fe bimetallic nanoparticles: Influencing factors, kinetics
1410 and mechanism. Sci. Total Environ. 485–486(0), 363-370.

1411 Xu, F., Deng, S., Xu, J., Zhang, W., Wu, M., Wang, B., Huang, J., Yu, G., 2012. Highly
1412 Active and Stable Ni–Fe Bimetal Prepared by Ball Milling for Catalytic
1413 Hydrodechlorination of 4-Chlorophenol. Environ. Sci. Technol. 46(8), 4576-4582.

1414 Xu, Y., Zhang, W.-x., 2000. Subcolloidal Fe/Ag Particles for Reductive Dehalogenation of
1415 Chlorinated Benzenes. Ind. Eng. Chem. Res. 39(7), 2238-2244.

1416 Yang, G.C.C., Lee, H.-L., 2005. Chemical reduction of nitrate by nanosized iron: kinetics
1417 and pathways. Water Res. 39(5), 884-894.

1418 Zeng, X., Massey Simonich, S.L., Robrock, K.R., KorytáR, P., Alvarez-Cohen, L., Barofsky,
1419 D.F., 2008. Development and validation of a congener-specific photodegradation
1420 model for polybrominated diphenyl ethers. Environ. Toxicol. Chem. 27(12), 2427-2435.

1421 Zhang, M., Lu, J., He, Y., Wilson, P.C., 2014. Photocatalytic degradation of
1422 polybrominated diphenyl ethers in pure water system. Front. Environ. Sci. Eng., 1-7.

1423 Zhuang, Y., Ahn, S., Luthy, R.G., 2010. Debromination of Polybrominated Diphenyl
1424 Ethers by Nanoscale Zerovalent Iron: Pathways, Kinetics, and Reactivity. Environ. Sci.
1425 Technol. 44(21), 8236-8242.

1426 Zhuang, Y., Ahn, S., Seyfferth, A.L., Masue-Slowey, Y., Fendorf, S., Luthy, R.G., 2011.
1427 Dehalogenation of Polybrominated Diphenyl Ethers and Polychlorinated Biphenyl by
1428 Bimetallic, Impregnated, and Nanoscale Zerovalent Iron. Environ. Sci. Technol. 45(11),
1429 4896-4903.

1430 Zhuang, Y., Jin, L., Luthy, R.G., 2012. Kinetics and pathways for the debromination of
1431 polybrominated diphenyl ethers by bimetallic and nanoscale zerovalent iron: Effects of
1432 particle properties and catalyst. Chemosphere 89(4), 426-432.

1433

1434
1435

**Figure Captions**

Fig. 1. (a) Number of different degradation technologies studied for the treatment of liquid systems contaminated with PBDEs; (b) Most studied PBDEs congeners in degradation experiments; (c) Percentage of publications about PBDEs degradation in liquid systems conducted at µg/L and mg/L levels and (d) Percentage of publications about PBDEs degradation in pure water and other solvents. Search in Scopus data base until the end of 2014 – www.scopus.com).

Fig. 2. The concentration of PBDE congeners and their photoproducts in hexane at different irradiation times: (a) BDE-28; (b) BDE-47; (c) BDE-99; (d) BDE-100; (e) BDE-153; (f) BDE-183. Reprinted from Chemosphere, volume 71, 258-267, Lei Fang, Jun Huang, Gang Yu, Lining Wang, Photochemical degradation of six polybrominated diphenyl ether congeners under ultraviolet irradiation in hexane, Copyright (2008), with permission from Elsevier.

Fig. 3. UV–Vis absorption spectrum of BDE-209 (5 mg/L in acetonitrile), acetone and the relative light irradiance filtered with the ZWB-2 filter. Reprinted from Chemosphere, volume 76, 1486-1490, Qing Xie, Jingwen Chen, Jianping Shao, Chang'er Chen, Hongxia Zhao, Ce Hao, Important role of reaction field in photodegradation of deca-bromodiphenyl ether: Theoretical and experimental investigations of solvent effects, Copyright (2009), with permission from Elsevier.

Fig. 4. Correlation of vertical excitation energy ($E_{ex}$) of BDE-209 and the photolytic reactivity ($\log k$) (a). Correlation of the average formal charges of Br ($q_{Br}^{+}$) and the photolytic reactivity ($\log k$) (b). Reprinted from Chemosphere, volume 76, 1486-1490, Qing Xie, Jingwen Chen, Jianping Shao, Chang'er Chen, Hongxia Zhao, Ce Hao, Important role of reaction field in photodegradation of deca-bromodiphenyl ether: Theoretical and experimental investigations of solvent effects, Copyright (2009), with permission from Elsevier.

Fig. 5. Mean net charges of individual halogen atoms in randomly selected PBDE molecules, calculated using the semiempirical AM1 method contained in the quantum chemical computation software HyperChem (release 7.0 for Windows). Those for deca congeners are drawn in empty symbols using the same color and are not included in generating the regression lines. Adapted with permission from (An Li, Chao Tai, Zongshan Zhao, Yawei Wang, Qinghua Zhang, Guibin Jiang, Jingtian. Debromination of Decabrominated Diphenyl Ether by Resin-Bound Iron Nanoparticles. Environmental Science and Technology. 2007; 41:6841-46). Copyright (2007) American Chemical Society.

Fig. 6. Production of reactive oxygen species by $TiO_2$ in 0.1% dimethyl sulfoxide under different operating conditions. (a) effect of pH levels on hydroxyl radicals production by $TiO_2$ (relative fluorescence units (RFU) ratio of treatment over controls); (b) effect of concentrations of humic acid on hydroxyl radicals production by $TiO_2$ (RFU ratio of treatment over controls); (c) effect of different crystalline structures of $TiO_2$ on hydroxyl radicals production by $TiO_2$ (RFU ratio of treatment over controls). Points with the same letter at the top were not significantly different ($p > 0.05$) according to one-way ANOVA test. Reprinted from Journal of Environmental Sciences, volume 24, 1670-1678, Ka Lai Chow, Yu Bon Man, Jin Shu Zheng, Yan Liang, Nora Fung Yee Tam, Ming Hung Wong, Characterizing the optimal operation of photocatalytic degradation of BDE-209 by nano-sized $TiO_2$, Copyright (2012), with permission from Elsevier.

Fig. 7. Effect of $TiO_2$ load on debromination efficiency ($Y_{Br-}$) of BDE-209 in UV-irradiated aqueous dispersions under air-saturated conditions. Adapted with permission from (Aizhen Huang, Nan Wang, Ming Lei, Lihua Zhu, Yingying Zhang, Zhifen Lin, Daqiang Yin, Heqing Tang. Efficient Oxidative Debromination of Decabromodiphenyl Ether by $TiO_2$ - Mediated Photocatalysis in Aqueous Environment. Environmental Science and Technology. 2012; 47:518-525). Copyright (2012) American Chemical Society.

Fig. 8. Temporal curves of the photocatalytic degradation of BDE-209 in 25 mL methanol solution under different conditions. $TiO_2$: in a suspension of pristine $TiO_2$; Pd–$TiO_2$: in a suspension of surface-palladized $TiO_2$; UV: under irradiation at

wavelength >360 nm; Ar: purged with argon; air: air-saturated; BDE-209: 10 μmol/L; photocatalysts: 0.2 g/L. Reprinted from Chemistry., 20, Lina Li, Wei Chang, Ying Wang, Hongwei Ji, Chuncheng Chen, Wanhong Ma, Jincai Zhao, Rapid, Photocatalytic, and Deep Debromination of Polybrominated Diphenyl Ethers on Pd–$TiO_2$: Intermediates and Pathways, 11163-70, Copyright © 2014 WILEY-VCH Verlag GmbH & Co. KGaA, Weinheim.

Fig. 9. Debromination efficiency ($Y_{Br-}$) of BDE-209 in systems of (1) UV/$CH_3CN$, (2) UV/$H_2O$, (3) UV/$TiO_2$/$CH_3CN$, and (4) UV/$TiO_2$/$H_2O$. Curve 5 was obtained in the system of curve 4 with the addition of methanol (0.2 mol/L). Adapted with permission from (Aizhen Huang, Nan Wang, Ming Lei, Lihua Zhu, Yingying Zhang, Zhifen Lin, Daqiang Yin, Heqing Tang. Efficient Oxidative Debromination of Decabromodiphenyl Ether by $TiO_2$ - Mediated Photocatalysis in Aqueous Environment. Environmental Science and Technology. 2012; 47:518-525). Copyright (2012) American Chemical Society.

Fig. 10. The effect of different ratio $CH_3OH$ on the photocatalytic debromination of BDE-209 in aqueous system; reaction conditions: 10 mg BDE-209/$TiO_2$ ($5.5 \times 10^{-6}$ mol/g), wavelength >360 nm, anaerobic condition. Reprinted from Chemosphere, volume 89, 420-425, Chunyan Sun, Jincai Zhao, Hongwei Ji, Wanhong Ma, Chuncheng Chen, Photocatalytic debromination of preloaded decabromodiphenyl ether on the $TiO_2$ surface in aqueous system, Copyright (2012), with permission from Elsevier.

Fig. 11. BDE209 removed by different Fe-based metallic particles (metallic particles, 4 g/L; initial concentration of BDE209, 2 mg/L; temperature, 28±2 °C; pH = 6.09; THF/water = 6/4, v/v). Reprinted from Desalination, volume 267, 34-41, Zhanqiang Fang, Xinhong Qiu, Jinhong Chen, Xiuqi Qiu, Degradation of the polybrominated diphenyl ethers by nanoscale zero-valent metallic particles prepared from steel pickling waste liquor, Copyright (2011), with permission from Elsevier.

Fig. 12. Comparison of decabromodiphenyl ether reaction with conventional NZVI, resin-templated NZVI and Ni–Fe bimetals. Decabromodiphenyl ether initial concentration = 2.0 mg/L, and resin = 2 g with ZVI = 0.46 g for both forms of NZVIs.

Reprinted from Journal of Colloid and Interface Science, volume 420, 158-165, Shou-Qing Ni, Ning Yang, Cation exchange resin immobilized bimetallic nickel–iron nanoparticles to facilitate their application in pollutants degradation, Copyright (2014), with permission from Elsevier.

Fig. 13. Effect of solvent conditions on the removal efficiency of BDE-209 (S-NZVI, 4 g/L; initial concentration of BDE-209, 2 mg/L; reaction time, 24 h; temperature, 28 ± 2 °C). (adapted from (Fang et al. 2011b)). Reprinted from Desalination, volume 267, 34-41, Zhanqiang Fang, Xinhong Qiu, Jinhong Chen, Xiuqi Qiu, Degradation of the polybrominated diphenyl ethers by nanoscale zero-valent metallic particles prepared from steel pickling waste liquor, Copyright (2011), with permission from Elsevier.

## Schemes

**(a)**

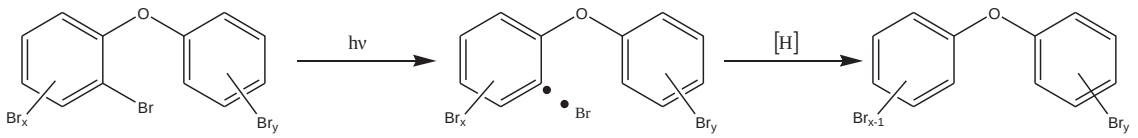


Favored in the presence of a labile solvent with regard to hydrogen atom donation (Rayne et al. 2006).

**(b)**

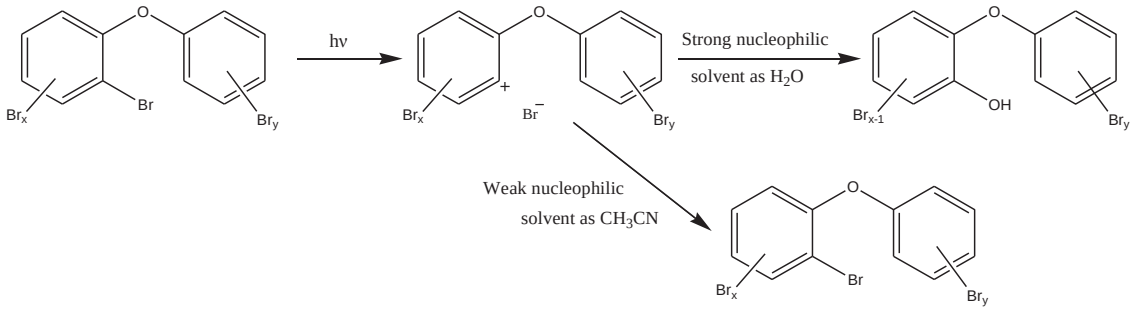


Favored in the presence of strong nucleophilic solvents (Christiansson et al. 2009, Eriksson et al. 2004).

**(c)**

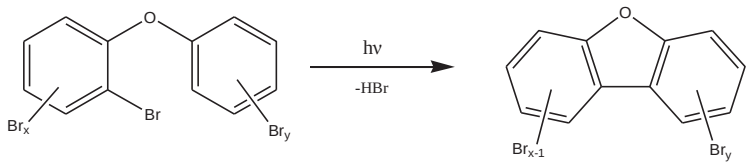


For PBDEs of any level of bromination as long as one *ortho* position is nonbrominated (Eriksson et al. 2004) or for PBDEs with ≤6 bromine substituents (Rayne et al. 2006, Watanabe and Tatsukawa 1987).

**(d)**

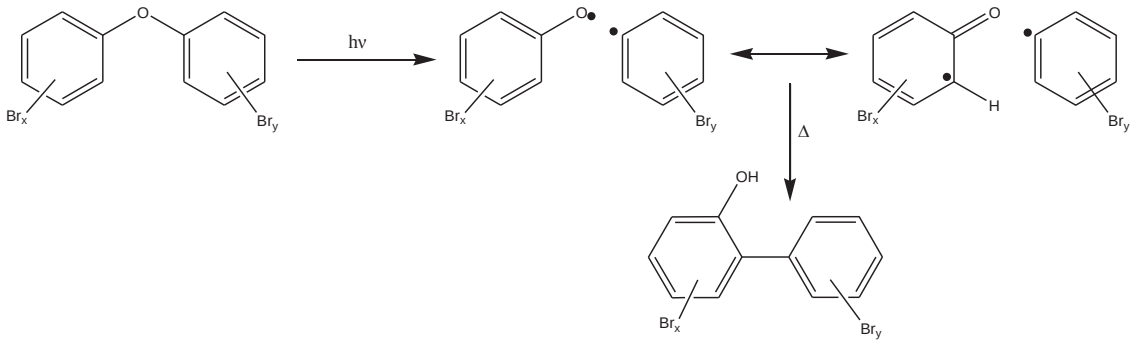


Favored in hydroxylic solvents (or their presence as co-solvents) (Ogata et al. 1970)

**(e)**

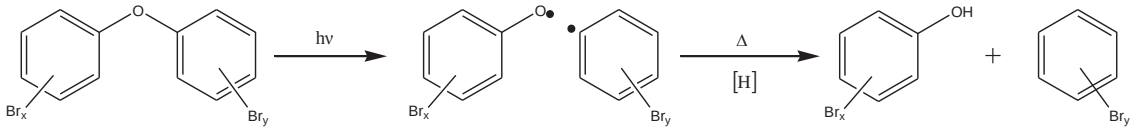


Favored in the presence of a labile solvent with regard to hydrogen atom donation (Rayne et al. 2006).

**(f)**

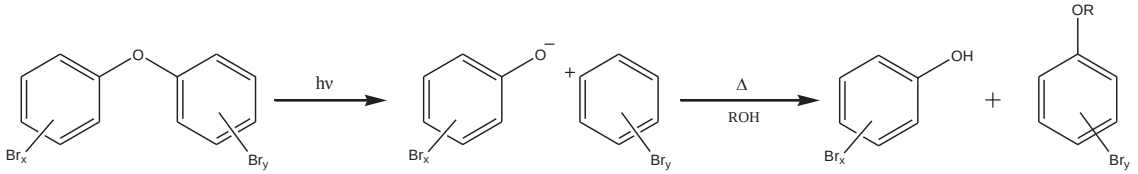


Favored in the presence of strong nucleophilic solvents (Christiansson et al. 2009, Eriksson et al. 2004).

Scheme 1. (a) Photochemically induced aryl-bromine bond cleavage by homolytic pathway; (b) Photochemically induced aryl-bromine bond cleavage by heterolytic pathway; (c) Formation pathways of PBDFs from PBDEs after irradiation; (d) Mechanism for the photo-Fries rearrangement of PBDEs; (e) Photochemically induced aryl-ether bond cleavage by homolytic pathway; (f) Photochemically induced aryl-ether bond cleavage by the heterolytic pathway.

**Route a**

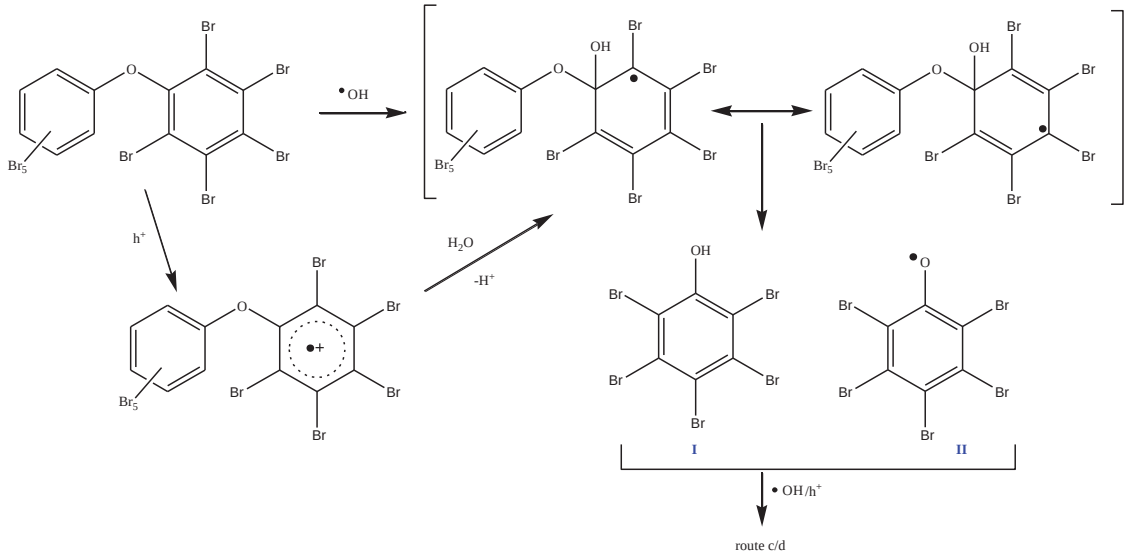


Scheme 2. Possible pathways for the photocatalytic oxidative degradation of PBDEs over $TiO_2$ in aqueous dispersions (adapted from (Huang et al. 2012)).

**Route b**

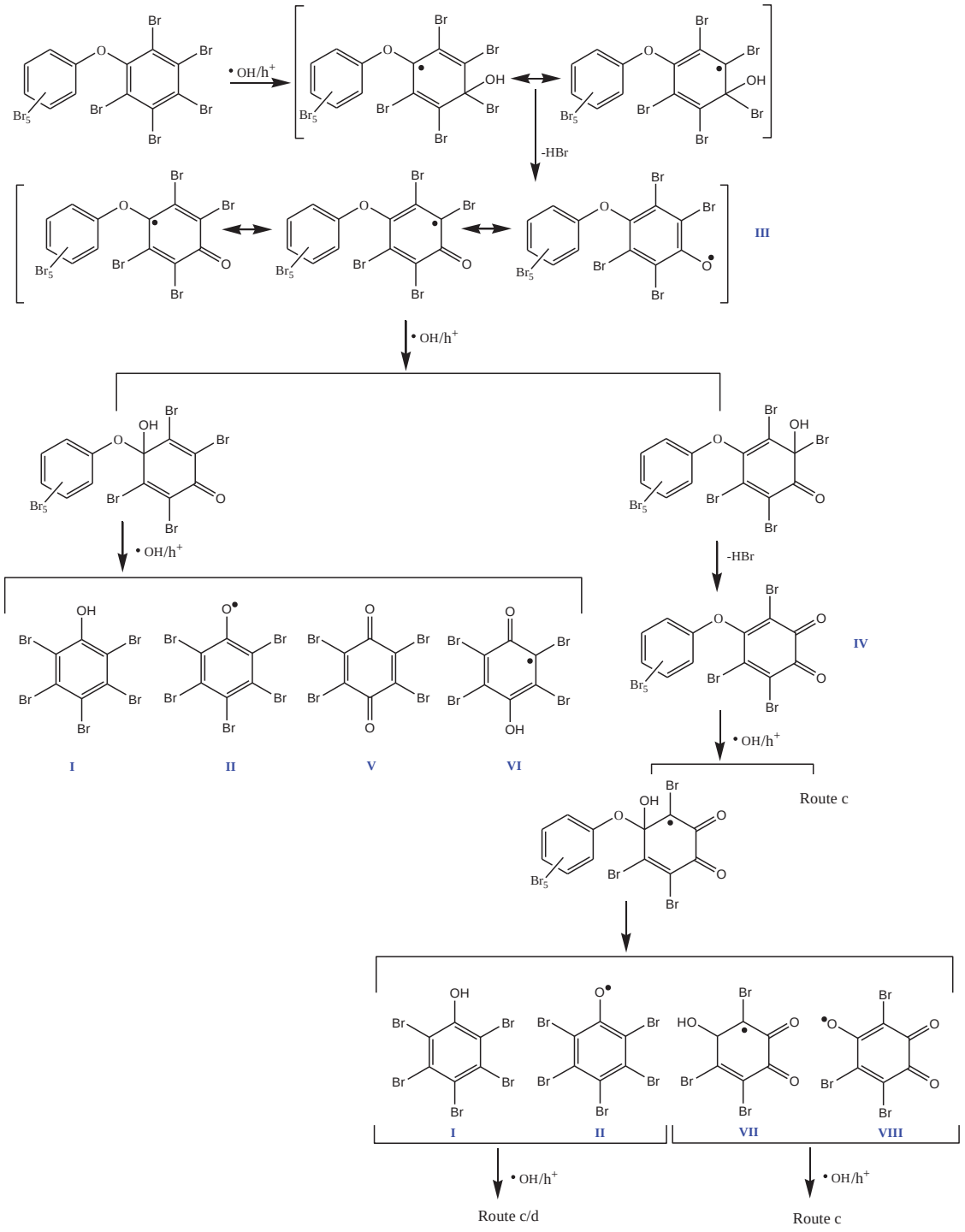


Scheme 2. Possible pathways for the photocatalytic oxidative degradation of PBDEs over $TiO_2$ in aqueous dispersions (adapted from (Huang et al. 2012)) – continued.

## Route c

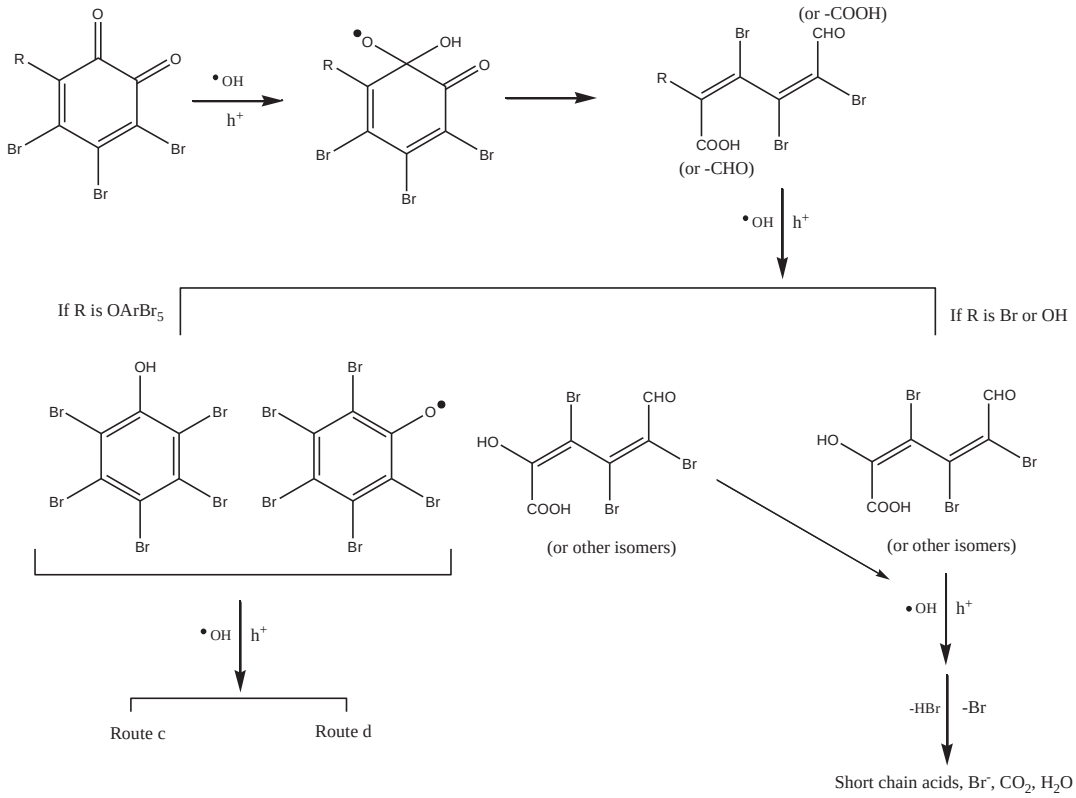


## Route d

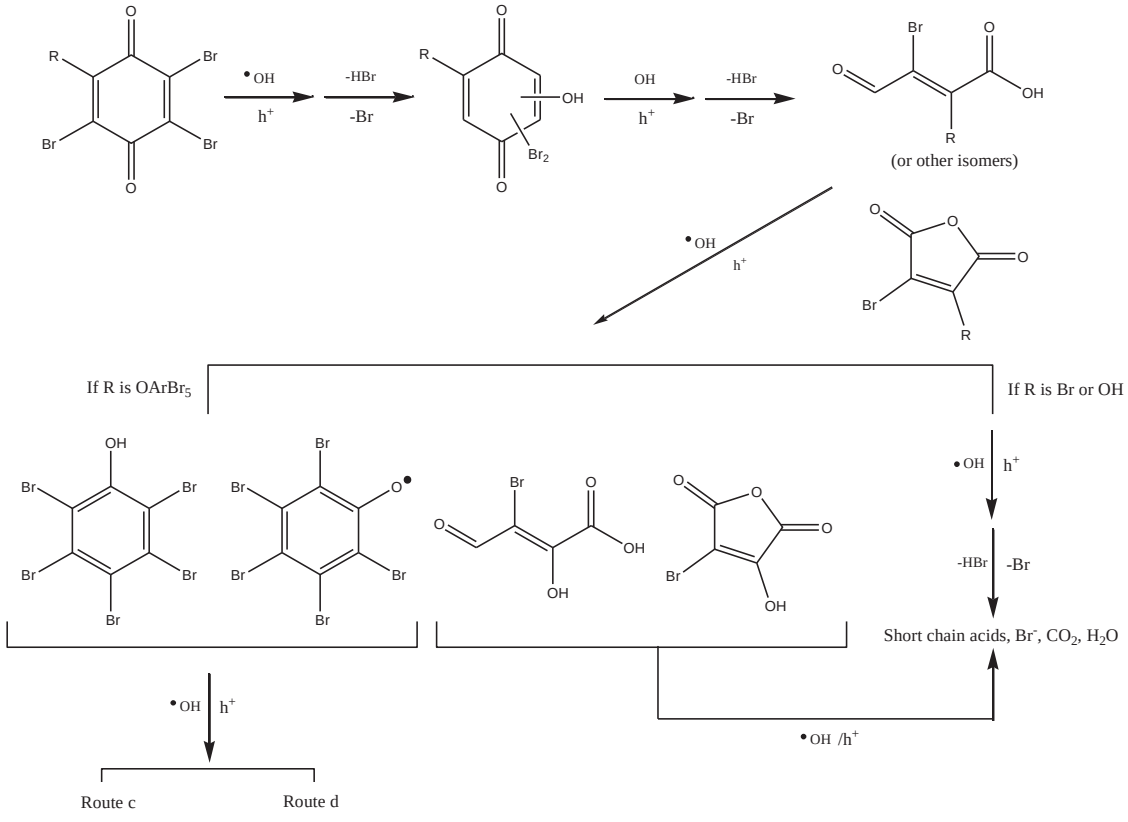

Scheme 2. Possible pathways for the photocatalytic oxidative degradation of PBDEs over $TiO_2$ in aqueous dispersions (adapted from (Huang et al. 2012)) – continued.

## Figures

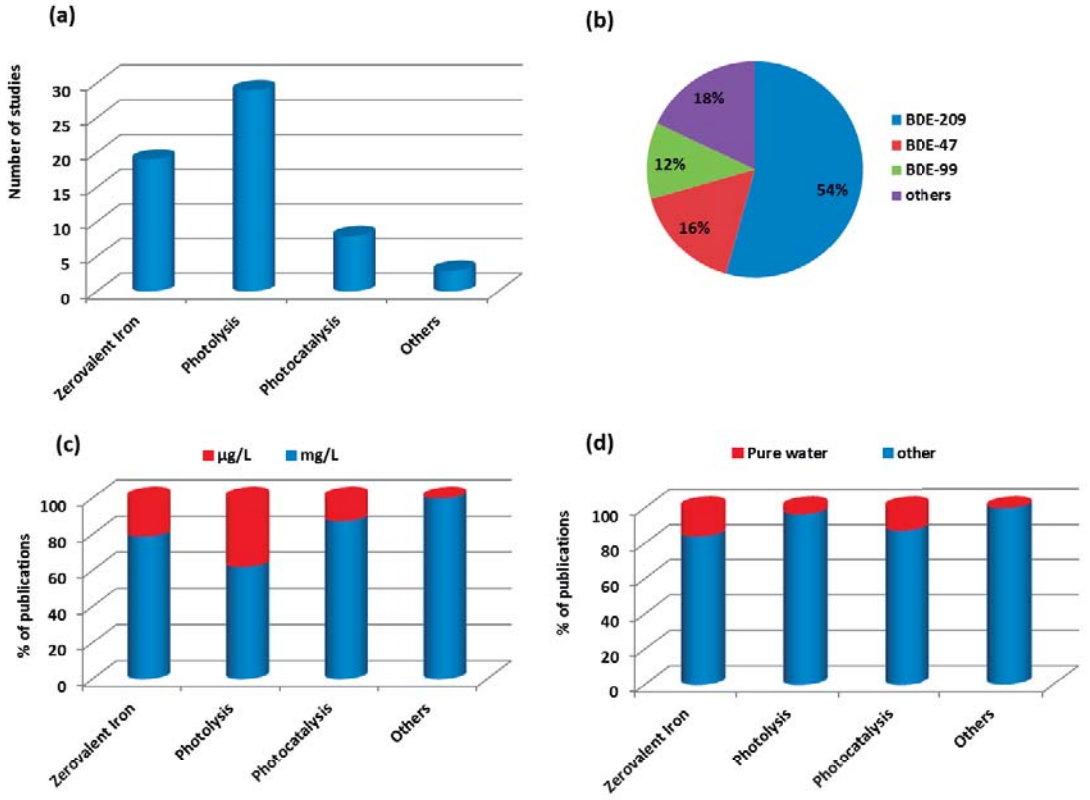


Fig. 1. (a) Number of different degradation technologies studied for the treatment of liquid systems contaminated with PBDEs; (b) Most studied PBDEs congeners in degradation experiments; (c) Percentage of publications about PBDEs degradation in liquid systems conducted at µg/L and mg/L levels and (d) Percentage of publications about PBDEs degradation in pure water and other solvents. Search in Scopus data base until the end of 2014 – www.scopus.com).

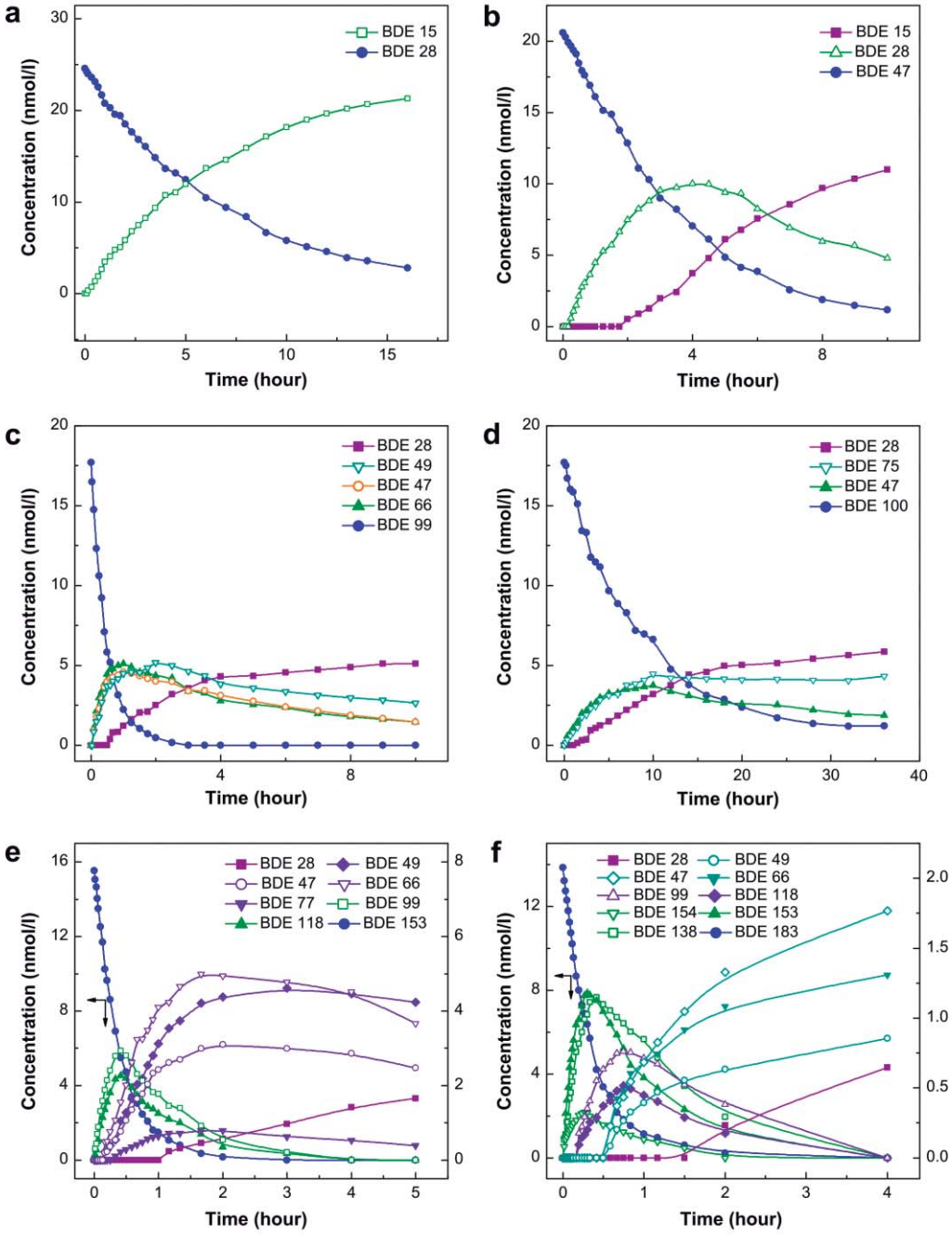


Fig. 2. The concentration of PBDE congeners and their photoproducts in hexane at different irradiation times: (a) BDE-28; (b) BDE-47; (c) BDE-99; (d) BDE-100; (e) BDE-153; (f) BDE-183. Reprinted from Chemosphere, volume 71, 258-267, Lei Fang, Jun Huang, Gang Yu, Lining Wang, Photochemical degradation of six polybrominated diphenyl ether congeners under ultraviolet irradiation in hexane, Copyright (2008), with permission from Elsevier.

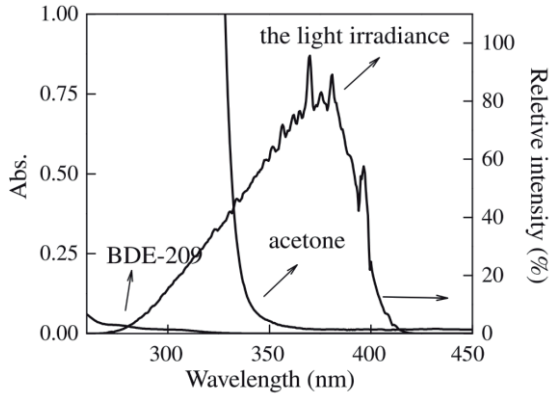


Fig. 3. UV–Vis absorption spectrum of BDE-209 (5 mg/L in acetonitrile), acetone and the relative light irradiance filtered with the ZWB-2 filter. Reprinted from Chemosphere, volume 76, 1486-1490, Qing Xie, Jingwen Chen, Jianping Shao, Chang'er Chen, Hongxia Zhao, Ce Hao, Important role of reaction field in photodegradation of deca-bromodiphenyl ether: Theoretical and experimental investigations of solvent effects, Copyright (2009), with permission from Elsevier.

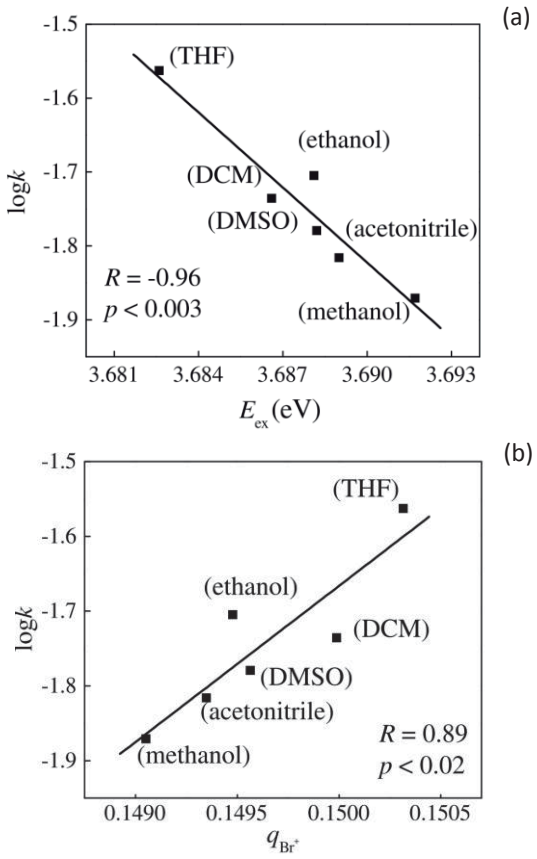


Fig. 4. Correlation of vertical excitation energy ($E_{ex}$) of BDE-209 and the photolytic reactivity ($\log k$) (a). Correlation of the average formal charges of Br ($q_{Br}^{+}$) and the photolytic reactivity ($\log k$) (b). Reprinted from Chemosphere, volume 76, 1486-1490, Qing Xie, Jingwen Chen, Jianping Shao, Chang'er Chen, Hongxia Zhao, Ce Hao, Important role of reaction field in photodegradation of deca-bromodiphenyl ether: Theoretical and experimental investigations of solvent effects, Copyright (2009), with permission from Elsevier.

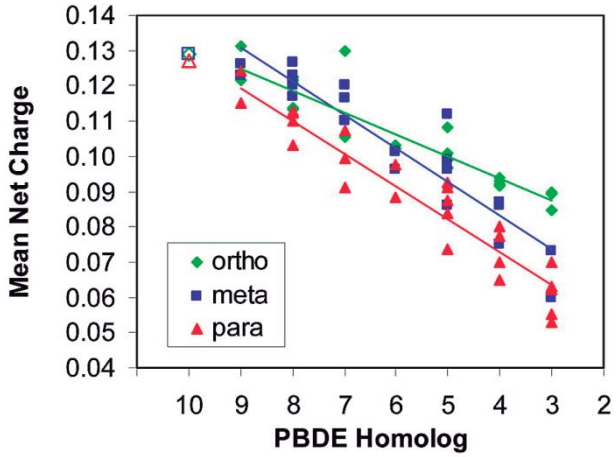


Fig. 5. Mean net charges of individual halogen atoms in randomly selected PBDE molecules, calculated using the semiempirical AM1 method contained in the quantum chemical computation software HyperChem (release 7.0 for Windows). Those for deca congeners are drawn in empty symbols using the same color and are not included in generating the regression lines. Adapted with permission from (An Li, Chao Tai, Zongshan Zhao, Yawei Wang, Qinghua Zhang, Guibin Jiang, Jingtian. Debromination of Decabrominated Diphenyl Ether by Resin-Bound Iron Nanoparticles. Environmental Science and Technology. 2007; 41:6841-46). Copyright (2007) American Chemical Society.

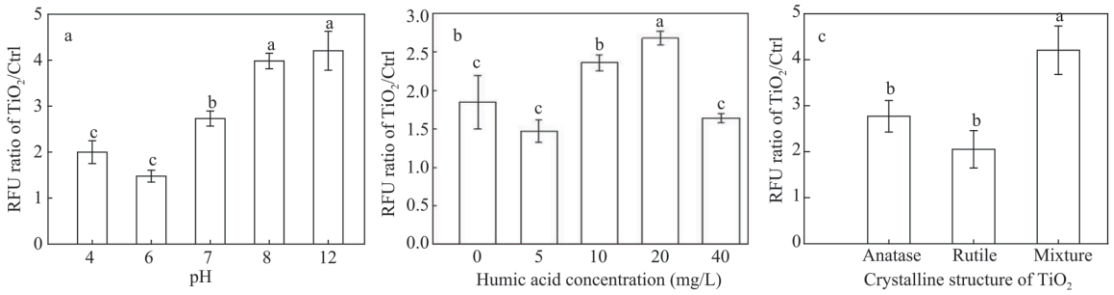


Fig. 6. Production of reactive oxygen species by $TiO_2$ in 0.1% dimethyl sulfoxide under different operating conditions. (a) effect of pH levels on hydroxyl radicals production by $TiO_2$ (relative fluorescence units (RFU) ratio of treatment over controls); (b) effect of concentrations of humic acid on hydroxyl radicals production by $TiO_2$ (RFU ratio of treatment over controls); (c) effect of different crystalline structures of $TiO_2$ on hydroxyl radicals production by $TiO_2$ (RFU ratio of treatment over controls). Points with the same letter at the top were not significantly different ($p > 0.05$) according to one-way ANOVA test. Reprinted from Journal of Environmental Sciences, volume 24, 1670-1678, Ka Lai Chow, Yu Bon Man, Jin Shu Zheng, Yan Liang, Nora Fung Yee Tam, Ming Hung Wong, Characterizing the optimal operation of photocatalytic degradation of BDE-209 by nano-sized $TiO_2$, Copyright (2012), with permission from Elsevier.

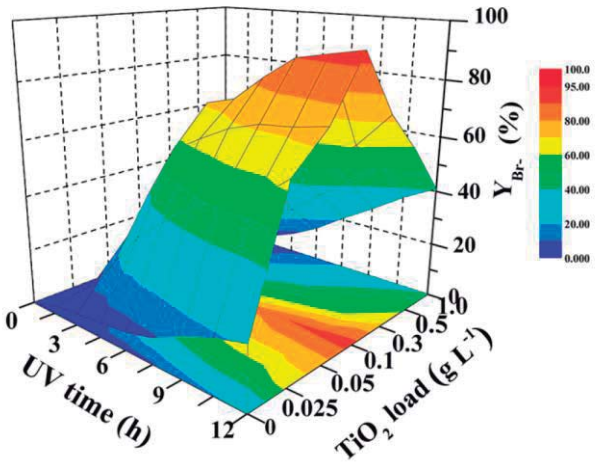


Fig. 7. Effect of $TiO_2$ load on debromination efficiency ($Y_{Br^-}$) of BDE-209 in UV-irradiated aqueous dispersions under air-saturated conditions. Adapted with permission from (Aizhen Huang, Nan Wang, Ming Lei, Lihua Zhu, Yingying Zhang, Zhifen Lin, Daqiang Yin, Heqing Tang. Efficient Oxidative Debromination of Decabromodiphenyl Ether by $TiO_2$ - Mediated Photocatalysis in Aqueous Environment. Environmental Science and Technology. 2012; 47:518-525). Copyright (2012) American Chemical Society.

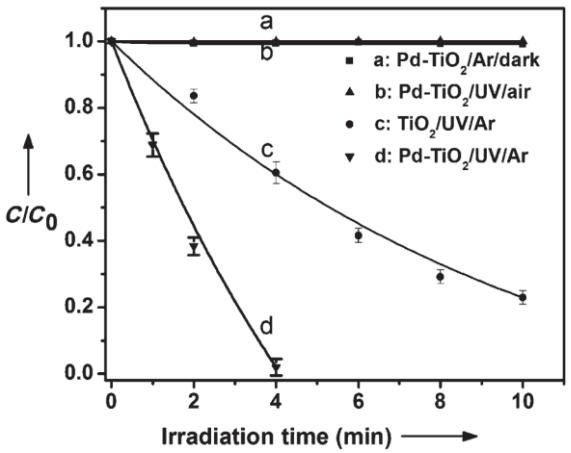


Fig. 8. Temporal curves of the photocatalytic degradation of BDE-209 in 25 mL methanol solution under different conditions. $TiO_2$: in a suspension of pristine $TiO_2$; Pd–$TiO_2$: in a suspension of surface-palladized $TiO_2$; UV: under irradiation at wavelength >360 nm; Ar: purged with argon; air: air-saturated; BDE-209: 10 μmol/L; photocatalysts: 0.2 g/L. Reprinted from Chemistry., 20, Lina Li, Wei Chang, Ying Wang, Hongwei Ji, Chuncheng Chen, Wanhong Ma, Jincai Zhao, Rapid, Photocatalytic, and Deep Debromination of Polybrominated Diphenyl Ethers on Pd–$TiO_2$: Intermediates and Pathways, 11163-70, Copyright © 2014 WILEY-VCH Verlag GmbH & Co. KGaA, Weinheim.

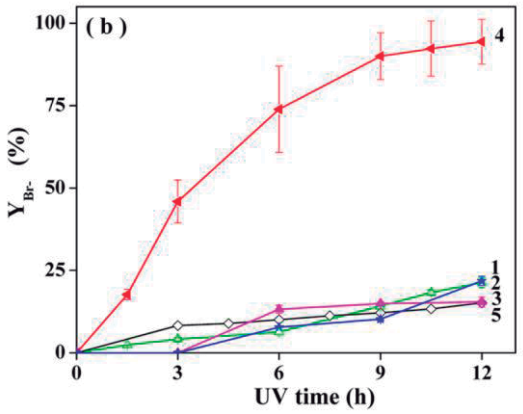


Fig. 9. Debromination efficiency ($Y_{Br-}$) of BDE-209 in systems of (1) UV/$CH_3CN$, (2) UV/$H_2O$, (3) UV/$TiO_2$/$CH_3CN$, and (4) UV/$TiO_2$/$H_2O$. Curve 5 was obtained in the system of curve 4 with the addition of methanol (0.2 mol/L). Adapted with permission from (Aizhen Huang, Nan Wang, Ming Lei, Lihua Zhu, Yingying Zhang, Zhifen Lin, Daqiang Yin, Heqing Tang. Efficient Oxidative Debromination of Decabromodiphenyl Ether by $TiO_2$ - Mediated Photocatalysis in Aqueous Environment. Environmental Science and Technology. 2012; 47:518-525). Copyright (2012) American Chemical Society.

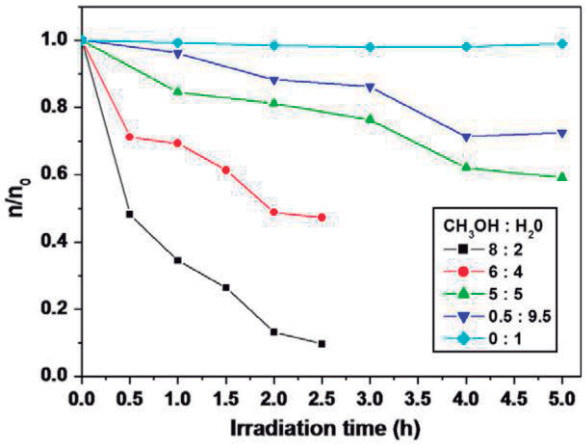


Fig. 10. The effect of different ratio $CH_3OH$ on the photocatalytic debromination of BDE-209 in aqueous system; reaction conditions: 10 mg BDE-209/$TiO_2$ ($5.5 \times 10^{-6}$ mol/g), wavelength >360 nm, anaerobic condition. Reprinted from Chemosphere, volume 89, 420-425, Chunyan Sun, Jincai Zhao, Hongwei Ji, Wanhong Ma, Chuncheng Chen, Photocatalytic debromination of preloaded decabromodiphenyl ether on the $TiO_2$ surface in aqueous system, Copyright (2012), with permission from Elsevier.

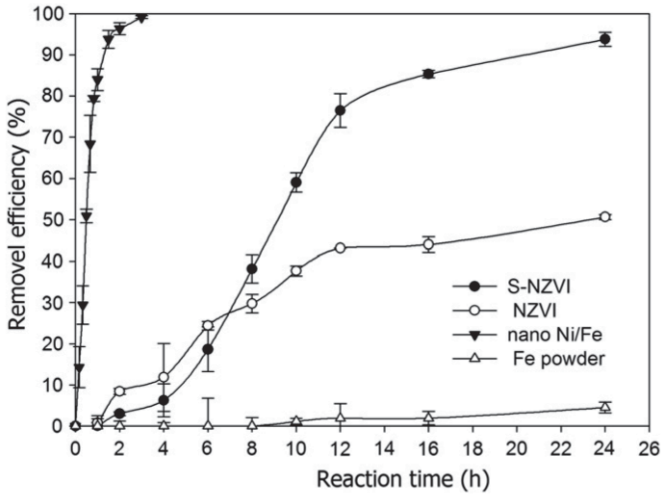


Fig. 11. BDE209 removed by different Fe-based metallic particles (metallic particles, 4 g/L; initial concentration of BDE209, 2 mg/L; temperature, 28±2 °C; pH = 6.09; THF/water = 6/4, v/v). Reprinted from Desalination, volume 267, 34-41, Zhanqiang Fang, Xinhong Qiu, Jinhong Chen, Xiuqi Qiu, Degradation of the polybrominated diphenyl ethers by nanoscale zero-valent metallic particles prepared from steel pickling waste liquor, Copyright (2011), with permission from Elsevier.

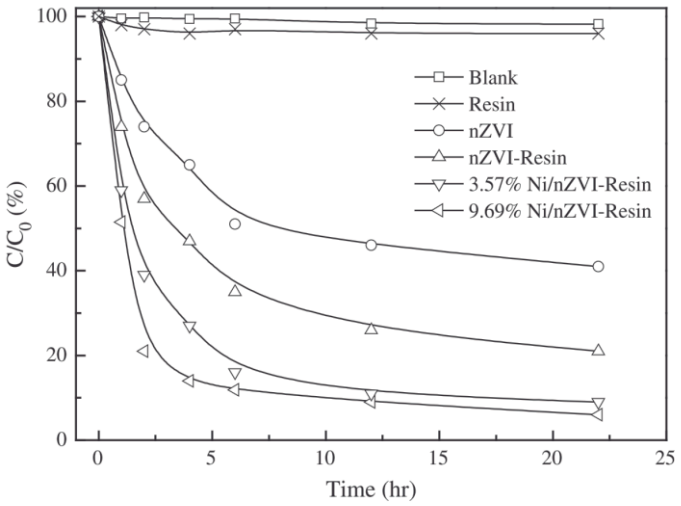


Fig. 12. Comparison of decabromodiphenyl ether reaction with conventional NZVI, resin-templated NZVI and Ni–Fe bimetals. Decabromodiphenyl ether initial concentration = 2.0 mg/L, and resin = 2 g with ZVI = 0.46 g for both forms of NZVIs. Reprinted from Journal of Colloid and Interface Science, volume 420, 158-165, Shou-Qing Ni, Ning Yang, Cation exchange resin immobilized bimetallic nickel–iron nanoparticles to facilitate their application in pollutants degradation, Copyright (2014), with permission from Elsevier.

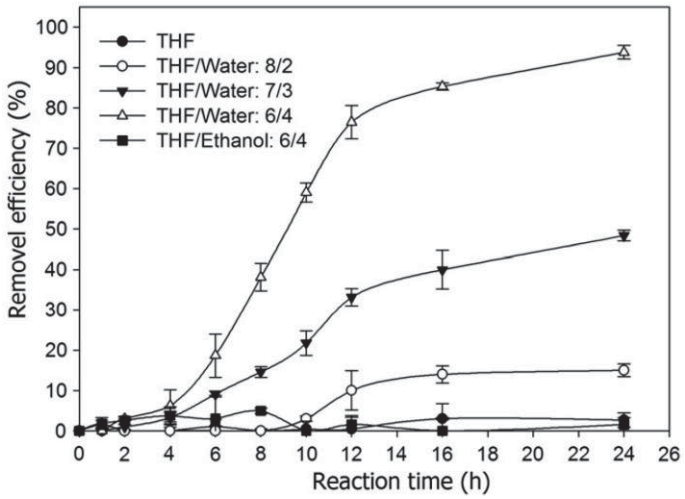


Fig. 13. Effect of solvent conditions on the removal efficiency of BDE-209 (S-NZVI, 4 g/L; initial concentration of BDE-209, 2 mg/L; reaction time, 24 h; temperature, 28 ± 2 °C). (adapted from (Fang, Qiu et al. 2011)). Reprinted from Desalination, volume 267, 34-41, Zhanqiang Fang, Xinhong Qiu, Jinhong Chen, Xiuqi Qiu, Degradation of the polybrominated diphenyl ethers by nanoscale zero-valent metallic particles prepared from steel pickling waste liquor, Copyright (2011), with permission from Elsevier.

# Chemical and Photochemical Degradation of Polybrominated Diphenyl Ethers in Liquid Systems – A Review

Mónica S. F. Santos[a*], Arminda Alves[a] and Luis M. Madeira[a*]

[a] LEPABE – Laboratory for Process, Environmental, Biotechnology and Energy Engineering, Faculty of Engineering, University of Porto, R. Dr. Roberto Frias, s/n, 4200-465 Porto, Portugal

**Figures**

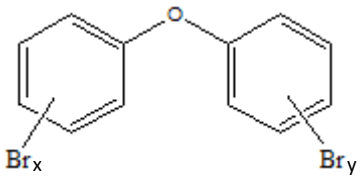


x+y = 1–10

| | |
|---|---|
| x+y = 1 Mono-BDEs | x+y = 6 Hexa-BDEs |
| x+y = 2 Di-BDEs | x+y = 7 Hepta-BDEs |
| x+y = 3 Tri-BDEs | x+y = 8 Octa-BDEs |
| x+y = 4 Tetra-BDEs | x+y = 9 Nona-BDEs |
| x+y = 5 Penta-BDEs | x+y = 10 Deca-BDEs |

Fig. S1. Chemical structure of PBDEs (adapted from (Eljarrat and Barceló 2004)).

* Corresponding authors. Tel.: +351-225081519; Fax: +351-225081449; E-mail adresses: mssantos@fe.up.pt (Mónica S. F. Santos), mmdeira@fe.up.pt (Luís M. Madeira)

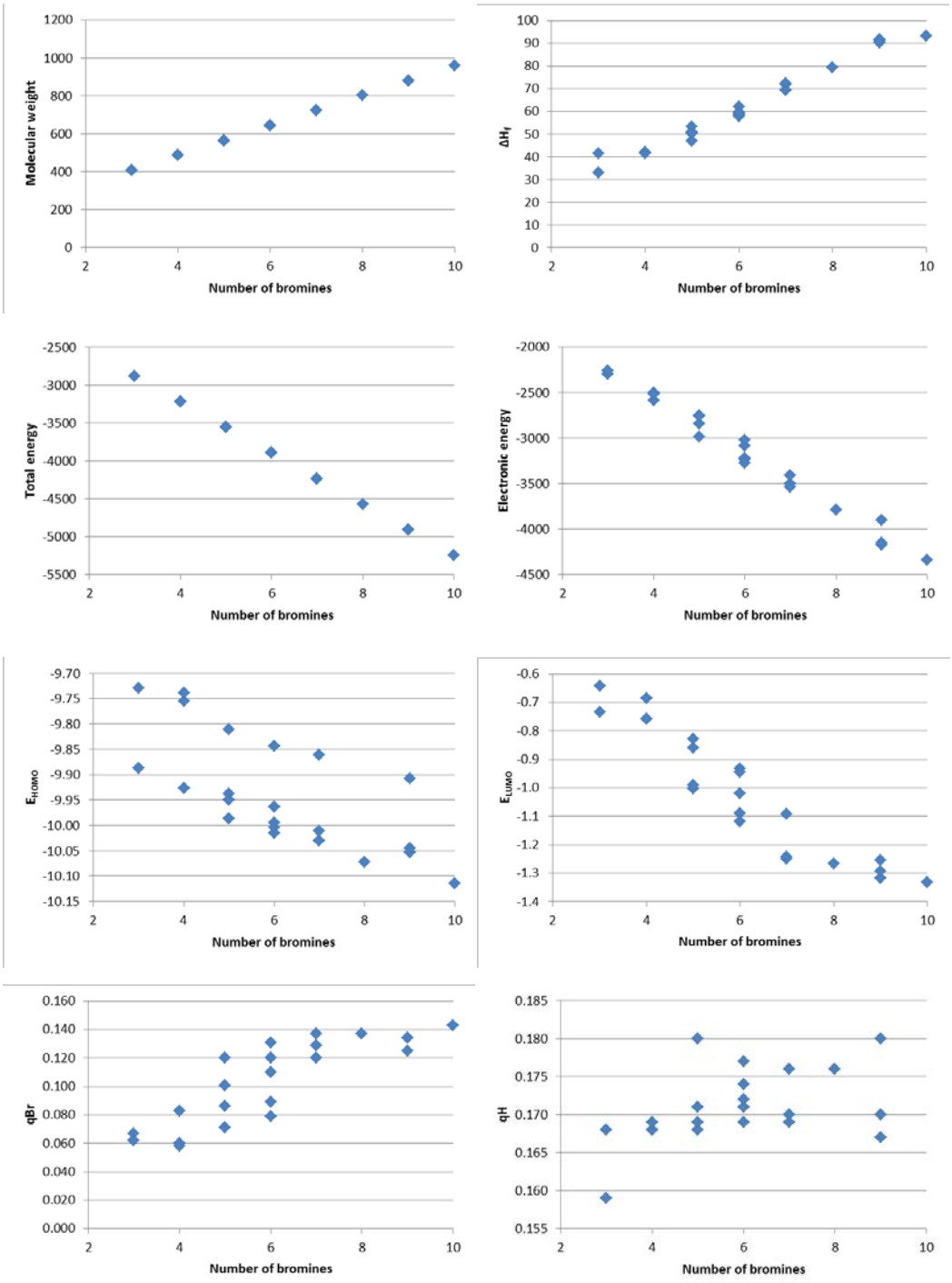


Fig. S2 – Dependence of selected semiempirical quantum chemical descriptors with the number of bromines in a PBDE molecule (Niu et al. 2006).

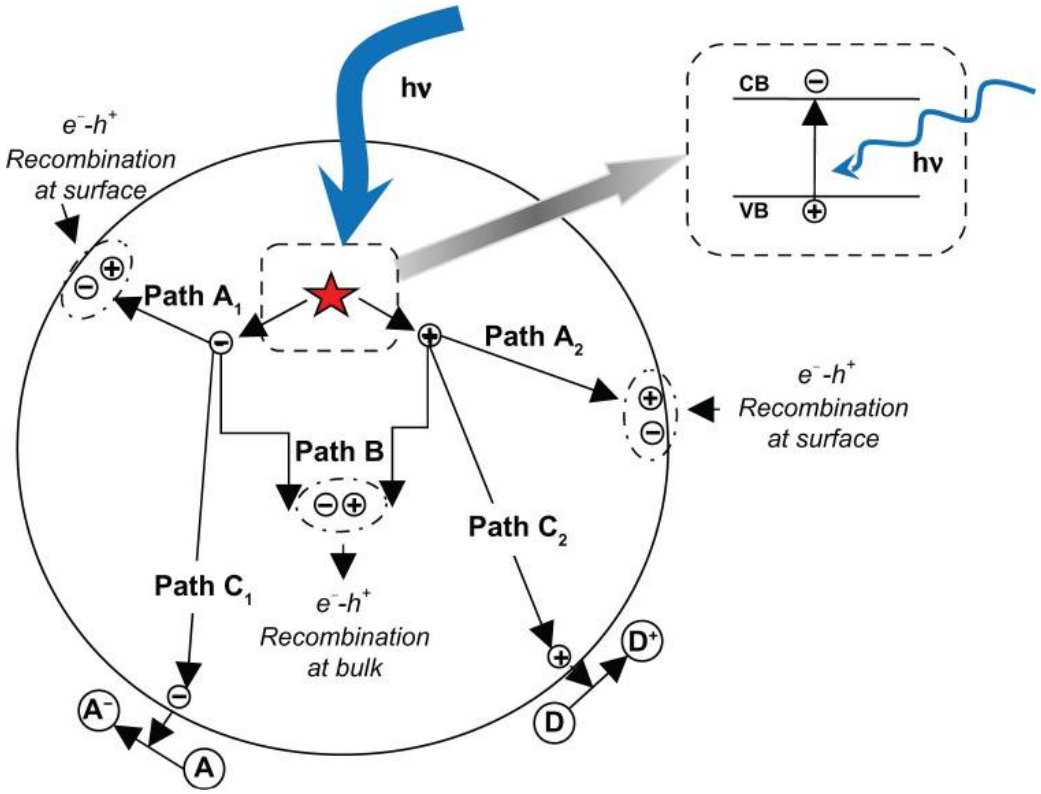


Fig. S3. Schematic representation of various de-excitation pathways for photogenerated electron and holes in a $TiO_2$ particle. Republished with permission of Dove Medical Press Ltd., from The design, fabrication, and photocatalytic utility of nanostructured semiconductors: focus on $TiO_2$-based nanostructures, Arghya Narayan Banerjee, 2011:4, 2011; permission conveyed through Copyright Clearance Center, Inc.

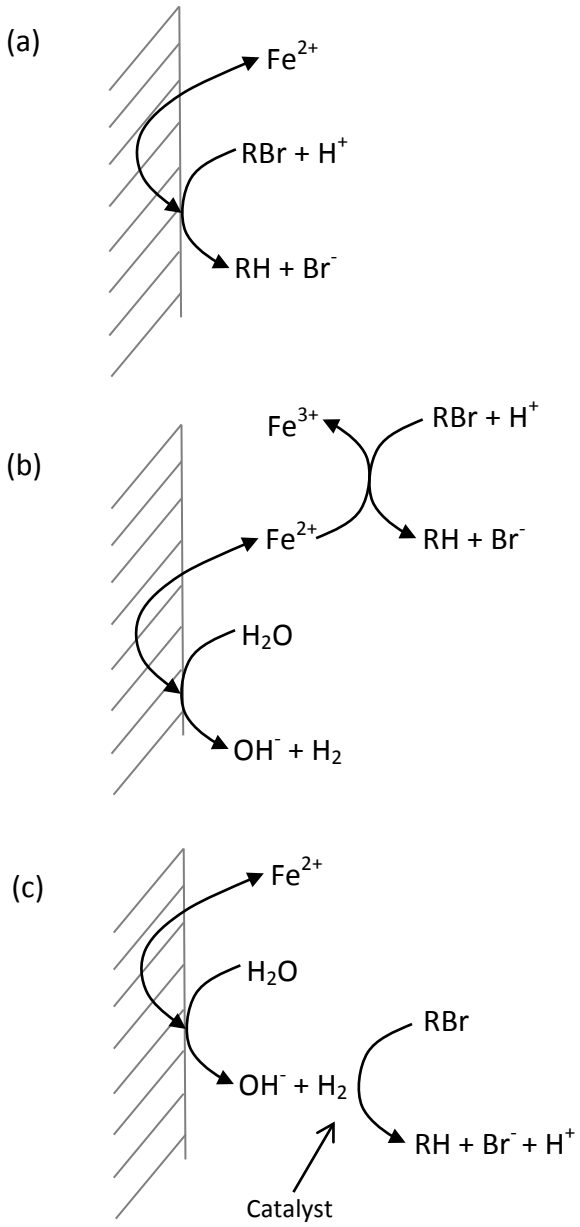


Fig. S4. The proposed pathway by Matheson and Tratnyek (Matheson and Tratnyek 1994) for reductive dehalogenation (adapted from(Ciblak 2011)).

## Tables

Table S1. Physical and chemical properties of technical PBDE mixtures.

| Property | Penta-BDE | Octa-BDE | Deca-BDE |
|---|---|---|---|
| **Color** | Clear, amber to pale yellow [a] | Off-white [a] | Off-white [a] |
| **Physical state** | Highly viscous liquid [a] | Powder [a] | Powder [a] |
| **Melting point** | -7 to -3 °C (commercial) [c] | 85-89 °C (commercial) [b] | 290-306 °C [a] |
| **Boiling point** | decomposes at >200 °C (commercial) [c] | decomposes at >330 °C (commercial) [b] | decomposes at >320 °C [a] |
| **Density at 25 °C (g/mL)** | 2.28 [a] | 2.8 (commercial) [b] | 3.0 [a] |
| **Solubility in water at 25 °C (μg/L)** | 13.3 (commercial) [c] | <1 (commercial) [b] | <0.1 [d] |
| **Log Kow** | 6.57 (commercial) [c] | 6.29 (commercial) [b] | 6.265 [a] |
| **Log Koc** | 4.89-5.10 [a] | 5.92-6.22 [a] | 6.80 [a] |
| **Vapor pressure (mmHg)** | $3.5\times10^{-7}$ (commercial) [a] | $4.9\times10^{-8}$ (commercial) [b] | $3.2\times10^{-8}$ [a] |

Note: The Kow is the octanol-water partitioning coefficient and the Koc is the soil organic carbon-water partitioning coefficient.
Values were extracted from a – (ATSDR and EPA, 2004), b – (ENVIRON International Corporation, 2003a), c – (ENVIRON International Corporation, 2003b), d – (Hardy et al. 2002)

Table S2. Literature review regarding the degradation of PBDEs in liquid-phase by direct photolysis.

| PBDE congeners | Initial Concentration | Matrix | Operating conditions | Analytical method | Results and comments | Ref. |
|---|---|---|---|---|---|---|
| BDEs 209, 208, 207, 206, 203, 190, 183, 181, 155, 154, 139, 138, 99, 77, 47 | $1\times10^{-6}$ M (1 mg/L for BDE-209 and 0.5 mg/L for BDE-47) | MeOH:$H_2O$ (80:20, v/v); MeOH; THF | **Radiation source:** 20 W UV lamp (Philips) | HPLC-UV | **Kinetics:** 1st order reaction<br>**Rate constants:** ranging from 0.003 $h^{-1}$ (BDE-47) to 1.44 $h^{-1}$ (BDE-209) in MeOH:$H_2O$; from 0.004 $h^{-1}$ (BDE-47) to 2.34 $h^{-1}$ (BDE-209) in MeOH; from 0.007 $h^{-1}$ (BDE-47) to 2.99 $h^{-1}$ (BDE-209) in THF.<br>**Quantum yields:** 0.22 (BDE-47); 0.29 (BDE-77); 0.14 (BDE-139); 0.14 (BDE-155); 0.10 (BDE-181); 0.16 (BDE-183); 0.12 (BDE-203); 0.17 (BDE-206); 0.09 (BDE-207); 0.10 (BDE-208); 0.14 (BDE-209) in MeOH:$H_2O$<br>**Degradation products:** lower brominated PBDEs (ten- down to six-), PBDFs (less than 6 bromines) and MeO-PBDFs | (Eriksson et al. 2004) |
| BDE-153 | 0.8 μg/L | ACN; Distilled water; Seawater | **Radiation source:** 6 W UV-lamp (302 nm) | HRGC-HRMS | **Kinetics:** 1st order reaction<br>**Rate constants:** 26±6 $h^{-1}$ in ACN; 9±2 $h^{-1}$ in seawater; cannot be calculated in distilled water.<br>**Global debromination*:** 27% after 1 min in ACN<br>**Degradation products:** lower brominated PBDEs, 1,2,4,7,8-PeBDF and tetrabrominated 2-hydroxybiphenyls (BDE-153 in ACN); only lower brominated PBDEs (BDE-153 in distilled and sea-waters). | (Rayne et al. 2006) |
| BDE-209 | 2-5 mg/L | Hexane | **Radiation source:** solar light | GC-μECD and GC-MS | **Kinetics:** 1st order reaction<br>**Rate constants:** 6.70 $h^{-1}$ (July 2 of 2003), 4.00 $h^{-1}$ (October 23 of 2003).<br>**Quantum yields:** 0.48 (July 2 of 2003), 0.46 (October 23 of 2003).<br>**Main mechanism**: consecutive reductive debromination<br>**Degradation products:** lower brominated PBDEs (43 BDEs were detected and 21 of them were identified). | (Bezares-Cruz et al. 2004) |
| BDEs 28, 47, 99, 100, 153 and 183 | 10 μg/L | Hexane | **Radiation source:** Hg 500 W filtered with Pyrex glass<br>**Irradiation time:** 40 h | GC-ECD | **Kinetics:** 1st order reaction<br>**Rate constants:** 0.10 $h^{-1}$ (BDE-100), 0.14 $h^{-1}$ (BDE-28), 0.30 $h^{-1}$ (BDE-47), 1.83 $h^{-1}$ (BDE-99), 2.30 $h^{-1}$ (BDE-153) and 2.64 $h^{-1}$ (BDE-183)<br>**Global debromination*:** 32% after 15 h (BDE-28), 52% after 10 h (BDE-47), 58% after 10 h (BDE-99), 48% after 35 h (BDE-100), 49% after 4 h (BDE-153), 83% after 4 h (BDE-183)<br>**Main mechanism**: consecutive reductive debromination<br>**Photoreactivity of bromines**: decrease from *ortho* to *para* positions for less brominated PBDEs; no differences were observed for higher brominated congeners.<br>**Degradation products:** lower brominated PBDEs and rather few PBDFs. | (Fang et al. 2008) |

| | | | | | | |
|---|---|---|---|---|---|---|
| Deca-BDE | $1\times10^{-6}$ M (1 mg/L for BDE-209) | THF<br>MeOH<br>THF/MeOH | **Radiation source:** Fluorescent tube TL 20 W/09N from Philips<br>**Irradiation time:** 100-200 min | GC-MS | **Global debromination*:** 28% after 100 min (THF), 24% after 100 min (MeOH)<br>**Main mechanism**: consecutive reductive debromination, intramolecular elimination of HBr.<br>**Degradation products:** BDEs (hexa- to nona-), PBDFs (mono- to penta-), MeO-PBDFs (tetra- to penta-), HO-PBDFs (di- to tetra-) and hydroxylated bromobenzenes | (Christiansson et al. 2009) |
| BDE-99 | 3 to 63 μg/L | $H_2O$<br>Aqueous surfactant solution (0.4 mM of Brij 35 and Brij 58) | **Radiation source:** two low-pressure Hg lamps (254 nm, $2.28\times10^{-7}$ Einstein $L^{-1}$ $s^{-1}$). | GC-μECD and GC-MS | **Kinetics:** pseudo first-order<br>**Rate constants:** 4.39 $h^{-1}$ in Brij 35/$O_2$; 5.26 $h^{-1}$ in Brij 35/$N_2$; 4.10 $h^{-1}$ in Brij 58/$O_2$; 4.72 $h^{-1}$ in Brij 58/$N_2$; 2.20 $h^{-1}$ in $H_2O/O_2$; 4.61 $h^{-1}$ in $H_2O/N_2$<br>**Quantum yields:** 0.109 in Brij 35/$O_2$; 0.131 in Brij 35/$N_2$; 0.102 in Brij 58/$O_2$; 0.117 in Brij 58/$N_2$; 0.054 in $H_2O/O_2$; 0.114 in $H_2O/N_2$<br>**Global debromination*:** 76% after 90 min (Brij 35)<br>**Main mechanism:** consecutive reductive debromination or intramolecular elimination of HBr.<br>**Degradation products:** lower brominated PBDEs (mono- to tetra-) and lower brominated PBDFs (mono- to tetra-).<br>**Toxicity/Biodegradability:** PBDFs are more toxic photoproducts. | (Li et al. 2010) |
| BDE-100 | 5 μg/L | $H_2O$ (ice and liquid) | **Freezer process:** in a laboratory freezer at -20 °C.<br>**Ice solid samples dimensions:** 6 cm diameter and 0.8 cm height.<br>**Radiation source:** two 8 W low-pressure Hg lamps (254 nm).<br>**Irradiation:** maximum 10 min | GC-MS | **Kinetics:** 1st order reaction<br>**Rate constants:** 10.68 $h^{-1}$ (ice), 9.72 $h^{-1}$ (water)<br>**Global debromination*:** 0% after 10 min (ice)<br>**Main mechanism:** consecutive reductive debromination and intramolecular elimination of HBr.<br>**Degradation products:** lower brominated PBDEs and PBDFs. | (Sanchez-Prado et al. 2012) |
| Deca-BDE | 100 mg/L | Hexane: benzene: acetone (8:1:1, v/v) | **Radiation source:** Hg lamp (254 nm) and sun light<br>**Irradiation time:** 16 h | GC-ECD and GC-MS | **Main mechanism:** consecutive reductive debromination.<br>**Degradation products:** lower brominated PBDEs (tri- to octa-), lower brominated PBDFs (mono- to hexa-) and bromobenzene (tetra- and penta-).<br>**Global debromination*:** 83% after 24 h (UV), 93% after 24 h (sunlight) | (Watanabe and Tatsukawa 1987) |

| | | | | | | |
|---|---|---|---|---|---|---|
| BDEs 206, 207, 208 and 209 | 0.5 mg/L for BDEs 206, 207 and 208; 0.3 mg/L for BDE-209 | Toluene, MeOH or THF | **Radiation source:** solar light (summer and early fall 2008) – North Carolina | GC-MS and LC-MS/MS | **Kinetics:** 1$^{st}$ order reaction<br>**Rate constants in Toluene:** 9.06 $h^{-1}$ for BDE-206, 12.12 $h^{-1}$ for BDE-207, 10.86 $h^{-1}$ for BDE-208 and 6.48 $h^{-1}$ for BDE-209<br>**Rate constants in MeOH:** 4.07 $h^{-1}$ for BDE-206, 7.14 $h^{-1}$ for BDE-207, 5.76 $h^{-1}$ for BDE-208 and 3.32 $h^{-1}$ for BDE-209<br>**Rate constants in THF:** 1.84 $h^{-1}$ for BDE-206, 3.28 $h^{-1}$ for BDE-207, 2.76 $h^{-1}$ for BDE-208 and 4.51 $h^{-1}$ for BDE-209<br>**Global debromination in Toluene*:** 27% after 5 min (BDE-206), 25% after 5 min (BDE-207), 27% after 5 min (BDE-208)<br>**Global debromination in MeOH*:** 7% after 5 min (BDE-206), 8% after 5 min (BDE-207), 12% after 5 min (BDE-208)<br>**Global debromination in THF*:** 23% after 5 min (BDE-206), 15% after 5 min (BDE-207), 17% after 5 min (BDE-208)<br>**Main mechanism:** consecutive reductive debromination<br>**Degradation products:** lower brominated PBDEs | (Davis and Stapleton 2009) |
| BDE-209 | 10.5 mg/L | Toluene | **Radiation source:** four Hg UV-lamps, Philips TLK40W/09N (1.6 mW/cm2) or natural sunlight (Umeå-Sweden, July 1997)<br>**Irradiation time:** 32 h | GC-MS | **Kinetics:** 1$^{st}$ order reaction<br>**Half-life:** <0.25 h<br>**Main mechanism:** consecutive reductive debromination and intramolecular elimination of HBr.<br>**Degradation products:** lower brominated PBDEs (nona- to tetra-) and PBDFs. | (Söderström et al. 2003) |

| | | | | | | |
|---|---|---|---|---|---|---|
| BDEs 28, 47, 85, 99, 100, 153, 154, 183, 196, 206, 207, 208 and 209 | 60 µg/L for BDE-209, 20 µg/L for nona-BDEs, 10 µg/L for BDE-196 and 9 µg/L for lower brominated congeners | hexane | **Radiation source:** natural sunlight (Chicago, August and September of 2008)<br>**Irradiation time:** 64 h | GC-ECNI-MS | **Kinetics:** 1st order reaction<br>**Rate constants:** 2.09 $h^{-1}$ (BDE-209), 2.38 $h^{-1}$ (BDE-208), 2.31 $h^{-1}$ (BDE-207), 1.34 $h^{-1}$ (BDE-206), 1.20 $h^{-1}$ (BDE-196), 0.28 $h^{-1}$ (BDE-183), 0.11 $h^{-1}$ (BDE-154), 0.21 $h^{-1}$ (BDE-153), 0.02 $h^{-1}$ (BDE-100), 0.18 $h^{-1}$ (BDE-99), 0.19 $h^{-1}$ (BDE-85), 0.02 $h^{-1}$ (BDE-47), 0.02 $h^{-1}$ (BDE-28)<br>**Global debromination*:** 36% after 8 h (BDE-207), 33% after 8 h (BDE-196), 28% after 64 h (BDE-154), 22% after 64 h (BDE-100), 38% after 64 h (BDE-85), 0% after 64 h (BDE-28), 47% after 8 h (BDE-209), 36% after 8 h (BDE-208), 38% after 8 h (BDE-206), 52% after 64 h (BDE-183), 45% after 64 h (BDE-153), 32% after 64 h (BDE-99), 24% after 64 h (BDE-47)<br>**Main mechanism:** consecutive reductive debromination and intramolecular elimination of HBr.<br>**Reactivity:** the observed rank of vulnerability was generally *meta* ≥ *ortho* > *para*<br>**Degradation products:** lower brominated PBDEs (nona- to tetra-) and PBDFs. | (Wei et al. 2013) |
| BDE-209 | 5 mg/L | THF, ethanol, DCM, DMSO, isopropanol, acetonitrile, methanol and acetone | **Radiation source:** 500 W Xe lamp; 365 nm with the irradiance of 340 µW$cm^{-2}$ | HPLC-DAD and GC-µECD | **Kinetics:** 1st order reaction<br>**Rate constants:** 1.642 $h^{-1}$ in THF, 1.184 $h^{-1}$ in ethanol, 1.103 $h^{-1}$ in DCM; 0.998 $h^{-1}$ in DMSO, 0.993 $h^{-1}$ in isopropanol, 0.917 $h^{-1}$ in acetonitrile, 0.808 $h^{-1}$ in methanol, 0.071 $h^{-1}$ in acetone.<br>**Quantum yields:** 0.38 in THF, 0.35 in ethanol, 0.27 in DCM; 0.60 in DMSO, 0.30 in isopropanol, 0.28 in acetonitrile, 0.23 in methanol.<br>**Main mechanism:** hydrogen addition process and intermolecular polymerization.<br>**Degradation products:** lower brominated PBDEs and other organic intermediates with high boiling points and low solubility (intermolecular polymerization). | (Xie et al. 2009) |

| | | | | | | |
|---|---|---|---|---|---|---|
| BDE-47 | 4.8 µg/L in water, 7.3 to 36.8 µg/L in Brij 35, 7.0 to 28.3 µg/L in Brij 58 and 6.3 to 23.1 µg/L in Tween 80 | nonionic surfactant solutions (Brij 35, Brij 58 and Tween 80) | **Radiation source:** two low-pressure mercury lamps, $2.28\times10^{-7}$ Einstein $L^{-1}s^{-1}$. | GC- µECD and GC-MS | **Kinetics:** 1st order reaction<br>**Rate constants:** 1.84 $h^{-1}$ in water, 2.87 to 3.00 $h^{-1}$ in Brij 35, 2.64 to 2.85 $h^{-1}$ in Brij 58, 0.88 to 4.28 $h^{-1}$ in Tween 80.<br>**Quantum yields:** 0.16 in water, 0.25 to 0.26 in Brij 35, 0.24 to 0.23 in Brij 58, 0.08 to 0.37 in Tween 80<br>**Global debromination*:** 73% after 90 min<br>**Main mechanism:** consecutive reductive debromination and intramolecular elimination of HBr.<br>**Reactivity:** higher reactivity of bromine atoms at *ortho* positions compared to that at *para* positions<br>**Degradation products:** lower brominated PBDEs (tri- to mono-) and PBDFs (tri- to mono-). | (Li et al. 2008) |
| Technical Octobromo Diphenyl Ether mixture – DE-79 (BDEs 153, 154, 183, 196, 197) | 8.4 mg/L for BDE-153, 0.69 mg/L for BDE-154, 21 mg/L for BDE-183, 6.2 mg/L for BDE-196 and 17 mg/L for BDE-197 | MeOH or MeOH-$d_4$ | **Radiation source:** sunlight simulator (SOL 500, 400 W, HÖnle, Gräfelfing, Germany) with a UV filter WG-295, λ>280 nm | HPLC-UV, GC/EI-MS and GC-ECD | **Kinetics:** 1st order reaction<br>**Half-lives in DE-79 mixture:** 0.40 h for BDE-154, 0.25 h for BDE-153, 0.29 h for BDE-183, 0.12 h for BDE-197 and 0.12 h for BDE-196<br>**Half-lives of isolated congener:** 0.16 h for BDE-154, 0.12 h for BDE-153, 0.15 h for BDE-183, 0.10 h for BDE-197 and 0.08 h for BDE-196<br>**Global debromination*:** 7% after 80 min<br>**Main mechanism:** consecutive reductive debromination<br>**Degradation products:** lower brominated PBDEs | (Bendig and Vetter 2010) |
| BDE-209 | 10 mg/L of BDE-209 and $1\times10^{-2}$ M of an aqueous solution of carboxylates | MeOH:$H_2O$ (100:1, v/v) or DMSO:$H_2O$ (100:1, v/v) | **Radiation source:** A PLS-SXE300 Xe lam (Beijing Trusttech Co. Ltd), λ≥420 nm | HPLC-UV and GC-µECD | **Kinetics:** 1st order reaction<br>**Rate constants:** 1.98 $h^{-1}$ and 3.36 $h^{-1}$ by adding ammonium oxalate and potassium oxalate, respectively<br>**Main mechanism:** consecutive reductive debromination based on the halogen binding interaction<br>**Degradation products:** lower brominated PBDEs | (Sun et al. 2013) |
| BDEs 47, 99, 100, 153 and 154 | 2 µg/L | $H_2O$ with 0.1% of acetone | **Radiation source:** natural sunlight (Santiago de Compostela-Spain, July of 2004)<br>or a Xenon arc lamp 1500 W (NXe 1500B, Atlas) | GC-MS | **Kinetics:** 1st order reaction<br>**Rate constants:** 10.02 $h^{-1}$ for BDE-47, 9.00 $h^{-1}$ for BDE-100, 19.02 $h^{-1}$ for BDE-99, 17.28 $h^{-1}$ for BDE-154 and 20.04 $h^{-1}$ for BDE-153<br>**Main mechanism:** consecutive reductive debromination and intramolecular elimination of HBr.<br>**Degradation products:** lower brominated PBDEs and PBDFs | (Sánchez-Prado et al. 2006) |

| | | | | | | |
|---|---|---|---|---|---|---|
| BDEs 153, 154, 183, 196 and technical octabromodiphenyl ether (DE-79) | 510 mg/L of DE-79, 21 mg/L of BDE-183, 8.5 mg/L of BDE-153, 6.25 mg/L of BDE-196 and 0.7 mg/L of BDE-154 | MeOH or MeOH/$H_2O$ | **Radiation source:** SOL 500 sunlight simulator (400 W, HÖnle, Gräfelfing, Germany), λ>280 nm | GC-MS | **Kinetics:** 1$^{st}$ order reaction<br>**Half-lives of BDE-183:** 0.15 h in pure MeOH, 0.4 h in 20% $H_2O$ and 0.7 h in 50% $H_2O$<br>**Main mechanism:** consecutive reductive debromination and ring cleavage<br>**Degradation products:** lower brominated PBDEs and bromophenols | (Bendig and Vetter 2013) |
| BDEs 47, 99 and 209 | 250 µg/L in isooctane; 30-40 pg/L in water of the Baltic Sea and the Atlantic Ocean | Isooctane or $H_2O$ | **Radiation source:** natural sunlight during the four seasons | GC-MS | **Kinetics:** 1$^{st}$ order reaction<br>**Half-lives in isooctane:** 0.6 h for BDE-209; 34 h for BDE-99 and 204 h for BDE-47<br>**Half-lives in $H_2O$ at the surface:** 0.5 h for BDE-209; 33.6 h for BDE-99 and 201.6 h for BDE-47<br>**Half-lives in Atlantic Ocean (30 m deep; 60 °N; summer):** 9.6 h for BDE-209; 648 h for BDE-99 and 2760 h for BDE-47<br>**Half-lives in Baltic Sea (10 m deep; summer):** 43.2 h for BDE-209; 2904 h for BDE-99 and 12624 h for BDE-47<br>**Half-lives in Atlantic Ocean (30 m deep; summer):** 4.8 h (0 °N ) to 9.6 h (60 °N ) for BDE-209; 288 h (0 °N ) to 648 h (60 °N ) for BDE-99; 1008 h (0 °N ) to 2784 h (60 °N ) for BDE-47<br>**Quantum yields in isooctane:** 0.28±0.04 for BDE-209; 0.16±0.02 for BDE-99 and 0.22±0.05 for BDE-47 | (Kuivikko et al. 2007) |
| **BDE-209** | 5 µg/L | $H_2O$ (0.1% ACN) or ethanol | **Radiation source:** sunlight simulator (55 W/m$^2$ (290–400 nm)) | HPLC-UV | **Kinetics:** 1$^{st}$ order reaction<br>**Rate constants:** 12.5 h$^{-1}$ in ethanol and 0.6 h$^{-1}$ in $H_2O$<br>**Quantum yields:** 0.23 in ethanol and 0.0102 in $H_2O$ | (Leal et al. 2013) |

| | | | | | | |
|---|---|---|---|---|---|---|
| BDEs 1, 2, 3, 8, 15, 17, 28, 33, 47, 52, 66, 85, 99, 100, 119, 153, 154 and 183 | 10 μg/L | Hexane or MeOH | **Radiation source:** two RPR-3000 A lamps | GC-μECD | **Kinetics:** 1st order reaction<br>**Rate constants in hexane:** 2.16 $h^{-1}$ (BDE-1), 2.83 $h^{-1}$ (BDE-2), 2.42 $h^{-1}$ (BDE-3), 3.77 $h^{-1}$ (BDE-8), 3.16 $h^{-1}$ (BDE-15), 9.76 $h^{-1}$ (BDE-17), 11.60 $h^{-1}$ (BDE-28), 10.24 $h^{-1}$ (BDE-33), 16.61 $h^{-1}$ (BDE-47), 10.60 $h^{-1}$ (BDE-52), 15.25 $h^{-1}$ (BDE-66), 25.54 $h^{-1}$ (BDE-85), 29.26 $h^{-1}$ (BDE-99), 11.54 $h^{-1}$ (BDE-100), 11.00 $h^{-1}$ (BDE-119), 39.84 $h^{-1}$ (BDE-153), 26.63 $h^{-1}$ (BDE-154) and 31.94 $h^{-1}$ (BDE-183)<br>**Rate constants in MeOH:** 2.37 $h^{-1}$ (BDE-1), 2.23 $h^{-1}$ (BDE-2), 3.07 $h^{-1}$ (BDE-3), 3.80 $h^{-1}$ (BDE-8), 3.62 $h^{-1}$ (BDE-15), 8.23 $h^{-1}$ (BDE-17), 8.13 $h^{-1}$ (BDE-28), 8.27 $h^{-1}$ (BDE-33), 12.23 $h^{-1}$ (BDE-47), 10.01 $h^{-1}$ (BDE-52), 13.62 $h^{-1}$ (BDE-66), 18.51 $h^{-1}$ (BDE-85), 24.85 $h^{-1}$ (BDE-99), 9.15 $h^{-1}$ (BDE-100), 8.34 $h^{-1}$ (BDE-119), 26.93 $h^{-1}$ (BDE-153), 19.83 $h^{-1}$ (BDE-154) and 25.66 $h^{-1}$ (BDE-183)<br>**Quantum yields in hexane:** 0.09 (BDE-1), 0.07 (BDE-2), 0.09 (BDE-3), 0.06 (BDE-8), 0.08 (BDE-15), 0.16 (BDE-17), 0.18 (BDE-28), 0.20 (BDE-33), 0.19 (BDE-47), 0.18 (BDE-52), 0.25 (BDE-66), 0.30 (BDE-85), 0.26 (BDE-99), 0.13 (BDE-100), 0.15 (BDE-119), 0.32 (BDE-153), 0.26 (BDE-154) and 0.33 (BDE-183)<br>**Quantum yields in MeOH:** 0.10 (BDE-1), 0.08 (BDE-2), 0.07 (BDE-3), 0.07 (BDE-8), 0.08 (BDE-15), 0.13 (BDE-17), 0.12 (BDE-28), 0.15 (BDE-33), 0.19 (BDE-47), 0.14 (BDE-52), 0.19 (BDE-66), 0.22 (BDE-85), 0.21 (BDE-99), 0.14 (BDE-100), 0.13 (BDE-119), 0.19 (BDE-153), 0.16 (BDE-154) and 0.18 (BDE-183) | (Fang et al. 2009) |

**Notes**: ACN – acetonitrile; DMSO – dimethylsulfoxide; DCM – dichloromethane; GC-ECD – gas chromatography with electron capture detector; GC/EI-MS – gas chromatography with electron ionization mass spectrometer; GC-μECD – gas chromatography with micro-cell electron capture detector; GC-ECNI-MS – gas chromatography coupled with electron capture negative chemical ionization mass spectrometer; HPLC-UV – high performance liquid chromatography with diode array detector; HRGC-HRMS – high resolution gas chromatography–mass spectrometry; HS-SPME – headspace solid phase microextraction; LC – liquid chromatography; MeOH – methanol; MS – mass spectrometry detector; PDMS – polydimethylsiloxane; THF – tetrahydrofuran; UV – ultraviolet.

*Global debromination values were estimated from the available information in the respective manuscript.

Table S3. Literature review regarding the degradation of PBDEs in liquid-phase by photocatalysis with $TiO_2$.

| PBDE congeners | Initial Concentration | Matrix | Operating conditions | Analytical method | Results and comments | Ref. |
|---|---|---|---|---|---|---|
| BDE 209 | 10 mg/L | $H_2O$:THF (95:5, v/v) | Addition of 0.3 g photocatalyst to BDE-209 (10 mg/L) in $H_2O$:THF (95:5, v/v); stir for 60 min; irradiation with a high-pressure mercury lamp 125 W (maximum at 365 nm); aerobic conditions | GC-MS and LC-MS/MS | **Kinetics:** 1st order reaction<br>**Rate constants:** ranged from 1.3 $h^{-1}$ for $TiO_2$:clay (1:4) to 4.1 $h^{-1}$ for $TiO_2$:clay (4:1)<br>**Main mechanism:** stepwise process; reductive debromination and oxidative process<br>**Degradation products:** lower brominated PBDEs (mono- to hexa-), hydroxylated-PBDEs, brominated phenoxy phenols, phenoxy phenols and small carboxylic acids | (An et al. 2008) |
| BDE-209 | 5-20 mg/L | BDE-209 adsorbed in $TiO_2$ and dispersed $H_2O$:MeOH (95:5, v/v) or pure MeOH | Addition of $TiO_2$ particles into a THF solution of BDE-209; stir until THF was volatilized completely; disperse BDE-209/$TiO_2$ in $H_2O$:MeOH (95:5, v/v) or pure MeOH; irradiation with a Xe lamp at λ>360 nm (PLS-SXE300); anoxic conditions | HPLC-UV | **Kinetics:** 30% of BDE-209 disappeared after 4 h of irradiation<br>**Main mechanism:** stepwise process (pure MeOH) or stepwise/concerted process (aqueous system); reductive debromination<br>**Degradation products:** lower brominated PBDEs<br>**Photoreactivity of bromines**: bromines at the *meta* position are much more susceptible for degradation than *ortho* (adsorption of BDE-209 onto $TiO_2$ and dispersion in a $H_2O$:MeOH (95:5, v/v) solution); bromines at the *ortho* position are much more susceptible for degradation than *meta* and *para* (pure MeOH). | (Sun et al. 2012) |
| BDE-209 | 20 mg/L | ACN, hexane, toluene, THF, acetone, dimethyl sulfoxide, MeOH or N,N-dimethylformamide | Addition of $TiO_2$ (1 g/L) and 0.33 M of isopropyl alcohol to 40 mL BDE-209 solution (20 mg/L); stir for 30 min (magnetic) and 1 min (ultrasound) in the dark; irradiation with a Xe lamp at λ>360 nm (PLS-SXE300); anoxic conditions | HPLC-UV and HRGC-HRMS | **Kinetics:** 1st order reaction<br>**Rate constants:** 20±13 $h^{-1}$, i.e. 90% after 0.13 h ($UV/TiO_2/ACN/N_2$)<br>**Global debromination*:** 42.7% after 24 h ($UV/TiO_2/ACN/N_2$)<br>**Main mechanism:** stepwise process; reductive debromination<br>**Degradation products:** lower brominated PBDEs (tetra- to nona-)<br>**Photoreactivity of bromines**: bromines at the *ortho* position are much more susceptible for degradation than those at the *para* positions | (Sun et al. 2008) |

| | | | | | | |
|---|---|---|---|---|---|---|
| BDE-209 | 75 μg/L | 0.1% DMSO | Preparation of 1% nano-sized $TiO_2$ solution in 20 mL of 0.1% DMSO at pH 7. Spiking with BDE-209 (75 μg/L); irradiation with visible light | GC-MS | **Kinetics:** 1$^{st}$ order reaction<br>**half-life:** 73.2 h<br>**Global debromination*:** 40-50% after 14 days (UV/$TiO_2$/0.1% DMSO/Air)<br>**Main mechanism:** reductive process<br>**Degradation products:** lower brominated PBDEs (tetra- to penta-) | (Chow et al. 2012) |
| BDE-209 | 10 mg/L | water, ACN and their mixtures with 1% THF | 100 mL BDE-209 (10 mg/L) + 10 mg $TiO_2$; stir for 1 min in ultrasound; irradiation with a Xe lamp (PLS-SXE300) at λ [360, 400] nm | HPLC-DAD, LC-MS and GC-MS | **Kinetics:** 96.8% BDE-209 removal after 12 h (UV/$TiO_2$/$H_2O$/Air)<br>**Global debromination*:** 96% after 12 h (UV/$TiO_2$/$H_2O$/Air)<br>**Main mechanism:** oxidative process (mainly)<br>**Degradation products:** brominated dienoic acids, carboxylic derivatives and hydroxylated compounds | (Huang et al. 2012) |
| BDE-209 | 10 mg/L | MeOH with 1% THF | 25 mL BDE-209 solution + 0.2 g/L $TiO_2$ or Pd/$TiO_2$; 2 min in ultrasound; 100 W mercury lamp | HPLC and GC-μECD | **Kinetics:** complete BDE-209 degradation after 4 min (Pd/$TiO_2$) and 40% of BDE-209 degradation after 4 min ($TiO_2$)<br>**Global debromination*:** 19.3% after 30 min (UV/$TiO_2$/MeOH with 1%THF/Ar), 100% after 60 min (UV/Pd-$TiO_2$/MeOH with 1%THF/Ar), 60% after 40 min (UV/Pd-$TiO_2$/MeOH with 1%THF/Ar)<br>**Main mechanism:** reductive process<br>**Degradation products:** lower brominated PBDEs and diphenyl ether | (Li et al. 2014) |
| BDE 209 | 2 mg/L | $H_2O$ with residual THF or $H_2O$:THF (1:1, v/v) | 100 mL BDE-209 (2 mg/L) + 2 g/L $TiO_2$; irradiation with six mercury lamps (3080 μW/(cm$^2$ nm) at 365 nm | GC-MS | **Kinetics:** 0.066 h$^{-1}$ for pH 3, 0.078 h$^{-1}$ for pH 5, 0.09 h$^{-1}$ for pH 7 and 0.138 h$^{-1}$ for pH 9 (all for BDE-209 degradation in $H_2O$ with residual THF)<br>**Global debromination*:** <50% (UV/$TiO_2$/$H_2O$:THF (1:1)/Air), >80% (UV/$TiO_2$/$H_2O$/Air) | (Zhang et al. 2014) |

ACN – acetonitrile; DCM – dichloromethane; GC-μECD – gas chromatography with micro-electron capture detector; GC-MS – gas chromatography with mass spectrometry detector; HPLC-DAD – high performance liquid chromatography with diode array detector; HPLC-UV – high performance liquid chromatography with ultraviolet detector; HRGC-HRMS - high resolution gas chromatography-high resolution mass spectrometry; LC-MS/MS – liquid chromatography tandem mass spectrometry; LLE – liquid-liquid extraction; MeOH – methanol; n.a. – not available; Pd/$TiO_2$ – $TiO_2$ with surface-loaded palladium; UV – ultraviolet.

*Global debromination values were estimated from the available information in the respective manuscript.

Table S4. Literature review regarding the degradation of PBDEs in liquid-phase by ZVI.

| PBDE congeners | Initial Concentration | Matrix | Operating conditions | Analytical method | Results and comments | Ref. |
|---|---|---|---|---|---|---|
| **BDEs 209, 100, 66, 47, 28, 7** | 5 mg/L | $H_2O$ | 1 mL of a PBDE solution in ethyl acetate (50 mg/L) was added to 5 g of iron. Solvent was removed and 10 mL of water was added. Shaken for 3 h to 40 days at 30 ºC and 60 rpm. | GC-ECD and HRGC-HRMS | **Kinetics:** 1st order reaction **Rate constants:** not available **Global debromination*:** 59% after 4 days (ZVI) for BDE-209 **Main mechanism:** stepwise process **Degradation products:** lower brominated diphenyl ethers. *Meta* and *ortho*-bromines were more susceptible to debromination than those at the *para* position. | (Keum and Li 2005) |
| **BDE-47** | 5 mg/L | $H_2O$ | 5 mL of BDE-47 solution in methanol (100 mg/L) was added to 0.1 g of NZVI/Ag. Solvent was removed and 100 mL of water was added. Ultrasoud wave shaker (40 kHz and 100 W) at 25±2 ºC. | HPLC-DAD, GC-MS and LC-MS/MS | **Kinetics:** not available **Rate constants:** BDE-47 was debrominated to diphenyl ether after 120 min by NZVI/Ag-ultrasound. **Global debromination*:** 100% after 15 min (NZVI/Ag/$H_2O_2$)**Main mechanism:** stepwise process **Degradation products:** lower brominated congeners and diphenyl ether **Toxicity/biodegradability:** the acute toxicity of the original solution was evidently lower than that of NZVI/Ag-ultrasound reduction-treated solution. | (Luo et al. 2011) |
| **BDE-209** | 2 mg/L | THF: $H_2O$ (60:40, v/v) | 2 mg/L BDE-209 solution in THF:$H_2O$ (60:40, v/v) was added to 4 g/L of Fe powder, NZVI, NZVI/Ni or S-NZVI); 200 rpm; dark; 28±2 °C. | HPLC-UV | **Kinetics:** pseudo-first order **Rate constants:** 0.002 $h^{-1}$ for Fe powder; 0.031 $h^{-1}$ for NZVI; 1.662 $h^{-1}$ for NZVI/Ni; 0.132 $h^{-1}$ for S-NZVI **Main mechanism:** stepwise process via catalytic hydrogenation **Degradation products:** lower brominated diphenyl ethers | (Fang et al. 2011b) |
| **BDE-209** | 0.5 mg/L to 4 mg/L | THF:$H_2O$ (60:40, v/v) | 2 mg/L BDE-209 solution in THF:$H_2O$ (60:40, v/v) was added to 4 g/L of NZVI/Ni or NZVI; 200 rpm; dark; 28±2 °C; 3 h cycle. | HPLC-UV and GC-MS | **Kinetics:** pseudo-first order **Rate constants:** Ranged from 5.04 $h^{-1}$ (0.5 mg/L BDE-209) to 1.38 $h^{-1}$ (4 mg/L BDE-209) **Main mechanism:** stepwise process via catalytic hydrogenation **Degradation products:** lower brominated diphenyl ethers | (Fang et al. 2011a) |
| **BDE-209** | 0.1 mg/L | $H_2O$: acetone (1:1, v/v) | 8 mL BDE-209 solution + 2 g resin (0.11 g NZVI); shaken 1 h to 10 days; 25±0.5 °C | GC-ECD and HRGC/HRMS | **Kinetics:** 1st order reaction **Rate constants:** 0.28±0.04 $h^{-1}$ **Global debromination*:** 46% after 10 days (NZVI) **Main mechanism:** stepwise process via catalytic hydrogenation **Degradation products:** nona- through tri- brominated diphenyl ethers. *Para*-bromines seem to be more unyielding than *meta* and *ortho*-bromines. | (Li et al. 2007) |

| | | | | | | |
|---|---|---|---|---|---|---|
| **BDE-209** | 10 mg/L | ethanol: n-heptane: $H_2O$ (1:1:10, v/v) | 10 mg/L BDE-209 solution + 0.05 wt.% of Pd in the steel wool + catalyst (at a ratio catalyst/contaminated water of 0.02); 20 ºC | GC-MS | **kinetics:** not provided<br>**Rate constant:** average BDE-209 concentrations decreased from 670 [illegible]2average BDE<br>**Degradation products:** lower brominated diphenyl ethers | (Kastanek et al. 2007) |
| **BDEs 3 and 209** | 1.83 mg/L (BDE-209) and 50 mg/L (BDE-3) | ethyl acetate: methanol; 1:1, v/v (BDE-209) and methanol (BDE-3) | 1.83 mg/L BDE-209 or 50 mg/L BDE-3 + 5 MZVI; 150 rpm; 27 °C; pH 7 | GC-µECD | **Kinetics:** 1st order reaction<br>**Rate constants:** 0.007 $h^{-1}$ (first period) and 0.217 $h^{-1}$ (follow-up period) for BDE-209; 0.003 $h^{-1}$ (first period) and 1.675 $h^{-1}$ (follow-up period) for BDE-3<br>**Global debromination*:** 10% after 30 days (MZVI) for BDE-209 in ethyl acetate:MeOH (1:1, v/v)<br>**Main mechanism:** stepwise process via electron transfer<br>**Degradation products:** lower brominated diphenyl ethers | (Peng et al. 2013) |
| **BDE-209** | 2.8 mg/L | $H_2O$ | 2.8 mg/L BDE-209 + 20 g/L NZVI or 480 g/L MZVI; 125 rpm; 25 °C; pH 5-10 | GC-µECD and GC-MS | **Kinetic:** 1st order reaction<br>**Rate constants for NZVI:** 1.32 $h^{-1}$ (without pH adjustment); 1.44 $h^{-1}$ (pH 5); 1.26 $h^{-1}$ (pH 7); 1.20 $h^{-1}$ (pH 8); 0.96 $h^{-1}$ (pH 10)<br>**Rate constant for MZVI:** 0.20 $h^{-1}$ (without pH adjustment)<br>**Global debromination*:** 86% after 15 min (NZVI)<br>**Main mechanism:** concerted process via electron transfer<br>**Degradation products:** nona- through mono- brominated diphenyl ethers (acid conditions); nona- through penta-brominated diphenyl ethers (alkaline conditions); *Para*-bromines seem to be more unyielding than *meta* and *ortho*-bromines. | (Shih and Tai 2010) |
| **BDEs 1, 47, 99, 153, 183 and 209** | 200 µg/L | acetone: $H_2O$ (1:1, v/v) | 10 mL BDEs solution (200 µg/L) + 1 g NZVI or 0.1-0.3 g NZVI/Pd or 0.25 g commercial NZVI or 0.5 mL commercial NZVI/Pd; 60 rpm; pH 7; anoxic conditions | GC-MS | **Kinetics:** 1st order reaction<br>**Rate constants:** 0.09 to 1.25 $h^{-1}$ (NZVI – BDE 47); 0.48 to 7.02 $h^{-1}$ (NZVI/Pd – BDE 1)<br>**Main mechanism:** stepwise process via electron transfer (NZVI) or catalytic hydrogenation (NZVI/Pd)<br>**Degradation products:** lower brominated PBDEs; *Para*-bromines seem to be more unyielding than *meta* and *ortho*-bromines (NZVI); *Ortho*-bromines seem to be more unyielding than *para*- and *meta*-bromines (NZVI/Pd). | (Zhuang et al. 2012) |

| | | | | | | |
|---|---|---|---|---|---|---|
| **BDEs 1, 2, 3, 8, 12, 21, 28, 33** | 250 µg/L | acetone: $H_2O$ (1:1, v/v) | 10 mL BDEs solution (250 µg/L) + 1 g NZVI or 0.1 g NZVI/Pd or 0.1 g synthesized NZVI/Pd-AC; 60 rpm; pH 7; anoxic or aerobic conditions | GC-µECD and GC-MS | **Kinetics:** $1^{st}$ order reaction<br>**Rate constants:** $1.13\times10^{-4}$ to $1.23\times10^{-2}$ $h^{-1}$ (NZVI and aerobic conditions); 0.016 to 0.126 $h^{-1}$ (NZVI/Pd and aerobic conditions); 0.273 to 0.335 $h^{-1}$ (NZVI/Pd and anoxic conditions)<br>**Main mechanism:** concerted process via catalytic hydrogenation (NZVI/Pd)<br>**Degradation products:** lower brominated PBDEs; *Para*-bromines were preferentially removed (NZVI/Pd). | (Zhuang et al. 2011) |
| **BDE-209** | 2 mg/L | DMSO: $H_2O$ (1:1, v/v) | 2 mg/L BDE-209 + NZVI or resin-bound NZVI or resin-bound NZVI/Ni; sonicated 1 min; 200 rpm; room temperature | HPLC-UV | **Kinetics:** $1^{st}$ order reaction<br>**Rate constants:** 0.164 $h^{-1}$ for 46 g/L resin-bound NZVI; 0.287 $h^{-1}$ for resin-bound NZVI/Ni (44 g/L $Fe^{2+}$ + 2 g/L $Ni^{2+}$); 0.493 $h^{-1}$ for resin-bound NZVI/Ni (41.5 g/L $Fe^{2+}$ + 4.5 g/L $Ni^{2+}$)<br>**Main mechanism:** stepwise process via catalytic hydrogenation<br>**Degradation products:** lower brominated PBDEs; *ortho*- and *meta*-positions were easier to be replaced than that at *para*-position. | (Ni and Yang 2014) |
| **BDEs 153, 183, 196, 197, 203 and 207 (Octa-BDE technical mixture)** | 1 mg/L | $H_2O$ and a small amount of iso-octane | 1 mg/L PBDEs + 10 g/L NZVI + surfactant (TX, CPC or SDDBS); 150 rpm | GC-ECD and GC-MS | **Kinetics:** $1^{st}$ order reaction<br>**Rate constants:** 0.124 $h^{-1}$<br>**Global debromination*:** 55% after 168 h (NZVI)<br>**Main mechanism:** stepwise process via electron transfer<br>**Degradation products:** lower brominated PBDEs | (Liang et al. 2014) |
| **BDEs 1, 2, 3, 5, 7, 12 and 21** | n.a. | acetone: $H_2O$ (1:1, v/v) | 10 mL BDEs solution (250 µg/L) + 1 g NZVI; 60 rpm; pH 7 | GC-MS | **Kinetics:** $1^{st}$ order reaction<br>**Rate constants:** $1.17\times10^{-4}$ $h^{-1}$ (BDE-1); $1.42\times10^{-4}$ $h^{-1}$ (BDE-2); $1.13\times10^{-4}$ $h^{-1}$ (BDE-3); $1.48\times10^{-3}$ $h^{-1}$ (BDE-5); $5.25\times10^{-4}$ $h^{-1}$ (BDE-7); $1.31\times10^{-3}$ $h^{-1}$ (BDE-12); $1.23\times10^{-2}$ $h^{-1}$ (BDE-21)<br>**Global debromination*:** 69% after 35 days (NZVI) for BDE-21<br>**Main mechanism:** stepwise debromination is the main mechanism, but concerted transformation may also occur; electron transfer<br>**Degradation products:** lower brominated PBDEs; *meta*-bromines were preferentially removed and the preferential difference between *ortho*- and *para*-bromines seems to be slight | (Zhuang et al. 2010) |

| | | | | | | |
|---|---|---|---|---|---|---|
| **BDEs 47 and 209** | 5 mg/L | THF (BDE-209) and methanol (BDE-47) | 5 mg/L BDEs solution + 2 g/L NZVI/Ag (Ag content, 1%, w/w); microwave energy of 800 W; pH 6.5±0.5 | HPLC-DAD, GC-MS and LC-MS/MS | **Kinetics:** $1^{st}$ order reaction<br>**Rate constants for NZVI/Ag:** 1.20 $h^{-1}$ (BDE-209 and 47)<br>**Rate constants for NZVI/Ag-MW:** 36.6 $h^{-1}$ (BDE-209); 11.4 $h^{-1}$ (BDE-47)<br>**Global debromination*:** 42% after 15 min (NZVI/Ag-MW) for BDE-209 in THF<br>**Main mechanism:** stepwise process via catalytic hydrogenation<br>**Degradation products:** lower brominated PBDEs | (Luo et al. 2012) |
| **BDE-209** | 2 mg/L | THF: $H_2O$ (60:40, v/v) | 2 mg/L BDE-209 solution + 4 g/L of NZVM + HA (0-40 mg/L) and/or $Cu^{2+}$, $Co^{2+}$, $Ni^{2+}$ (0-0.5 mM); 28±2 °C; 200 rpm; anoxic conditions | HPLC-UV | **Kinetic:** $1^{st}$ order reaction<br>**Rate constants:** 1.10 $h^{-1}$ (NZVM); 0.76 $h^{-1}$ (NZVM + 10 mg/L HA); 0.48 $h^{-1}$ (NZVM + 20 mg/L HA); 0.37 $h^{-1}$ (NZVM + 40 mg/L HA); 9.40 $h^{-1}$ (NZVM + 0.025 mM $Cu^{2+}$); 23.03 $h^{-1}$ (NZVM + 0.05 mM $Cu^{2+}$); 9.19 $h^{-1}$ (NZVM + 0.025 mM $Co^{2+}$); 16.16 $h^{-1}$ (NZVM + 0.05 mM $Co^{2+}$); 24.74 $h^{-1}$ (NZVM + 0.025 mM $Ni^{2+}$); 46.59 $h^{-1}$ (NZVM + 0.05 mM $Ni^{2+}$) | (Cai et al. 2014) |
| **BDE-209** | 2 mg/L | THF: $H_2O$ (60:40, v/v) | 2 mg/L BDE-209 solution + 4 g/L of NZVI + HA (0-40 mg/L) and/or $Cu^{2+}$, $Co^{2+}$, $Ni^{2+}$ (0-0.5 mM); 28±2 °C; 200 rpm; anoxic conditions | HPLC-UV | **Kinetic:** $1^{st}$ order reaction<br>**Rate constants:** 1.02 $h^{-1}$ (NZVI); 0.71 $h^{-1}$ (NZVI + 10 mg/L HA); 0.49 $h^{-1}$ (NZVI + 20 mg/L HA); 0.30 $h^{-1}$ (NZVI + 40 mg/L HA); 8.99 $h^{-1}$ (NZVI + 0.025 mM $Cu^{2+}$); 21.79 $h^{-1}$ (NZVI + 0.05 mM $Cu^{2+}$); 7.28 $h^{-1}$ (NZVI + 0.025 mM $Co^{2+}$); 13.82 $h^{-1}$ (NZVI + 0.05 mM $Co^{2+}$); 24.00 $h^{-1}$ (NZVI + 0.025 mM $Ni^{2+}$); 42.32 $h^{-1}$ (NZVI + 0.05 mM $Ni^{2+}$) | (Tan et al. 2014) |

CPC – cationic cetylpyridinium chloride; DCM – dichloromethane; GC-ECD – gas chromatography with electron capture detector; GC-μECD – gas chromatography with micro-electron capture detector; GC-MS – gas chromatography with mass spectrometry detector; HA – humic acid; HPLC-DAD – high performance liquid chromatography with diode array detector; HPLC-UV – high performance liquid chromatography with ultraviolet detector; HRGC-HRMS - high resolution gas chromatography-high resolution mass spectrometry; LC-MS/MS – liquid chromatography tandem mass spectrometry; MeOH – methanol; MZVI – microscale zerovalent iron particles; n.a. – not available; NZVI – nanoscale zerovalent iron particles; MW – microwave energy; NZVI/Ag – bimetallic iron-silver nanoparticles; NZVI/Ni – bimetallic iron-nickel nanoparticles; NZVI/Pd – bimetallic iron-palladium nanoparticles; NZVI/Pd -AC– bimetallic iron-palladium nanoparticles immobilized on activated carbon; NZVM – nanoscale zerovalent metal prepared from steel pickling liquor; SDDBS – anionic sodium dodecyl benzenesulfonate; S-NZVI – nanoscale zerovalent iron particles prepared from steel pickling waste liquor; TX – nonionic polyethylene glycol octylphenol ether.
*Global debromination values were estimated from the available information in the respective manuscript.

**References**

ATSDR and EPA, 2004. Toxicological profile for polybrominated biphenyls and polybrominated diphenyl ethers. U.S. Department of Health and human Services, Agency for Toxic Substances and Disease Registry, Georgia.

ENVIRON International Corporation, 2003a. Voluntary Children's Chemical Evaluation Program Pilot (VCCEPP): Tier 1 Assessment of the Potential Health Risks to Children Associated with Exposure to the Commercial octabromodiphenyl ether Product. Great Lakes Chemical Corporation, West Lafayette, Indiana, USA.

ENVIRON International Corporation, 2003b. Voluntary Children's Chemical Evaluation Program Pilot (VCCEPP): Tier 1 Assessment of the Potential Health Risks to Children Associated with Exposure to the Commercial pentabromodiphenyl ether Product. Great Lakes Chemical Corporation, West Lafayette, Indiana, USA.

An, T., Chen, J., Li, G., Ding, X., Sheng, G., Fu, J., Mai, B., O'Shea, K.E., 2008. Characterization and the photocatalytic activity of TiO2 immobilized hydrophobic montmorillonite photocatalysts: Degradation of decabromodiphenyl ether (BDE 209). Catal. Today 139(1–2), 69-76.

Bendig, P., Vetter, W., 2010. Photolytical Transformation Rates of Individual Polybrominated Diphenyl Ethers in Technical Octabromo Diphenyl Ether (DE-79). Environ. Sci. Technol. 44(5), 1650-1655.

Bendig, P., Vetter, W., 2013. UV-Induced Formation of Bromophenols from Polybrominated Diphenyl Ethers. Environ. Sci. Technol. 47(8), 3665-3670.

Bezares-Cruz, J., Jafvert, C.T., Hua, I., 2004. Solar Photodecomposition of Decabromodiphenyl Ether: Products and Quantum Yield. Environ. Sci. Technol. 38(15), 4149-4156.

Cai, Y., Liang, B., Fang, Z., Xie, Y., Tsang, E., 2014. Effect of humic acid and metal ions on the debromination of BDE209 by nZVM prepared from steel pickling waste liquor. Front. Environ. Sci. Eng., DOI 10.1007/s11783-014-0764-8.

Chow, K.L., Man, Y.B., Zheng, J.S., Liang, Y., Tam, N.F.Y., Wong, M.H., 2012. Characterizing the optimal operation of photocatalytic degradation of BDE-209 by nano-sized TiO2. J. Environ. Sci. (China) 24(9), 1670-1678.

Christiansson, A., Eriksson, J., Teclechiel, D., Bergman, Å., 2009. Identification and quantification of products formed via photolysis of decabromodiphenyl ether. Environ. Sci. Pollut. Res. 16(3), 312-321.

Davis, E.F., Stapleton, H.M., 2009. Photodegradation Pathways of Nonabrominated Diphenyl Ethers, 2-Ethylhexyltetrabromobenzoate and Di(2-ethylhexyl)tetrabromophthalate: Identifying Potential Markers of Photodegradation. Environ. Sci. Technol. 43(15), 5739-5746.

Eljarrat, E., Barceló, D., 2004. Sample handling and analysis of brominated flame retardants in soil and sludge samples. Trends Anal. Chem. 23(10–11), 727-736.

Eriksson, J., Green, N., Marsh, G., Bergman, Å., 2004. Photochemical Decomposition of 15 Polybrominated Diphenyl Ether Congeners in Methanol/Water. Environ. Sci. Technol. 38(11), 3119-3125.

Fang, L., Huang, J., Yu, G., Li, X., 2009. Quantitative structure–property relationship studies for direct photolysis rate constants and quantum yields of polybrominated diphenyl ethers in hexane and methanol. Ecotox. Environ. Safe. 72(5), 1587-1593.

Fang, L., Huang, J., Yu, G., Wang, L., 2008. Photochemical degradation of six polybrominated diphenyl ether congeners under ultraviolet irradiation in hexane. Chemosphere 71(2), 258-267.

Fang, Z., Qiu, X., Chen, J., 2011a. Debromination of polybrominated diphenyl ethers by Ni/Fe bimetallic nanoparticles: Influencing factors, kinetics, and mechanism. J. Hazard. Mater. 185(2-3), 958-969.

Fang, Z., Qiu, X., Chen, J., 2011b. Degradation of the polybrominated diphenyl ethers by nanoscale zero-valent metallic particles prepared from steel pickling waste liquor. Desalination 267(1), 34-41.

Hardy, M.L., Schroeder, R., Biesemeier, J., Manor, O., 2002. Prenatal Oral (Gavage) Developmental Toxicity Study of Decabromodiphenyl Oxide in Rats. Int. J. Toxicol. 21(2), 83-91.

Huang, A., Wang, N., Lei, M., Zhu, L., Zhang, Y., Lin, Z., Yin, D., Tang, H., 2012. Efficient Oxidative Debromination of Decabromodiphenyl Ether by TiO2-Mediated Photocatalysis in Aqueous Environment. Environ. Sci. Technol. 47(1), 518-525.

Kastanek, F., Maleterova, Y., Kastanek, P., Rott, J., Jiricny, V., Jiratova, K., 2007. Complex treatment of wastewater and groundwater contaminated by halogenated organic compounds. Desalination 211(1–3), 261-271.

Keum, Y.-S., Li, Q.X., 2005. Reductive Debromination of Polybrominated Diphenyl Ethers by Zerovalent Iron. Environ. Sci. Technol. 39(7), 2280-2286.

Kuivikko, M., Kotiaho, T., Hartonen, K., Tanskanen, A., Vähätalo, A.V., 2007. Modeled Direct Photolytic Decomposition of Polybrominated Diphenyl Ethers in the Baltic Sea and the Atlantic Ocean. Environ. Sci. Technol. 41(20), 7016-7021.

Leal, J.F., Esteves, V.I., Santos, E.B.H., 2013. BDE-209: Kinetic Studies and Effect of Humic Substances on Photodegradation in Water. Environ. Sci. Technol. 47(24), 14010-14017.

Li, A., Tai, C., Zhao, Z., Wang, Y., Zhang, Q., Jiang, G., Hu, J., 2007. Debromination of decabrominated diphenyl ether by resin-bound iron nanoparticles. Environ. Sci. Technol. 41, 6841-6846.

Li, L., Chang, W., Wang, Y., Ji, H., Chen, C., Ma, W., Zhao, J., 2014. Rapid, Photocatalytic, and Deep Debromination of Polybrominated Diphenyl Ethers on Pd–TiO2: Intermediates and Pathways. Chem. Eur. J. 20(35), 11163-11170.

Li, X., Huang, J., Fang, L., Yu, G., Lin, H., Wang, L., 2008. Photodegradation of 2,2’,4,4’-tetrabromodiphenyl ether in nonionic surfactant solutions. Chemosphere 73(10), 1594-1601.

Li, X., Huang, J., Yu, G., Deng, S., 2010. Photodestruction of BDE-99 in micellar solutions of nonionic surfactants of Brij 35 and Brij 58. Chemosphere 78(6), 752-759.

Liang, D.-W., Yang, Y.-H., Xu, W.-W., Peng, S.-K., Lu, S.-F., Xiang, Y., 2014. Nonionic surfactant greatly enhances the reductive debromination of polybrominated diphenyl ethers by nanoscale zero-valent iron: Mechanism and kinetics. J. Hazard. Mater. 278(0), 592-596.

Luo, S., Yang, S., Sun, C., Gu, J.-D., 2012. Improved debromination of polybrominated diphenyl ethers by bimetallic iron–silver nanoparticles coupled with microwave energy. Sci. Total Environ. 429(0), 300-308.

Luo, S., Yang, S., Xue, Y., Liang, F., Sun, C., 2011. Two-stage reduction/subsequent oxidation treatment of 2,2′,4,4′-tetrabromodiphenyl ether in aqueous solutions: Kinetic, pathway and toxicity. J. Hazard. Mater. 192(3), 1795-1803.

Ni, S.-Q., Yang, N., 2014. Cation exchange resin immobilized bimetallic nickel–iron nanoparticles to facilitate their application in pollutants degradation. J. Colloid Interface Sci. 420(0), 158-165.

Niu, J., Shen, Z., Yang, Z., Long, X., Yu, G., 2006. Quantitative structure–property relationships on photodegradation of polybrominated diphenyl ethers. Chemosphere 64(4), 658-665.

Peng, Y.-H., Chen, M.-k., Shih, Y.-h., 2013. Adsorption and sequential degradation of polybrominated diphenyl ethers with zerovalent iron. J. Hazard. Mater. 260(0), 844-850.

Rayne, S., Wan, P., Ikonomou, M., 2006. Photochemistry of a major commercial polybrominated diphenyl ether flame retardant congener: 2,2′,4,4′,5,5′-Hexabromodiphenyl ether (BDE153). Environ. Int. 32(5), 575-585.

Sanchez-Prado, L., Kalafata, K., Risticevic, S., Pawliszyn, J., Lores, M., Llompart, M., Kalogerakis, N., Psillakis, E., 2012. Ice photolysis of 2,2′,4,4′,6-pentabromodiphenyl ether (BDE-100): Laboratory investigations using solid phase microextraction. Anal. Chim. Acta 742, 90-96.

Sánchez-Prado, L., Lores, M., Llompart, M., García-Jares, C., Bayona, J.M., Cela, R., 2006. Natural sunlight and sun simulator photolysis studies of tetra- to hexa-brominated diphenyl ethers in water using solid-phase microextraction. J. Chromatogr. A 1124(1–2), 157-166.

Shih, Y.-H., Tai, Y.-T., 2010. Reaction of decabrominated diphenyl ether by zerovalent iron nanoparticles. Chemosphere 78(10), 1200-1206.

Söderström, G., Sellström, U., de Wit, C.A., Tysklind, M., 2003. Photolytic Debromination of Decabromodiphenyl Ether (BDE 209). Environ. Sci. Technol. 38(1), 127-132.

Sun, C., Chang, W., Ma, W., Chen, C., Zhao, J., 2013. Photoreductive Debromination of Decabromodiphenyl Ethers in the Presence of Carboxylates under Visible Light Irradiation. Environ. Sci. Technol. 47(5), 2370-2377.

Sun, C., Zhao, D., Chen, C., Ma, W., Zhao, J., 2008. TiO2-Mediated Photocatalytic Debromination of Decabromodiphenyl Ether: Kinetics and Intermediates. Environ. Sci. Technol. 43(1), 157-162.

Sun, C., Zhao, J., Ji, H., Ma, W., Chen, C., 2012. Photocatalytic debromination of preloaded decabromodiphenyl ether on the TiO2 surface in aqueous system. Chemosphere 89(4), 420-425.

Tan, L., Liang, B., Fang, Z., Xie, Y., Tsang, E., 2014. Effect of humic acid and transition metal ions on the debromination of decabromodiphenyl by nano zero-valent iron: kinetics and mechanisms. J. Nanopart. Res. 16(12), 1-13.

Watanabe, I., Tatsukawa, R., 1987. Formation of brominated dibenzofurans from the photolysis of flame retardant decabromobiphenyl ether in hexane solution by UV and sun light. Bull. Environ. Contam. Toxicol. 39, 953-959.

Wei, H., Zou, Y., Li, A., Christensen, E.R., Rockne, K.J., 2013. Photolytic debromination pathway of polybrominated diphenyl ethers in hexane by sunlight. Environ. Pollut. 174, 194-200.

Xie, Q., Chen, J., Shao, J., Chen, C.e., Zhao, H., Hao, C., 2009. Important role of reaction field in photodegradation of deca-bromodiphenyl ether: Theoretical and experimental investigations of solvent effects. Chemosphere 76(11), 1486-1490.

Zhang, M., Lu, J., He, Y., Wilson, P.C., 2014. Photocatalytic degradation of polybrominated diphenyl ethers in pure water system. Front. Environ. Sci. Eng., 1-7.

Zhuang, Y., Ahn, S., Luthy, R.G., 2010. Debromination of Polybrominated Diphenyl Ethers by Nanoscale Zerovalent Iron: Pathways, Kinetics, and Reactivity. Environ. Sci. Technol. 44(21), 8236-8242.

Zhuang, Y., Ahn, S., Seyfferth, A.L., Masue-Slowey, Y., Fendorf, S., Luthy, R.G., 2011. Dehalogenation of Polybrominated Diphenyl Ethers and Polychlorinated Biphenyl by Bimetallic, Impregnated, and Nanoscale Zerovalent Iron. Environ. Sci. Technol. 45(11), 4896-4903.

Zhuang, Y., Jin, L., Luthy, R.G., 2012. Kinetics and pathways for the debromination of polybrominated diphenyl ethers by bimetallic and nanoscale zerovalent iron: Effects of particle properties and catalyst. Chemosphere 89(4), 426-432.